Mathematical Sciences School
Queensland University of Technology

Mathematical Modelling of Fumigant Transport in Stored Grain

Mat Isa, Zaiton
Bachelor of Science (Mathematics)
Masters of Science (Mathematics)

A thesis submitted for the degree of Doctor of Philosophy in the Science and Engineering Faculty, Queensland University of Technology according to QUT requirements.

Principal Supervisor: Associate Professor Troy W. Farrell
Associate Supervisors: Dr Glenn R. Fulford
Dr Neil A. Kelson

2014

Abstract

The research presented in this thesis investigates phosphine gas fumigation of wheat beds in unsealed, sealed and leaky grain storage, typical of Australian agricultural settings. Fumigation by phosphine gas is a common method used for killing insects in stored grain in order to preserve quality standard requirements. The hydrodynamic behaviour of the phosphine gas movement and distribution is not very well known but is crucial as the fumigant is only effective if kept in contact with the insects for sufficient time at the required concentration. If fumigation is insufficient, potential zones may exist within the stored grain that provide a refuge where insects can survive and breed.

The main body of the thesis is in the form of three research papers where computational fluid dynamics (CFD) simulation, analytical solutions, and mathematical modelling approaches are used to gain insights into the fumigant distribution with time under the various storage and delivery regimes. Two types of commonly used delivery method, namely fan forced and tablet fumigation, are considered in this work to investigate the hydrodynamic behaviour of phosphine gas in the stored grain. Overall, the work progresses from the simpler case of fan forced fumigation of a grain bed in an unsealed cylindrical store, to the more complex situation of a completely sealed or leaky grain storage silo subject to either fan forced or tablet fumigation.

The work begins by developing initial CFD simulation models to describe the flow of fumigant in a prototype geometry for a typical on farm silo, in the form of an unsealed open-top vertical cylindrical grain store. The objective is to understand the hydrodynamics of the phosphine gas during fan-forced fumigation, and the mainly advection driven flow is mathematically described as a porous medium using

either a Darcy or Navier Stokes model. These are implemented in the widely used Comsol and Fluent CFD solvers, respectively. The study also serves to compare the two CFD modelling approaches as a basis for adopting one of these (Fluent) for the later work. The results of this study are reported in the first of the three included papers, where the flow predictions are explored in detail to identify features such as high flow regions and zones in the grain storage that might provide refuge for breeding insects.

An additional study of fan forced fumigation of the open-top vertical cylindrical store is also included in this thesis, where the search for analytic solutions is now the main focus. To this end, the case of relatively low fan-forced fumigant injection velocities is modelled as Darcy flow in a porous medium. This study is reported in the second of the three included papers, where new closed form analytic solutions are derived for the pressure, velocity components and streamlines in the grain bed. These closed form solutions provide a flow description for a range of storage radius, height and circular or annular inlet conditions, from which traverse times describing the extent of the fumigant flow into the grain can be numerically computed. A leading order closed form expression for the traverse time is also obtained and found to be reasonable for inlet configurations close to the central axis of the grain storage. Results are interpreted for the case of a representative 6m high on farm wheat store, where the time to advect the phosphine to almost the entire grain bed is found to be approximately one hour.

In the final study reported in the third paper included in this thesis, the more complex situation of grain stored in a completely sealed or leaky silo is considered. For this study, a mathematical model is developed which accounts for the transport of a multicomponent gas phase, along with a grain phase. The model also accounts for sorption of phosphine into the grain kernels, along with insect extinction within the grain bed as a function of their exposure to the fumigant. The resultant mathematical model is implemented for numerical solution and subsequent analysis via a user modified version of the CFD solver ANSYS Fluent as a fully three-dimensional, compressible, multicomponent gas transport model.

For the case of the completely sealed or leaky silo, the two types of fumigation delivery are again studied, namely, fan-forced from the inlet at the base of the silo,

and tablet close to the grain bed surface within the silo. An analysis of the numerical simulations for a small scale on farm leaky silo shows that during fan forced fumigation, the position of the leaky area is very important to the development of the gas flow field and the phosphine distribution in the silo. For a typical silo and fan-forced fumigation strategy, there may, for example, be insufficient phosphine within the upper part of the silo to eradicate insects if the leak is located near the silo base, even after extended periods of fumigation. In contrast, during tablet fumigation the position of a leaky area has little effect on the phosphine distribution, and for fumigation in a typical silo configuration, phosphine concentrations remain low near the base of the silo. Furthermore, we find that a commonly used indicator of required dosage and dosage time, namely, the half-life pressure test (HLP), does not have any significant effect on the fumigant distribution during tablet fumigation. Overall, the results from this study for both fan forced and tablet delivery have implications of potential importance regarding the efficacy and efficiency of current on farm fumigation practices for stored grain.

Keywords

diffusion, advection, partial diferential equations, porous media, Darcy's Law, Laplace equation, Bessel function, mathematical modelling, fumigation, control volume method, computational fluid dynamics, streamlines, traverse time, incompressible flow, compressible flow, phosphine, grain storage, silo

List of publications & manuscript

The following papers are included in this thesis as chapters:

Chapter 3: **Z.M.Isa**, G.R.Fulford, N.A.Kelson. Simulation of phosphine flow in vertical grain storage: a preliminary numerical study. ANZIAM J., 2011, 52, C759-C772.

Chapter 4: **Z.M.Isa**, G.R.Fulford, N.A.Kelson, T.W.Farrell. Flow field and traverse times for fan forced injection of fumigant via circular or annular inlet into stored grain. Submitted to Applied Mathematical Modelling.

Chapter 5: **Z.M.Isa**, T.W.Farrell, G.R.Fulford, N.A.Kelson. Mathematical modelling and numerical simulation of phosphine flow during grain fumigation in leaky cylindrical silos. Submitted to Journal of Stored Product Research.

Acknowledgements

My deep and sincere gratitude to my supervisors, Assoc. Prof. Troy Farrell, Dr Glenn Fulford, and Dr Neil Kelson for their support, motivation and valuable advice throughout the course of my thesis work. Thank you for the patience and kindness in giving me continuous ideas and guidance that have been a major part in the success of this thesis. Without that, I would not have been able to complete my thesis. Also thank you to Professor Ian Turner who has always been available to advise me and provide assistance in numerous way.

Thanks to all the staff and friends in the School of Mathematical Sciences for helping me out all the time. Also to everyone in the High Performance Computing Group who give me advice in order to conduct my simulations.

I would also like to acknowledge Ministry of Higher Education, Malaysia and Universiti Teknologi Malaysia, Malaysia for the financial support in pursuing this doctoral study. The financial support of the Queensland University of Technology is also sincerely acknowledged.

Finally, a very special thanks to my husband, Masnizam who has always been full of patience, support, and encouragement. Also my thanks go to my children, Danial, Iffah, and Izwah for keeping my life happy and enjoyable. This thesis, and everything I do, I dedicate to my lovely family.

Contents

List of Figures

List of Tables

Statement of Original Authorship

The work contained in this thesis has not been previously submitted to meet requirements for an award at this or any other higher education institution. To the best of my knowledge and belief, the thesis contains no material previously published or written by another person except where due reference is made.

Signed: ___

Date: 16/7/2014

Chapter 1

Introduction

The research presented in this thesis investigates phosphine gas fumigation of wheat beds in unsealed, sealed and leaky grain storage, typical of Australian agricultural settings. The main body of the thesis is in the form of three research papers (Chapters 3 to 5) where computational fluid dynamics (CFD) simulation, analytical solutions, and mathematical modelling approaches are used to gain insights into the fumigant distribution with time under the various storage and delivery regimes. Two types of commonly used delivery method, namely fan forced and tablet fumigation, are considered in this work to investigate the hydrodynamic behaviour of phosphine gas in the stored grain. Overall, the work progresses from the simpler case of fan forced fumigation of a grain bed in an unsealed cylindrical store, to the more complex situation of a completely sealed or leaky grain storage silo subject to either fan forced or tablet fumigation. For the latter case, mathematical modelling is also developed to account for sorption of phosphine into the grain and bug extinction based on fumigant exposure. The resultant mathematical model is implemented for numerical solution and analysis via a user modified version of the CFD solver ANSYS Fluent as a fully three-dimensional, compressible, multicomponent gas transport model.

This introductory chapter provides an overview of the thesis and serves to motivate the research undertaken. Section 1.1 provides some background remarks on the research topic of grain fumigation and problems that are faced by the grain industry, with a more detailed review being deferred until the next chapter. In

Section 1.2, the research questions around fumigation practices and regimes are introduced that serve as the motivation to conduct this study. The specific aims and objectives are given in Section 1.3, followed by a statement in Section 1.4 of the importance and significance of the thesis contribution to the grain industry. Finally, in Section 1.5 a chapter by chapter outline of the thesis structure is presented.

1.1 Background

Wheat is Australia's major crop and major export grain [59] and contributes significantly to Australia's income. For example, in 2010-11, export earnings for Australia from wheat totalled $5,526 million [80]. The existence of insects, such as weevils, grain borers, beetles, moths, and booklice in grain storage affects the total amount of quality grain that can be exported and accepted by the customers. Thus, producing high quality wheat, by making sure that it is free from insects and damage, has attracted major attention.

During production, wheat is first transferred from a harvester to a terminal elevator or storage. In this thesis the main interest is on smaller scale Australian on-farm storage where the most common grain storage arrangement is in the form of a vertical or tower silo [156]. For this work, these are divided into two basic types, referred to as (a) unsealed or open-top silos, and (b) sealed or closed silos. In practice, silos are often not completely sealed, so the situation of an incompletely sealed silo due to leaks is also considered. Further details of typical on-farm grain storage and fumigant leakage are provided in Chapter 2.

During the process from harvesting to storage, wheat is exposed to the attack from grain insects which are present in the harvesting machinery and handling equipment, and transportation vehicles, or from insects that fly between farms and storage [43, 93, 159]. Furthermore, the contaminated wheat may remain in the storage from a few days to several years before entering the market [92]. During storage, insects cause damage directly by consuming large quantities of grain, producing water that contributes to mould growth, or leaving their dead body fragments in the grain mass [90]. This damage must be eliminated otherwise the

product will be rejected by most buyers and the export trade would be adversely affected. For these reasons, the Australian export standards (Export Grain Regulations made under the Custom Act 1901 – 1971) require zero live insects in commodities destined for export [42, 91, 157].

Several ways to kill the insects have been introduced, including: (i) cooling the grain with aeration, (ii) controlled atmosphere and (iii) thermal disinfestation techniques. The most common and cost effective method, however, is fumigation by chemicals such as phosphine, methyl bromide, and ethyl formate. Of these, methyl bromide used to be one of the most widely used fumigants due to its speed of action [115]. However, its use has ceased because of the adverse environmental impact. The 1987 Montreal Protocol on Substances that Deplete the Ozone Layer [77, 113, 136] allowed for critical use of methyl bromide up until 1 January 2005, after which it was completely phased out [26, 27, 83]. Another widely use fumigant is phosphine, which started with phosphine in solid formulation (i.e tablet) during the 1930s [53]. In the early 1980's, delivery via fan-forced fumigation using phosphine (PH_3) gas technology began. Due to the progressive phase-out of methyl bromide since the mid-1990s, the industry has become dependent on the use of phosphine [59, 77] to kill stored product insects and it has become established as the most relied upon and preferred fumigant in Australia [96, 154], being cheap, easy to apply, and leaving little residue in the grain [35, 43, 50, 60, 118, 132]. Its combined benefits relative to other available chemicals are such that, statistically over 80% of Australia's grain is fumigated with phosphine [71, 159]. In this thesis the focus is on the use of phosphine gas for fumigation with fan-forced and tablet methods of delivery.

In practice, grain insects may still be present in a well-managed storage system, even after many improvements in the processes of fumigation using phosphine have been achieved. As a result grain needs to be fumigated repeatedly, which may result in insects developing resistance to the fumigant. This failure and the development of insect resistance, have threatened the use and the sustainability of this valuable agrochemical. Already, a number of pest species have developed significant levels of resistance [61, 67, 59, 68, 91, 109, 122, 127, 133, 140, 146, 148, 147]. This situation is of concern to the industry since phosphine as a fumigant of choice is unlikely to

change in the next few years [117].

Owing to the high dependence on phosphine and the need for sustaining its use into the future, efforts to identify the causes of fumigation failure and the development of strategies for effective phosphine use amid the threat of insect resistance have started to take place. Central to these efforts is the need for a good understanding of how the fumigant behaves in grain storage and the factors that influence the distribution of the fumigant gas. Surprisingly, this understanding is currently lacking, as highlighted by the following statement [59]:

> *"Our current short-term priority is the control of phosphine resistance outbreaks, while our more strategic research is aimed at gaining a fundamental* ***understanding of fumigant behaviour in grain storages****, the movement and colonisation of grain by insect pests and the mechanisms of selection in insect populations information that will underpin the development of long-term resistance management."*
>
> *"Rapid, even application of fumigant to all parts of a grain store is fundamental to effective pest management and avoidance of under-dosing and the risk of selection for resistance.* ***Surprisingly little is known of the behaviour of fumigants in grain storages, however****."*

The importance of understanding the flow of the gas during fumigation has been highlighted in a more recent proposals to experimentally determine the movement of phosphine fumigant in large grain storages and to use the information to actively improve fumigant application (see e.g. [128]). However, performing appropriate field experiments to understand the fumigant flow behavior and concentration levels during fumigation is expensive to organize. Therefore, in this thesis the focus is on mathematical modelling and simulation as a cost effective approach.

A number of mathematical models have been developed on fumigation of stored grain and a detailed review of previous works is given in Chapter 2. Overall, comprehensive studies on the modelling of phosphine distribution in grain silos are lacking, regardless of the application method of fumigation. For example, spatial variations in fumigant concentration with time during tablet delivery are unrealistically ignored, or oversimplified approaches to leakage modelled as a constant is

used [16]. For tablet fumigation, previous work has not dealt with the common practice of placing the tablets on the grain surface. In addition, fan-forced fumigation in alternative geometries, such as those relevant to horizontal storage practices [55], and alternative storage contents, such as flour [112], has been investigated. However to date, a mathematical model of the distribution of phosphine gas, due to fan-forced application, in an on-farm, cylindrical silo has not been developed. Previous investigations also lack in the treatment of practical situations where the grain storage is closed everywhere, except at leaky holes where the fumigant gas can escape. A treatment of the fumigant as a multicomponent gas mixture where phosphine losses to sorption can be precisely accounted for has also been lacking. The term sorption is used here for the combined processes of adsorption and absorption, where adsorption refers to molecules of gas adhering to the surface of the material, and absorption is where gas enters into the cells of the material [125]. While sorption together with desorption and degradation of phosphine in wheat has been proven to occur [70, 72, 149] it is not considered e.g. as in one of the relatively small number of CFD studies in the literature [32]. Importantly, none of the theoretical modelling studies mentioned here and in more detail in Chapter 2 have tried to account for insect extinction.

The knowledge gaps identified above have motivated the development of the thesis, which aims to develop more comprehensive modelling that include key factors such as phosphine distribution, silo integrity (gas tightness), sorption of fumigant, and extinction of insects.

In this work, Computational fluid dynamics (CFD) software will be used to implement the modelling in stored grain for solution and subsequent analysis. The development of such a tool could play an important role in contributing knowledge in this field of research since the model can be adjusted to understand the behaviour for different fumigants, application regimes and storage geometry. Results obtained from the model will potentially improve fumigant application so that insect control is effectively achieved and selection for resistance is avoided.

1.2 Research questions

The work in this thesis attempts to provide answers to the following questions.

What is the hydrodynamics of the fumigant gas during fumigation?

During fumigation, the fumigant, which is normally placed in the grain silo in the form of solid (tablets), or pumped through an injection inlet as a gas (fan-forced) is dispersed in a gaseous form throughout the silo whether by natural convection or by the action of fans. For tablet fumigation, the main transport process for the gas flow is diffusion, while during fan forced flow, the diffusion may be less significant with advective transport dominating. The behaviour of fumigant hydrodynamics is very important to provide insight into where the fumigant can or cannot reach.

How does the half-life pressure test value (HLP) affect the fumigant distribution?

The silo must be sufficiently gas tight to retain a lethal concentration for a sufficient time. However, although silos are closed, most are not perfectly sealed and hence allow the fumigant to leak out during fumigation. The "leakiness" (or gas tightness) of a silo is characterized by a half-life pressure (HLP) test that is conducted before fumigation is started. Currently, the standard is a HLP of 5 minute for empty silos [154] and a 3 minute HLP for storage filled to capacity [11]. The importance of this value and its effect will be investigated in this thesis.

Does the position of a leaky hole affect the fumigant distribution?

Generally, the position of holes in the silo walls are not known prior to fumigation. We can, however, use numerical simulation to observe the phosphine distribution in silos having leaks in various locations. It is expected that changing the hole location will affect how uniform the steady-state phosphine concentration is, and how quickly this steady-state is approached.

Where are the areas in the grain storage that do not receive sufficient dosage?

In addition to leaks in the storage silos, phosphine is also lost due to absorption into the grain. Consequently, there may be areas of low dosage during fumigation and an understanding of where and when these occur is crucial. In addition, the development of a supplementary extinction model should assist significantly in identifying the storage areas that do not receive a sufficient dosage.

How much phosphine residue is in the grain kernel?

It is also important to know the amount of phosphine inside the grain kernels after fumigation. The maximum residue limit (MRL) for phosphine in raw cereal is recommended at 0.1 ppm by the Codex Alimentarius Commission of the World Health Organization (WHO) and Food Agriculture Organization (FAO) [7, 108]. By developing a multicomponent gas model that incorporates sorption into the grain, the phosphine inside the grain kernel can be predicted.

Ultimately, the answers to the above questions will assist us to obtain a good understanding of phosphine behaviour in grain silos. Such an understanding can help grain growers and silo manufacturers to design efficient and effective fumigation regimes which could lead to reduced costs and higher insect morbidity.

1.3 Thesis aims and objectives

The primary aim of this thesis is to develop mathematical models that facilitate the simulation of the flow of phosphine fumigant within small-scale (on-farm) grain silos under the regimes of fan-forced and tablet fumigation. Such models will allow us to extend our knowledge of such fumigation practices by providing a means for assessing hypotheses that many suggest new avenues of investigation. The specific objectives of the thesis are as follows:

1. To understand the hydrodynamics of fumigant transport in stored grain via:
   - the development of simple analytic models for the flow of gas in open-top silos,

   - the evaluation of relevant computational fluid dynamics packages for the implementation of flow field equations in open and closed grain storage systems.

2. To model the phosphine concentration field in a closed silo whilst accounting for the important factors that characterize realistic grain storage including:

   - gas leaks in the silo,
   - fumigant sorption and degradation,
   - high dimensional geometry of the domain,
   - the multicomponent nature of the fumigant gas,
   - the effect of the fumigant concentration field on the extinction of grain pests.

1.4 Contribution of the thesis

The contribution of this thesis can be divided into two main contributions relating to the analytic work, and the numerical work. An analytic solution [99, 100], exists that relates to the grain store geometries examined in this work. However, it is approximate only, and considers gas injected at the inlet of a cylindrical silo to be a point source rather than a finite size inlet. This thesis provides instead an exact and more general analytic closed form solution to this problem that accounts for a realistic fixed width circular and annular inlet geometry. The results of this analytic study provide information on the hydrodynamic behaviour of the gas in the investigated domains.

The numerical work involves the development of a full three-dimensional fumigant transport model. Previous models do not treat the fumigant as a multicomponent gas despite its potential to behave differently from a single mixture, especially the ability of phosphine to undergo sorption and degradation. The inclusion of a sorption term contributes to new knowledge concerning fumigant transport. Furthermore, the addition of an insect extinction model to predict areas of refuge

provides an initial attempt at addressing the question of insect resistance to fumigation.

The present mathematical modelling will generate information on the behaviour of fumigant gas in grain silos. Specifically, the thesis findings will result in the following contributions to the literature:

- An analytic solution to gas flow in a silo will provide a benchmark against which numerical simulations can be validated (in the future).
- The fumigant transport model provides a tool to predict the gas concentration within a silo during fan-forced and tablet fumigation, and could be extended to any storage shape.
- The fumigant transport model accounts for fumigant sorption which will provide a better prediction of the concentration distribution.
- The investigation of the effect of gas tightness within a silo will result in furthering our understanding of how the fumigant disperses and distributes in storage. In turn this will provide an insight into where in the grain storage, insects may find refuge.
- An extinction model provides a useful tool to determine possible areas within silos and under certain fumigation regimes, where insect extinction is incomplete.

As for the practical implications of this work, the results could be adopted for developing future fumigation design guidelines for the use of phosphine as an efficient fumigant in both fan-forced and tablet fumigation and hence, contribute to its long-term cost-effectiveness and sustainability.

1.5 Thesis outline

The thesis has 6 chapters with Chapters 3 to 5 in the form of published and submitted papers. An overview of the research work connecting the objectives and each of the chapters is depicted in Figure 1.1. A brief outline of each chapter is as

follows.

Chapter 2: Chapter 2 provides a detailed literature review of the work related to the thesis scope and aims. Initially, the chapter provides an overview of the grain fumigation systems and practices, specifically phosphine on wheat as well as the overview of the relevant grain pests. Explanations aim to provide basic knowledge concerning the fumigation practices and the issue of failure. Following this, an overview of previous mathematical modelling of stored grain is given in order to refine and identify the knowledge gaps in the current literature. The review is categorized into two sections, namely, a review of fumigant flow equations focusing on gas hydrodynamics, gas velocity and traverse time. This is followed by a review of mass transport modelling relevant to grain storage. In addition, some details of the mathematical models presented in this work together with an explanation of the assumptions used, are given. The chapter ends with some details of the widely used CFD solvers COMSOL and FLUENT which are utilized in this work.

Chapter 3: This chapter deals with gas flow modelling (velocity profiles) in a cylindrical silo (axisymmetric flow). The purpose of this work is to perform an initial study of advection-driven phosphine transport, and to this end we focus on a prototype geometry for a typical, cylindrical, farm silo. Knowledge of the flow patterns in stored grain are also used to gain an indication of the zones in the grain storage that might provide areas of refuge for breeding insects. The study also serves as a comparison exercise of the simulation results obtained using COMSOL Darcy flow and FLUENT Navier-Stokes solvers. The outcomes of this comparison serve as a basis for adopting FLUENT in subsequent work.

Chapter 4: This chapter also investigates gas flow in a cylindrical silo, however this time, analytic solutions are the main focus. The overall objective of this chapter is to extend the work of Chapter 3 in order to investigate fumigant flow for a circular and annular inlet. The specific aim of the chapter is to derive closed form analytic solutions for pressure, velocity and streamlines in a cylindrical silo for incompressible Darcy flow. From these closed form expressions for the traverse times

of the gas are then obtained. These exact analytic closed form solutions provide a detailed flow solution, and additionally can provide benchmark against which future numerical simulation models involving more complex physical processes or geometrical silo configurations could be validated.

Chapter 5: This chapter develops a three-dimensional mathematical model of fumigant transport in a cylindrical grain silo. The model takes into account key factors that are characteristic of this type of grain storage, including leakiness of the silo, sorption of fumigant, and extinction of insects. Two types of fumigant delivery are studied, namely fan-forced and tablet fumigation. Binary gas flow is modelled and a range of gas tightnesses and leak positions are investigated. The incorporation of an extinction model assists in effectively determining areas of insufficient fumigant dosage. Unlike Chapter 4, the aim of this Chapter is not to pursue analytical solutions of simplified model equations but rather to develop a more complicated and relatively complete model of an actual grain storage silo. Given the nonlinear nature of this model and the complicated domain on which it is defined, it is unlikely that closed form analytical solutions exist. Thus, a user modified version of the FLUENT CFD solver is used to implement the fully three-dimensional, compressible, multicomponent, gas transport model to study the phosphine concentration during fumigation as a function of space and time.

Chapter 6: Chapter 6 summarizes the outcomes of the thesis. In addition, several future research prospects are discussed.

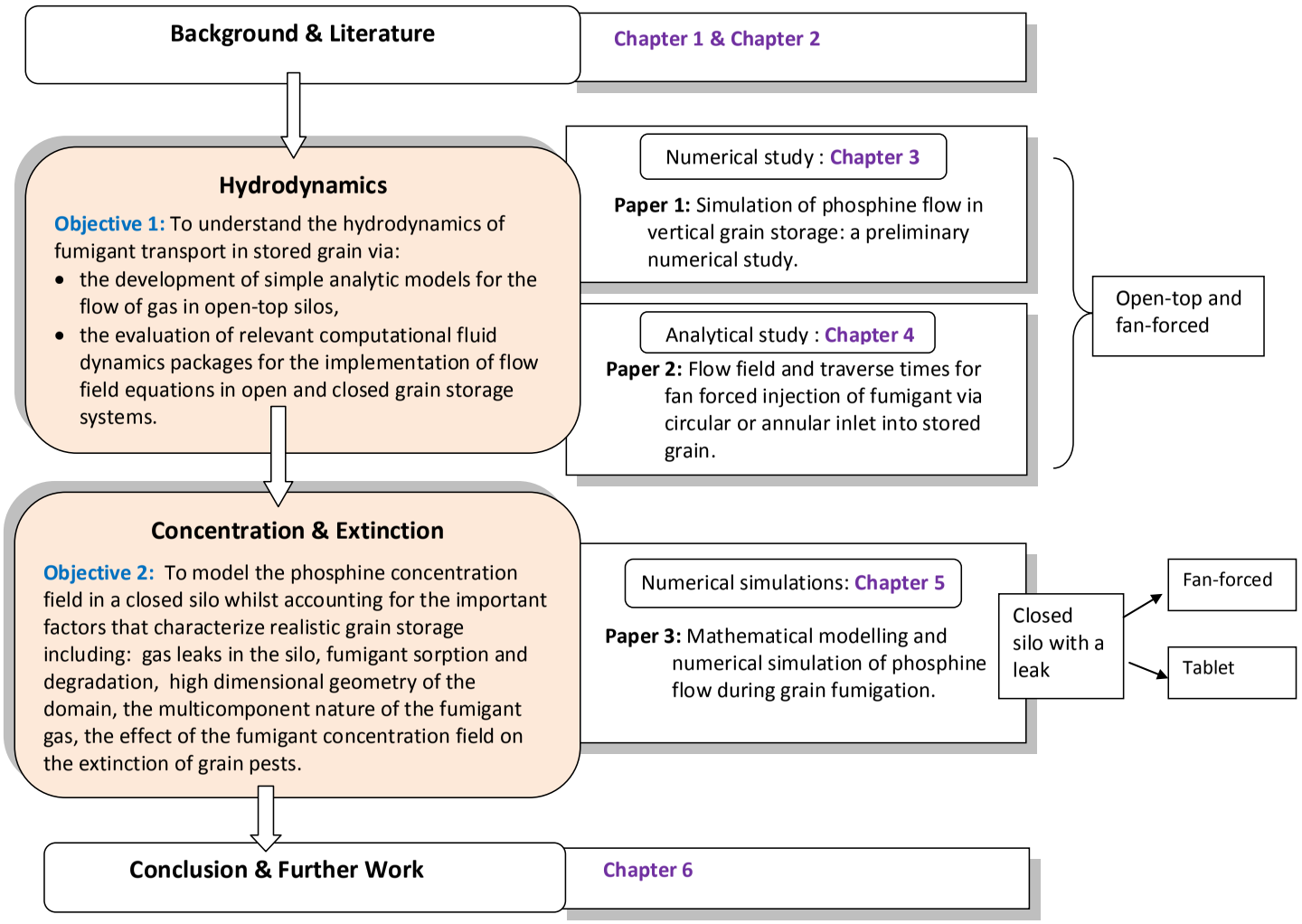

FIGURE 1.1: Overview of the research work.

Chapter 2

Literature review and the mathematical model

2.1 Introduction

This chapter provides a detailed literature review of the work relating to the thesis aims and identifies the knowledge gaps in the current literature. The review covers the target insects, the practical fumigation systems and the mathematical literature and methods. The mathematical modelling work presented in this thesis requires an understanding of transport, partial differential equations and numerical schemes. Thus, the remainder of this chapter is structured to provide a necessary understanding of this material.

2.2 An overview of the insects, fumigation practices and issues

Prior to investigating the fumigant movement in a silo, it is important to have an understanding of the insects that colonize the storage. Among the stored grain insects, the resistance to phosphine fumigant is highest in *R.dominicia* [61]. It is possible that this type of insect might not receive enough dosage since most of their developmental stage takes place within the grain kernel. In addition, the types of available storage, the fumigation method and the factors concerning fumigation failure are also reviewed.

2.2.1 Stored grain insects

In reality, grain is not totally undamaged when it enters the storage. The grain may have chipped seed coats, which occur during harvesting, handling or transportation [75]. Such damage also encourages insect attacks. The grain can be attacked externally or internally by several types of insect with different behaviour. The group of insects comprising external feeders like to feed outside the grain kernels causing damage externally. At the larvae stage, they produce silken threads that result in "caking" or "crusting" on the surface of the grain. Included in the external feeders group are saw-toothed grain beetles and flour beetles. Whereas, the internal feeders of insects deposit their eggs inside the kernels and remain in the grain kernel during the developmental stage until they reach the adult stage. Then, they chew their way out of the kernels [82]. Lesser grain borers and weevils are examples of insects in the internal feeders group.

Table 2.1 gives examples of some common stored grain insects.

Insect	**Description**
Flat grain beetle (*Cryptolestes pusillus*) 	• Pest capable of significant damage • External feeders

Lesser grain borer (*Rhyzopertha dominica*) 	• A very serious pest that is capable of rapid and extensive damage • 2–3 mm in length • Reddish-brown to dark-brown in color • Internal feeders • Adult beetles are strong flyers and live for 2-3 months • Life-cycle completed in 4 weeks at 35^{o}C and 7 weeks at 22^{o}C and stop below 18^{o}C • The most difficultinsect pests to control
Psocids (*Liposcelis spp.*), booklice 	• Pest capable of causing damage • Very small with 1 mm in length

Rice weevil (*Sitophilus oryzae*) 	• Major pest that is capable of rapid and extensive damage • 3–4.6 mm in length • Internal feeders • Larvae spin webs on the grain surface and consume kernels within the webbing • Adults live two to three months on average
Saw-toothed grain beetle (*Oryzaephilus surinamensis*) 	• Major pest that is capable of rapid and extensive damage • 1.7–3.2 mm in length • External feeders • Adults live six to 10 months on average

TABLE 2.1: Common grain storage pests [90, 93, 82, 78]

The insect's life cycle consists of four stages, egg, larvae, pupae and adult as depicted in Figure 2.1. On average, stored product insects spend 61 - 79% of the time in the larval stage [93] and the time required for the complete life cycle ranges between 26 days to 9 weeks [79]. While the larvae and adults are mobile, eggs and pupae are not. The temperature is known to influence the rate of development and reproduction of the insect [116]. For example, Table 2.2 provides data for the egg to adult developmental times for five different species.

During fumigation, poisonous gases enter the bodies of the insects mainly

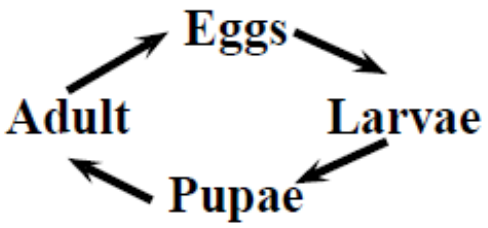

FIGURE 2.1: Life cycle of insects.

through the respiratory system [53]. Therefore, the uptake of fumigant is generally proportionate to the rate of respiration. Same as the rate of development, the rate of respiration of insects is largely dependent on grain temperature [46, 51]. Among all the stages, the egg and pupae are harder to kill their immobility which lowers the respiratory rate [28, 37]. Meanwhile, beetles and other insects that develop outside of the grain kernels are usually more susceptible to fumigants than certain moths and beetle species that develop inside the grain kernels. The biochemical aspects and the toxicity process of fumigant on grain pests can be sought from [38], [39], [52], [53], [114], [129] and [130]. Specifically, *Sitophilus oryzae* and *Rhyzopertha dominica*, it is known that insects at all stages of maturation survive longer at a given temperature, with *R. dominica* being more resistant to fumigation than *S. oryzae* [24].

Phosphine is a comparatively slow-acting poison [61]. Therefore, for a complete kill, insects should be exposed to a lethal dose for a sufficient time. A mortality of less than 90%, is regarded as a failure. In practice, mortalities after treatment should exceed 99%, or even 99.9%, for the results to be considered satisfactory [95]. The equation describing the relationship between the concentration (C) and time of exposure (t), also known as Haber's rule [14, 18, 25, 61, 158], is given as

$$C^n t = k,$$

where n is the toxicity index, a measure of the relative importance of fumigant concentration and k is a constant. There are two indicators that are usually used

	Temperature (^{o}C)							
Insect species	**20**	**22.5**	**25**	**27.5**	**30**	**32.5**	**35**	**37.5**
C. ferrugineus	...	53.4	37	28.1	23.2	20.6	19.0	18.2
O. surinamensis	...	48.5	36.4	27.9	22.4	19.8	20.8	27
R. dominica	...	...	58.8	49.9	42.4	36.1	31.0	...
S. oryzae	52.9	43.2	35.9	30.6	27.4	26.7	29.1	66.7
T. castaneum	...	...	41.8	32.7	28.4	26.3	23.4	21.7

TABLE 2.2: Egg to adult developmental times, in days at different temperature[93].

to determine the efficacy of fumigation, namely, the time required to kill 99.9% of the insect population (or lethal time, $LT_{99.9}$), and the time to total population extinction (TPE). The $LT_{99.9}$ value assumes a possibility of 0.1% of live insects remaining at a certain phosphine concentration and exposure time, whereas TPE guarantees no emergence of live insects. Table 2.3 provides TPEs for some common insects. The findings from [61] show that the relationship between concentration and exposure period for the strongly resistant *Rhyzopertha dominica* is $C^{0.6105}t = 4.0404$ (C in mg/L and t in day). These particular values of constants n and k will be adopted in Chapter 5 of this thesis.

The mortality of the insects depend significantly on temperature [24, 63, 76, 151, 151] as can be seen in the Table 2.3. This is because the body temperature of the insect follows their surrounding temperature [75]. This temperature has a high effect on insect development, as mentioned above, and the stages in which insects are harder to kill (namely, egg and pupae) can become prolonged. As a result, the ability of an insect to survive depends upon the surrounding temperature.

Insect species	**Fumigation condition**	$LT_{99.9}$ (day)	**TPE** (day)	**Remark**	**Reference**
Rhyzopertha dominica	0.2 mg/L at 25^{o}C		14	high resistant strain, mixed age	[61]
	0.3 mg/L at 25^{o}C		10		
	1 mg/L at 25^{o}C		5		
Rhyzopertha dominica	0.04 mg/L at 25^{o}C		13	weak resistant strain, mixed age	[61]
	1 mg/L at 25^{o}C		4		
	1.5 mg/L at 25^{o}C		2		
Sitophilus oryzae	0.02 mg/L at 25^{o}C	27		resistant mixed age	[67]
	0.02 mg/L at 25^{o}C	8		susceptible mixed age	
	1 mg/L at 25^{o}C	4		mix of resistance and susceptible, mixed age	
L. bostrychophila	0.1 mg/L at 15^{o}C		19	all life stages,	[118]
	1 mg/L at 15^{o}C		11		
	0.1 mg/L at 35^{o}C		4		
	1 mg/L at 35^{o}C		2		

TABLE 2.3: Mortality based on $LT_{99.9}$ and TPE from reported works.

2.2.2 Grain storage types

Grain storage comes in a wide range of sizes and shapes. Some are permanently built and others are constructed prior to storage. The total load capacity varies, with some examples given in Table 2.4. At the farm, grain storage is generally small-scale with sizes ranging between 15 t and 3000 t [156]. Permanent storage includes horizontal sheds with a concrete floor and steel or timber frame walls and vertical, concrete or steel silos. Silos are the most common grain storage, constituting 79% of all on farm grain storage in Australia.

Location	**Storage description**	**Remark**
Apamurra	3,300 t steel bins 1,500 t concrete vertical 5,000 t unsealed shed 40,000 t bunker	Adelaide workshop
Melrose	20,000 t shed	[111]
Port Kwinana, Perth	300,000 t shed	[97]
Merredin, Western Australia	240,000 t shed	[47]

TABLE 2.4: Examples of large grain storage capacity available at bulk handling facilities in Australia. On farm storage is much more smaller ranging between 15 t - 3000 t [156].

Temporary structures are necessary when available storage capacities are likely to be exceeded. Options for temporary storage include grain bags, ground dumps and bunker storage. Usually, they are formed on a ground sheet and covered with protective sheeting. The risk of damage by water, insects, animals and moulds is greater than for other fixed storage types. Bunkers conctitute 12% and grain bags, 9% of all on farm grain storage in Australia [156]. Pictures of various storage types are provided in Figure 2.2.

(a) Shed

(b) Vertical steel silo

(c) Bunker

(d) Grain bags

FIGURE 2.2: Storage types examples (images retrieved from the internet).

2.2.3 Phosphine application practices

Grain fumigation is the process of adding a chemical, called the fumigant, to the grain storage with the objective of killing the insects. In addition to phosphine, sulfuryl fluoride, carbonyl sulphide and ethyl formate are examples of some of the fumigants. At room temperature the fumigants are in a gaseous form. Phosphine is colourless and odourless at concentrations of up to 2 ppm [154]. It has a similar density to that of air (relative density 1.13:1) [53]. Phosphine can ignite spontaneously in air at concentrations over 18,000 ppm [47, 96]. Synonyms for phosphine include hydrogen phosphide and phosphorated hydrogen [110, 138]. The following specifically explains the application of phosphine. There are two common methods

of phosphine application during fumigation, which are described below.

(a) Cylinder-based (fan-forced)

In cylinder-based fumigation gas is released from a cylinder containing phosphine, sometimes mixed with carbon dioxide or nitrogen. The most common gas formulations available in the market are ECO$_2$Fume [1] and VaporPH$_3$OS [2, 65]. ECO$_2$Fume (previously known as Phosfume) was patented by BOC Gases of Australia [48]. It is a mixture of 2% phosphine and 98% carbon dioxide (CO_2) by weight making it a non-flammable and ready to use fumigant [47]. Delivery of phosphine into the silo requires dispensing equipment that allows the user to control the dispensing rate. On the other hand, VaporPH$_3$OS is a pure phosphine formulation of 99.3% phosphine by weight. This pure phosphine must be used with special blending equipment to dilute the phosphine to the desired concentration with either carbon dioxide (CO_2) or air. When blended with CO_2, the final product is similar to the ready to use ECO$_2$Fume [2] gas mixture. A clear advantage of the on site blending of VaporPH$_3$OS is that it greatly reduces the number of cylinders that are required.

Siroflo [111] is a cylinder based fumigation method that involves the mixing of fumigant with air by injecting phosphine from the cylinders into a fan supplied air stream and blowing continuously into the grain silo at a controlled rate. The fumigant is applied at a low concentration for a relatively long period of time. Further technical aspects of Siroflo can be obtained from [111, 120, 139, 152]. Sirocirc is identical to Siroflo except that it incorporates a recirculation system consisting of ducting that connects an outlet on the roof of the silo to a fan at the inlet near the base of the silo. Such system is also known as closed loop fumigation (CLF). The fumigation recirculation procedures can be obtained in [106, 123, 139, 163].

In cylinder-based applications, the cylinder is connected to the grain storage through a system that consists of an inlet duct, mixing/blending equipment and designed metering orifices to control the concentration. The gas is mixed/blended to the intended concentration and blown continuously into the mass grain with the

help of a fan through the duct, generally located near the base of the silo [120]. Available blending equipment has the capability of dispensing phosphine with the rates shown in Table 2.5.

Mass flow rate	**Remark**	Reference
1.2 kg/hr	HDS 80,	[47]
3 kg/hr	HDS 200,	[47]
12 kg/hr	HDS 800,	[47]

TABLE 2.5: Available blending equipment capability. HDS stands for Horn Diluphos System; a commercial blending system developed in 2001 [97].

Cylinder-based fumigation is normally used at bulk handling facilities with a large grain volume capability. On farm fumigation most commonly uses solid formulations, which are described below.

(b) Solid application

Solid applications may exist in the form of a tablet, pellet, blanket, or a bagchain. The fumigant is usually present as either aluminium phosphide or magnesium phosphide [84, 137]. Commercial names include Phostoxin, Gastion, Detia, Gas XT, Fumitoxin, quickphos, and celphos. Normally, the chemical is placed in an open container or tray, attached to a rope and hung above the grain surface. Otherwise, it is placed directly on the surface of the grain or inserted into the grain using a commercial probe. The solid formulation will start evolving fumigant as soon as it is exposed to the moisture in the air. The breakdown of the solid starts slowly, gradually accelerates, and then tapers off [41, 84, 160]. Some examples of solid application are shown in Figure 2.3.

The tablet evolution rate varies depending on the type of formulation, moisture and temperature. If the moisture content and temperature are high ($24 - 29\,^{\circ}\mathrm{C}$), aluminium phosphide formulations evolve completely within three days [40], or

in about 70-90 hours [124]. Tablets are 3 g in weight and each can produce 1 g of phosphine gas [15, 138]. The recommended application rate is two tablets (2 g phosphine) per tonne of storage capacity to obtain a concentration of 200-300 ppm, one bag chain per 60 t, or a single blanket per 600 t [154].

(a) Tablets on tray (b) Bagchain in headspace

FIGURE 2.3: Solid formulation [4]

During the fumigation period, the concentration within the grain is monitored regularly. With cylinder-based formulations, the dosage can be adjusted from time to time to be above the minimum concentration. However, with a solid formulation, the dosage should be carefully determined prior to application, which takes into account such factors as sorption and leaks. This is because phosphine is a poisonous gas and humans should not enter the storage to add tablets/pellets if undesirable concentrations are detected.

For successful insect control in grain storage, the phosphine must be effectively distributed to all areas of the silo and kept in contact with the insects for a sufficient time at the required concentration. If this does not occur, then there will be potential zones that can provide areas of refuge where the insects can survive and breed. However, this does not mean that one can fumigate using a very high concentration for a short time. This is because phosphine is slowly absorbed by insects. Therefore, high concentrations may not increase toxicity, but, instead may cause insects to go into a protective narcosis [40]. Moreover, phosphine is also toxic to humans. At high concentrations, it has to be handled with care and can pose a

serious threat to the workplaces around silos and in the surrounding environment. The recommended dosage are given in Table 2.6 with the highest recommendation being 700 ppm.

Recommended dosage	Year	Remark	Reference
min of 100 ppm for 14 days	1998	$15-20^{o}$C	[111]
min of 215 ppm for 10 days	2006	$25-29^{o}$C	[47]
min of 360 ppm for 7 days		$25-29^{o}$C	[47]
min of 700 ppm for 5 days		$25-29^{o}$C	[47]
min of 300 ppm for 7 days	2007		[43], [154]
min of 200 ppm for 10 days	2007		[43]
100 ppm for 21 days	2009		Adelaide workshop
70 ppm for 28 days			Adelaide workshop
350 ppm for 10 days			Adelaide workshop
700 ppm for 7 days			Adelaide workshop

TABLE 2.6: Recommended dosage.

2.2.4 Factors affecting fumigation failure

Phosphine fumigation failure is generally caused by the fumigant not being retained for long enough at the desired concentration [15, 28]. Either the distribution of the gas is poor or where the distribution is good enough, the gas is not retained for a sufficient time [155]. The possible conditions that provide poor distribution and insufficient dosage are silo leakage and fumigant sorption in the grain. Furthermore, the emergence of resistant insect strains makes it harder to successfully fumigate. The following gives further explanation on the factors for fumigation failure.

(a) Sorption

Fumigant sorption between the phosphine gas and the grain kernel has been proven to occur by several authors [17, 20, 31, 30, 49, 69, 82, 108, 134, 135, 149, 138]. In addition, phosphine degrades, through reaction with air into other substances. Sorption reduces the amount of phosphine available in the inter-granular air for killing insects and may cause the phosphine concentration to decrease below the lethal dosage before all the insects are killed.

(b) Leakage

Fumigant is also often lost through leakage due to holes, cracks and crevices within the storage structure [64]. Leaks commonly occur at the bottom outlet, at the aeration inlet seal, via damaged lids, between the bottom cone or base and the silo wall joint at the roof and wall joint, and where the lid ring joins the roof [154]. The importance of sealing has been consistently discussed in the literature [13, 112, 121, 131, 156] and demonstrates that leaking is one of the major causes of fumigation failure. Moreover, during a fumigation trial in a silo with small leaks, a phosphine concentration as low as 3 ppm was found close to a leaking hole with the remaining area also suffering from reduced gas level [154]. Therefore, to retain a lethal concentration for a sufficient time, the storage must be sufficiently gas tight.

The gas tightness of the silo is determined by a half-life pressure test value (HLP). When a pressure test is undertaken, the time taken for a fall of oil level in the pressure relief valve from 25 mm to 12.5 mm is noted (i.e. from a gas pressure of 250 Pa above atmospheric pressure to a pressure of 125 Pa above atmospheric pressure). Only silos that pass a predetermined value are categorized as truly sealed [154]. The standard is 5 minutes for empty silos [154] and 3 minutes for storage filled to capacity [11].

(c) Insect resistance

The effectiveness of phosphine can be reduced considerably by the development of resistance in insects. A number of pest species have developed significant levels of resistance to phosphine [29, 50, 58, 59, 60, 61, 66, 91, 122, 127, 140, 148]. In

Australia itself, strong resistance to phosphine was first detected in 1997 in *R. dominica*, followed by *T. castaneum* and *Oryzaephilus surinamensis(L.)* in 2000, *Cryptolestes ferrugineus (Stephens)* in 2007 and in *S. oryzae* in 2009 [59]. Some insects are considerably more tolerant to phosphine than others. Among the stored grain insects, the resistance is highest in *R. dominicia* [61].

Two major factors that cause the development of phosphine resistance in grain insects are:

- Under dosing due to an insufficient application rate, uneven distribution of fumigant within storage, poor sealing of the structure, insufficient fumigation period, external environmental conditions, or grain temperatures that are either too high or too low for the dose to be effective.

- Multiple fumigations due to repeated fumigation with phosphine of the same bulk of grain. The outcome of this practice is the repeated exposure of the same insect population to phosphine. Every application, particularly where there is a risk of under-dosing, can potentially build up resistance.

Obviously silo leakage contributes to under dosing. Thus, the behaviour of phosphine flow in leaky silos is crucial to understand.

The necessity for the improvement in grain fumigation has motivated a number of theoretical studies to date. Sections 2.3 and 2.4 review these previous works. The review initially comprises the modelling of the fumigant flow involving only the gas velocity, streamlines and traverse time, and subsequently in Section 2.4, the review focuses on the modelling of fumigant transport for concentration distribution.

2.3 A review of the mathematical modelling of fumigant flow

This section presents an overview of the reported mathematical models of fumigant flow in a grain storage. This review has motivated the development of the articles in Chapter 3 and 4 of this thesis.

The flow in grain is considered as porous media flow where over the full range of velocity, the pressure gradient satisfies Darcy's Law, namely [23],

$$\boldsymbol{v} = -\frac{k}{\mu}\boldsymbol{\nabla} p, \tag{2.1}$$

where p (Pa) is pressure, $\boldsymbol{v}$ (m/s) is velocity, μ (kgm^{-1}s^{-1}) is the viscosity of the gas and k (m^2) is permeability. This has been used by most researchers [100, 126, 143, 144, 161] for modelling gas flow in grain storage. Usually, simplifying assumptions, such as assuming that the gas is incompressible ($\boldsymbol{\nabla} \cdot \mathbf{v} = 0$), are made to reduce the complexity [73, 89, 100, 143, 144]. Combining (2.1) with the incompressibility assumption yields Laplace equation for the gas pressure, namely,

$$\boldsymbol{\nabla}^2 p = 0. \tag{2.2}$$

The solution to (2.2) for pressure p facilitates the determination of $\boldsymbol{v}$ in (2.1). From the literature, reported works differ in the dimension of the spatial domain (1, 2 or 3-dimensional), and the method of solution. In terms of boundary conditions, the following are always implemented:

1. The gas enters the grain mass through the inlet with constant pressure [89, 142, 144] or constant volumetric flow rate [100].

2. The surface of the grain, where the gas exits, is considered as having atmospheric pressure [89, 142, 144]. This boundary condition is reasonable for open-top storage but not for closed storage.

3. The walls are impermeable to the flow, $\boldsymbol{\nabla} p \cdot \boldsymbol{n} = 0$, where $\boldsymbol{n}$ is a unit vector normal to the wall.

An analytic solution for calculating the pressure drop within grain storage was obtained in [99] for planar two-dimensional flows. The pressure drop was calculated using a conformal mapping approach. However, the pressure solution is not further used to obtain the velocity profiles.

Formulae for traverse times were later developed in [100] for a few particular geometries, including some of the plane flows in [99]. For a circular cylindrical store, having a conical base, a traverse time was also obtained but the solution was only

an approximation. This is because [100] combined an approximate expression for the traverse time on the centre line and also along the x axis to give the solution for the entire field. In addition, the inlet was treated as a point source.

A Darcy flow in a rectangular bin studied in [100] was further studied in detail in [89]. They reproduced the analytic solution in [100] for pressure, velocity, streamlines, and traverse time for a bin of infinite height. Then, a bin with a finite height was analysed. It was found that their solution for a semi-infinite height is accurate for all bins with a height greater than 1.25 m. However, once again, the gas that entered the bin was also treated as a point source inlet at the floor centre and furthermore the storage is assumed to have two-dimensional rectangular geometry. The flow was also extended to solve Ergun's equation [89, 73] by using perturbation expansions and the finite difference method. An analytic solution to this Ergun flow problem was later obtained by [73], but by reducing the two-dimensional flow to unidirectional flow instead.

Conformal mapping was also used in [144] to obtain the gas pressure via solution of Laplace's equation. The geometry considered was also a rectangular symmetrical bin. However, different from [100] and [89] was the inlet where the gas entered the bin was treated as a finite curved shape instead of a point source. They also gave a formula for the stream function and the air traverse time.

To solve the airflow in a two-dimensional, rectangular drying bin with a curved bottom, [126] also used a conformal mapping approach. The physical plane was transformed onto a reference plane, and then they numerically solved the mapping equations. They only considered Darcy flow.

Numerically, using the finite element method, [142] studied two-dimensional Ergun flow. The geometry considered had a triangular cross section with a triangular inlet.

In all the above studies, the grain storage was modelled either as a two dimensional rectangular or cylindrical geometry, while the flow was based on Darcy flow (velocity proportional to pressure gradient) or Ergun flow (Darcy flow with a square velocity correction). For mathematical convenience the analytical works mentioned above treated the inlet as a point source, which is not readily achievable in practice for real farm silo flows. Also, the most relevant of these prior studies

([100]) only considered a centrally positioned inlet attached to the cylindrical silo base, from which only approximate closed form solutions could be obtained. Therefore, as a more realistic approach, the mathematical analysis undertaken in this thesis work considers a physically realisable finite size inlet which, additionally, can be arbitrarily positioned at any radial location on the base of a cylindrical geometry. The use of a finite width inlet in the mathematical model also results in exact closed form solutions for a cylindrical silo of arbitrary radius and height. The resulting flow solutions allow for the effects of these various geometric changes to be investigated, as presented and discussed later in Chapter 4.

2.4 A review of the mathematical modelling of fumigant transport (concentration)

Here we initially review the previous literature on mass transport in grain silos before concluding with a summary of the key knowledge gaps in this area.

To date, there have been a number of studies investigating fumigant concentration in grain storage during fumigation. The reported models differ in the use of storage geometry (1,2 or 3-dimensional), the method of solving the governing equations and the fumigation methods that have been modelled. Some studies focus on the use of dry ice as a fumigant, which sublimes into CO_2 [8, 9, 143, 145, 161], while others have studied phosphine gas fumigation generated by tablets of metallic phosphide [16]. Fan forced fumigation was first introduce in the 1980's and to date, very few theoretical studies have been conducted [112].

Solid application of fumigant involves sublimation of tablets (or pellet or bag chains) into gas in the first stage and distributed through diffusion and advection. In cylinder-based application, gas is injected directly into the silo from a gas source assisted by a fan. For both types of fumigant application, the general form of the mass conservation equation that governs the gas transport is

$$\frac{\partial C}{\partial t} + \boldsymbol{v} \cdot \nabla C = D\nabla^2 C - S \tag{2.3}$$

where C is the fumigant gas concentration, $\boldsymbol{v}$ is the gas velocity, D is the diffusion

coefficient and S is a source term. For this equation, most studies impose the following boundary conditions:

1. The gas enters the grain mass through the inlet with constant or time varying concentration [9, 8, 145].

2. The grain surface is considered as having constant concentration [9, 8], zero for infinite height [145] or $\partial C/\partial n = 0$ if the grain is covered with a plastic sheet [9, 8].

3. The walls are impermeable to flow, $\mathbf{J} \cdot \mathbf{n} = 0$, where $\mathbf{J}$ is mass flux of gas and $\mathbf{n}$ is a unit vector normal to the wall.

In the models of fumigant transport in grain storage to date, simplifying assumptions have been made to reduce the complexity including; ignoring gas sorption [143, 161], assuming sorption is a constant [16], assuming that the storage is open-topped [8, 9], assuming that fumigant leakage is at a constant rate per day [16] and assuming the fumigant to be a single component gas [16, 8, 9].

Various approaches have been developed and introduced to solve (2.3). Analytical solutions were obtained by simplifying (2.3) to a one dimensional problem with $\boldsymbol{v} = 1$ [145]. Others wrote their own computer code based on the finite element method [9, 8]. For more complex problems, commercial pde solvers were the preferred choice [112].

In this thesis, we focus on phosphine fumigation in a cylindrical silo. However, the reviews on CO_2 will also be included here as these studies should provide a theoretical understanding of gas transport in bulk grain, the results of which are applicable for phosphine gas.

A study in [16] proposed a mathematical model to predict the average phosphine concentration over time, in three types of storage filled with wheat under metallic phosphide fumigation (tablet). The model did not account for an advection diffusion equation, instead it used a simple time step calculation where a spatially independent phosphine concentration was updated at each time step. Thus, at any location in the storage, the predicted phosphine concentration is the

same, which is not physically realistic. Although leakage and sorption were also accounted for, they were both modelled as constants.

The movement of CO_2 in a cylindrical silo was studied in [9]. CO_2 gas was generated from dry ice and fed into the silo through an inlet at the silo's base. Three different inlets, consisting of a circular geometry at the centre line, rectangular floor opening and circular geometries near the wall, were investigated. The transport equation was modelled as a 3-dimensional diffusion equation and was solved using the finite element method. This diffusion only model predicted much lower CO_2 concentrations when compared with experimental data at every sampling point and at all times. The inaccurate predictions were attributed to the mass displacement when the dry ice sublimated into CO_2. The model was modified to incorporate an empirically derived "apparent flow coefficient", of the form $D_{app} = a + b\ln(t)$ where $a, b =$ constant, for the initial 3 hours of the simulation. The diffusion model with the apparent flow diffusion coefficient improved the predicted concentration distribution, however, large errors were still observed during the first 3 hours. The authors showed that the model predictions were further improved when sorption of CO_2 into the wheat was included.

The work in [9] was further studied in [8]. This time, the diffusion coefficient was replaced by the effective diffusivities in the longitudinal, D_L (m^2/s) and lateral D_T (m^2/s) directions during the ice sublimation period (first 3 hours) as follows;

$$D_L = \frac{1}{2} v L_g \left(\ln \frac{3 v \tau_0}{L_g} - \frac{1}{12} \right),$$

and

$$D_T = \frac{3}{16} v L_g.$$

Here, L_g (m) is the grain size, v (m/s) is the Darcy velocity created due to sublimation of dry ice into gas, and $\tau_0 = L_g^2/2D_m$ (1/s), with D_m (m^2/s) is the molecular diffusion. The velocity was calculated using the formula

$$v = (\frac{\Delta p}{A})^{1/B},$$

where p is pressure and A and B are empirical constants. The pressure created by the sublimation was calculated using the universal gas equation. The predicted concentrations were observed to be close to the experimental data for times greater

than 12 hours, however for initial sampling times, the errors were still high. The possible reasons for the errors were suggested as being due to inaccurate calculation of the velocity and also due to the effect of gravity, which was not included in the model.

The modelling of the movement of CO_2 by advection, diffusion, and sorption was also investigated in [143]. A silo with a circular inlet on the centreline was studied. The advection was modelled using Darcy's law while the diffusion coefficient was taken to be a function of time. The model predictions were compared with the experimental data and found to be in reasonable agreement.

Perturbation methods were used to obtain a semianalytic solution to the advection-diffusion of CO_2 in a cylindrical storage [145]. The governing equation (2.3) was reduced into a 1-dimensional problem and the advection velocity was set to $\boldsymbol{v} = 1$, for simplification.

By simplifying mass transport as a 1-dimensional advection-diffusion problem, [161] modelled the CO_2 distribution through connected columns of hot and cold wheat. Again, the pressure gradient was used to calculate the velocity according to Darcy's Law, however, the transport equation did not account for sorption.

A fumigation method, with fan forced application and recirculation, was proposed in [112] for combating dilution in a horizontal storage. The phosphine distribution in a domain that had eight injection inlets and eight suction outlets was simulated using the CFD package CFX. Leakage of gas was modelled as a thin layer near the leakage points with a porosity of 0.005. The aims were to study the effect of external air flow over the outside of the storage on phosphine concentration within the storage. The fan speed and the rate of gas input varied over time for 26 days. The new system was found to preserve phosphine concentrations at all locations, including the bulk periphery.

A CFD (FLUENT) simulation to predict fumigant distribution and leakage in a flour mill during a 24-hour, fan circulation assisted, sulfuryl fluoride fumigation was conducted in [54], [56] and [57]. The model was divided into external and internal flow models. The external flow model was set up as a rectangular volume that contained buildings in a grain processing facilities. The resulting pressure on the walls was used to provide an input pressure to the internal flow model in one

of the mill buildings. The simulation results showed minor discrepancies from the experimental concentration data acquired in [55].

The previous modelling works on fumigant distribution in stored grain are summarized in Table 2.7. In conclusion, studies on the modelling of the fumigant distribution have general focused on CO_2. The only modelling for phosphine gas as conducted in [16] using an overly simple transport model and a tablet application technique. Furthermore, transport modelling for phosphine gas using fan forced application in a cylindrical storage has not yet been studied.

Experimentally, phosphine gas distribution has been studied in [21, 35, 42, 49, 105, 157]. The experiments conducted in [157] involved fumigation in a large scale silo using phosphine gas that was generated by an aluminium phosphide blanket. The blanket was introduced at the top of a sufficiently gas tight, vertical steel bin, filled with wheat. Phosphine gas was observed to be released immediately following the introduction of the blanket. The time taken for the gas to distribute to all areas of the bin was found to be dependent on the temperature gradient within the grain. During summer or early autumn, the phosphine reaches the base of the bin in 120 hours, while during late autumn and winter, it only took 48 hours.

The authors of [35] studied a system that could assist phosphine distribution during tablet fumigation in which tablets were placed on the surface of the grain of a tall concrete silo. The system consisted of recirculation ducting that drew the gases downward and returned them through an external duct to the headspace. The system appeared to be practically successful in that a good distribution of phosphine was achieved.

As noted earlier, in this thesis we develop a comprehensive model of the transport of phosphine in a small-scale (on farm) cylindrical silo. The model will account for tablet and fan forced fumigant application, the multicomponent nature of the fumigant gas mixture, sorption of phosphine into the grain kernel, degradation of phosphine in air, the leaking of gas from the silo and the extinction of grain pests. To date, no such comprehensive model, incorporating all these features, exists for small-scale grain storage.

Author	**Fumigant**	**Method**	**Features**
[16]	phosphine (tablet)	Stepwise calculation using Excel	1D, tablet only, numerical only
[145]	CO_2 from dry ice	analytic	1D, analytic, tablet only, assume $\|\boldsymbol{v}\| = 1$
[161]	CO_2 from dry ice	finite difference method written in FORTRAN	1D, tablet only, numerical only
[143]	CO_2 from dry ice	numerical	2D axisymmetric, tablet only, numerical only
[9],[8]	CO_2 from dry ice	Finite element method written in FORTRAN	3D, tablet only, numerical only, single mixture, nil grain adsorption, unsealed
[112]	phosphine (fan-forced)	CFX	unknown modelling approach, unconventional storage configuration
[10]	sulfuryl fluoride	FLUENT	3D simulation,single mixture, include leaking, flour mill building
[54], [56] and [57]	sulfuryl fluoride	FLUENT	single mixture,rectangular volume of a mill building,

TABLE 2.7: Summary of previous modelling work related to fumigant distribution in grain storage.

2.5 Supplementary modelling material and modelling assumption

In this section we expand on component of the mathematical model introduced in Chapter 5. In addition we introduce an expanded discussion of the key assumption of the modelling work of this thesis. This expanded material is designed to supplement the more succinct discussions of such given in Chapters 3, 4 and 5 that follow.

The sorption of gas into the grain kernel is a component of the transport model introduced in Chapter 5. The sorption model given in Chapter 5 is due to [70] and [72]. These researchers have suggested that the relationship between the fumigant concentration in the interstices between the grain, C_{ph}, and the average concentration of fumigant within the grain kernel $\overline{q}$, is modelled by

$$\frac{\partial C_{\text{ph}}}{\partial t} + B_1 C_{\text{ph}} - B_2 \overline{q} = 0 \tag{2.4}$$

and

$$\frac{\partial \overline{q}}{\partial t} + B_3 \overline{q} - B_4 C_{\text{ph}} = 0. \tag{2.5}$$

The coefficients B_1, B_2, B_3, and B_4, are independent of C_{ph} and $\overline{q}$. The values are given in [70],

$$B_1 = \frac{S_{\text{sorp}} k_f}{B_{fill}},$$

$$B_2 = \frac{S_{\text{sorp}} k_f}{B_{fill} F},$$

$$B_3 = \frac{S_{\text{sorp}} k_f}{(1-\varepsilon) F} + k_{bind}$$

and

$$B_4 = \frac{S_{\text{sorp}} k_f}{1-\varepsilon},$$

with

$$B_{fill} = \varepsilon + \frac{1 - R_{fill}}{R_{fill}}.$$

Here S_{sorp} is the specific adsorption surface area, k_f is a linear mass transfer coefficient, F is the partition relation coefficient; ε is the porosity of the bulk grain; k_{bind} is the coefficient for irreversible reaction/binding of the adsorbed fumigant in the grain kernel, and R_{fill} is the filling ratio.

The study in [70] was further extended in [72] where the parameters become

$$B_1 = \frac{S_{\text{sorp}} k_{fA}}{B_{fill}} - \frac{\epsilon}{B_{fill}} r_{fA} - \frac{S_{\text{sorp}} \rho_g k_{fA} k_{fA}}{B_{fill} A_1 F},$$

$$B_2 = \frac{S_{\text{sorp}} k_{fA} \rho_g k_{fG}}{B_{fill} A_1 F},$$

$$B_3 = \frac{S_{\text{sorp}} k_{fG}^2}{A_1 (1-\epsilon) \rho_g} - \frac{S_{\text{sorp}} k_{fG}}{(1-\epsilon)\rho_g} + r_{fG},$$

and

$$B_4 = \frac{S_{\text{sorp}} k_{fA} k_{fG}}{A_1 (1-\epsilon) \rho_g},$$

with

$$A_1 = k_{fG} + \frac{k_{fA} \rho_g}{F}.$$

Here k_{fA} is a linear mass transfer coefficient in the gas phase, k_{fG} is the linear mass transfer coefficient in the adsorbed phase; F is the partition relation coefficient; ρ_g is the "true" density of grain kernels; r_{fA} is the coefficient for the rate of reaction of gaseous fumigants in the air according to first order kinetics; S_{sorp} is the specific surface area for fumigant sorption; ϵ is the porosity of the bulk grain; and r_{fG} is the coefficient for irreversible reaction/binding of the adsorbed fumigant in the grain kernel according to first order kinetics.

The parameter values in [72] are for the ethyl formate sorption by wheat. In this thesis the parameter values are based on [70] where $F = 0.3$, $S_{\text{sorp}} k_f = 0.0125$ (h^{-1}), and $k_{bind} = 0.0569$ (h^{-1}) have been proven to fit the experimental data for the phosphine sorption into wheat and are hence applicable for use in the present study.

2.5.1 Discussion of modelling assumptions

The following assumptions are considered in the present thesis.

Compressibility

The gas mixture has a possibility to be compressed during fumigation due to the resistance of the porous media. However, due to the high porosity (of 0.43) it is most likely that this compression will be small. The assumption regarding

compressibility in this thesis depends on the problem that is being solved. For the preliminary study presented in Chapter 3 and the analytic solution presented in Chapter 4, the grain surface is assumed to be open to the atmosphere. Therefore, in these chapters the gas mixture is assumed incompressible as in [143] and [145].

However, for the comprehensive modelling of fumigant transport in Chapter 5, pressure inside a sealed silo can build up. Thus, in this chapter the gas mixture is assumed to be compressible. For a compressible flow, the model will involve solving for the density as an additional variable and we no longer have $\nabla \cdot \boldsymbol{v} = 0$.

Use of Darcy's law

In Chapter 3 and 4, we assume the use of Darcy's law to govern the flow. It is expected that during fan forced or tablet fumigation of grain, the flow is very slow and thus it is not necessary to include additional inertial terms. In Chapter 5 however, we use FLUENT to solve the full Navier-Stokes equations into which an external Darcy friction force is incorporated.

Variation in the grain temperature

In this research, we assume that the variation in the grain (wheat) temperature is negligible during fumigation. Particularly in Australia, most grain is harvested at the beginning of summer so that warm grain (30 °C) is harvested and held in a storage throughout the hot summer months of the year [91]. Changes in stored grain temperatures caused by the changes of ambient temperature are expected to be minimal since grain has a low thermal conductivity and heat conduction within stored grain is slow [44, 46]. Therefore, the grain retains much of its heat.

In addition, [45] have conducted a computer simulation to predict the changes in wheat temperature for 600 days of storage in a sealed cylindrical steel bin. The size of the storage is about 2.5 m radius and 6 m height, which is close to that considered in our study. The temperature prediction is given in Figure 2.4. Node 16 is located at the middle (2.45 m from the wall and 1.907 m distance from the base), while node 18 is also located at the same distance from the base but only 0.82 m from the bin wall. On the first day of storage, the wheat temperature

at both nodes is the same. Then, the wheat temperature is observed to slowly increase. We can see that seasonal temperature variation is considerably more significant than daily variation when it comes to affecting the grain temperature.

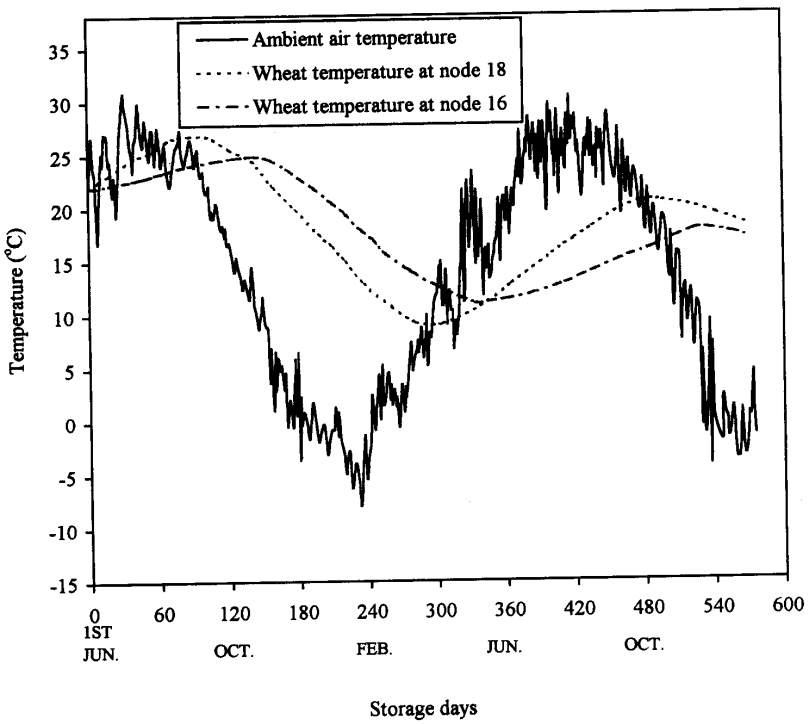

FIGURE 2.4: Predicted wheat temperature at various radial locations from the bin wall during storage (Beijing, from 1 June 1992 to 1 January 1994). [45].

In other work in [141], where a bunker like store (10 x 20 x 5 m) is filled with maize initially at 30 °C, and is subjected to temperature of 10 °C on the external surface, the maximum predicted temperature gradient is 8 °C in 90 days, which again shows that the temperature variation in the grain is small over the time scale of a fumigation.

The fumigant simulations presented in this work extend to a maximum time of approximately 25 days. Given the above observations we therefore, as a first approximation, assume that the grain is isothermal throughout this fumigation period.

2.6 Simulation and numerical procedure

In this thesis, both the COMSOL and FLUENT CFD software is used. COMSOL is based on the finite element method whereas FLUENT is based on the finite volume method. There is a significant amount of research related to gas transport and COMSOL is widely used such as in [22], [88], [94], [107], and [162]. On the other hand, examples of the use of FLUENT in gas flow simulation are [87] and [150]. The following sections discuss the simulation procedures as well as the numerical approach by both pieces of software.

2.6.1 COMSOL

COMSOL is use in Chapter 3 of this thesis which involves the study of the hydrodynamics of gas flow in an open-top grain storage bin. The steps involved in the simulation by COMSOL are summarized in the flow chart given in Figure 2.5. COMSOL provides a number of predefined templates and user interfaces already set up with equations and variables for specific areas of physics. COMSOL can implement the Laplace equation,

$$-\nabla \cdot (\nabla u) = 0 \tag{2.6}$$

for any variable u. The equation is solved via a GMRES linear system solver using a geometric multigrid preconditioner [62].

2.6.2 FLUENT

FLUENT is used in Chapter 3 and Chapter 5. FLUENT uses a control-volume-based technique to convert the governing equations to algebraic equations that can be solved numerically. The governing equations implemented in this work are the equations of conservation of mass and momentum. Mass here can be separated into the overall and the individual species mass. The simplified form of these governing equations are as follows [6]:

Overall mass (continuity equation):

$$\frac{\partial \rho}{\partial t} + \nabla \cdot (\rho \boldsymbol{v}) = 0 \tag{2.7}$$

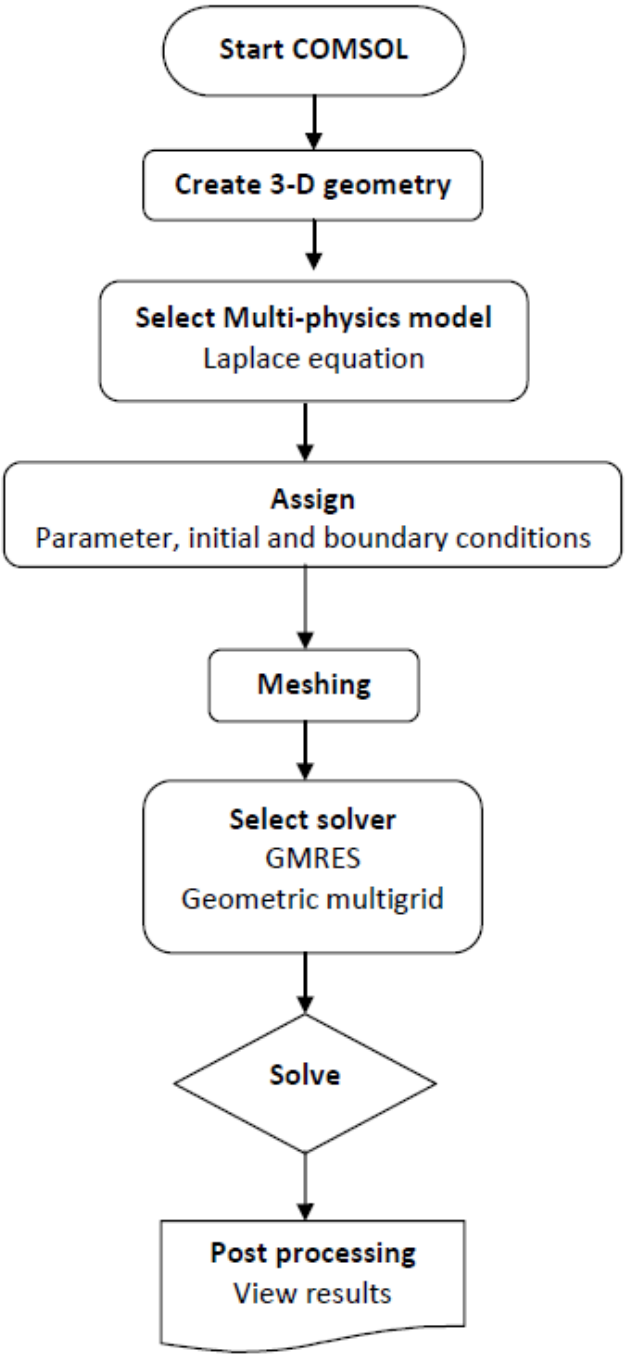

FIGURE 2.5: COMSOL modelling steps. COMSOL is also known as FEMLAB. Chart was adapted from [34].

Momentum (Navier-Stokes equation):

$$\frac{\partial}{\partial t}(\rho \boldsymbol{v}) + \boldsymbol{\nabla} \cdot (\rho \boldsymbol{v}\boldsymbol{v}) = -\boldsymbol{\nabla} p + \boldsymbol{\nabla} \cdot (\boldsymbol{\tau}) + \rho \boldsymbol{g} + \boldsymbol{F} \tag{2.8}$$

Species mass:

$$\frac{\partial}{\partial t}(\rho Y_i) + \boldsymbol{\nabla} \cdot (\rho \boldsymbol{v} Y_i) = \boldsymbol{\nabla} \cdot (\Gamma \nabla Y_i) + S_i \tag{2.9}$$

Here, ρ (kg/m^3), $\boldsymbol{v}$ (m/s), and p (Pa) are the density, velocity and pressure of the gas respectively. While, $\boldsymbol{\tau}$ (kgm^{-1}s^{-2}) is the stress tensor, $\boldsymbol{g}$ (m/s^2) is the gravity and $\boldsymbol{F}$ (kgms^{-2}) is the external body forces. In the species mass equation, Y_i refers to the mass fraction of species i, Γ is the diffusion coefficient and, S_i is the source term.

The finite volume method consists of the following steps [6, 153]:

- Integrating the governing equations over all the control volumes in the domain.
- Discretising the resulting integral equations to construct an algebraic equation.
- Solving the the resulting algebraic equations using an iterative method.

For an arbitrary control volume V, the integral form of the governing equations are [6]:
Continuity equation:

$$\int_V \frac{\partial \rho}{\partial t} dV + \oint \rho \boldsymbol{v} \cdot d\mathbf{A} = 0 \tag{2.10}$$

Momentum equation:

$$\int_V \frac{\partial \rho \boldsymbol{v}}{\partial t} dV + \oint \rho \boldsymbol{v}\boldsymbol{v} \cdot d\mathbf{A} = -\oint p\mathbf{I} \cdot d\mathbf{A} + \oint \boldsymbol{\tau} \cdot d\mathbf{A} + \int_V \bar{F} dV \tag{2.11}$$

Species equation:

$$\int_V \frac{\partial \rho Y_i}{\partial t} dV + \oint \rho Y_i \boldsymbol{v} \cdot d\mathbf{A} = -\oint \Gamma \nabla Y_i \cdot d\mathbf{A} + \int_V S dV \tag{2.12}$$

Discretization of these equations over a given control volume yields an equation that contains the unknown scalar variables at the cell centre as well as the unknown

values in surrounding neighbour cells. The discretized governing equations are given below [6]:

Continuity equation:

$$\frac{\partial \rho}{\partial t} V + \sum_{f}^{N_{\text{faces}}} \rho_f \boldsymbol{v}_f \cdot \mathbf{A}_f = 0, \tag{2.13}$$

or (steady state)

$$\sum (\rho \boldsymbol{v} A)_f = 0, \tag{2.14}$$

Momentum equation:

$$\frac{\partial \rho \boldsymbol{v}}{\partial t} V + \sum_{f}^{N_{\text{faces}}} \rho_f \boldsymbol{v}_f \boldsymbol{v}_f \cdot \mathbf{A}_f = - \sum_{f}^{N_{\text{faces}}} p_f \mathbf{I} \cdot \mathbf{A}_f + \sum_{f}^{N_{\text{faces}}} \boldsymbol{\tau} \cdot \mathbf{A}_f + \bar{F} V, \tag{2.15}$$

or in the linearized form (steady state)

$$a_P \boldsymbol{v} = \sum_{nb} a_{nb} \boldsymbol{v}_{nb} + \sum p_f A \cdot i + S, \tag{2.16}$$

Species equation:

$$\frac{\partial \rho Y_i}{\partial t} V + \sum_{f}^{N_{\text{faces}}} \rho_f (Y_i)_f \boldsymbol{v}_f \cdot \mathbf{A} = - \sum_{f}^{N_{\text{faces}}} \Gamma_f \nabla (Y_i)_f \cdot \mathbf{A}_f + S V, \tag{2.17}$$

or in the linearized form (steady state)

$$a_P (Y_i)_P = \sum_{nb} a_{nb} (Y_i)_{nb} + b. \tag{2.18}$$

where N_{faces} is the number of faces enclosing a given cell, $\mathbf{A}_f$ is area of face f, V is cell volume, nb is neighbouring cell, a_P, a_{nb} is linearized coefficient, and I is an identity matrix.

The simulation procedure used by FLUENT is given in Figure 2.6. Either a segregated (decoupled) or coupled algorithm can be implemented in FLUENT. The coupled solver is recommended [6] for a strong inter-dependence between density, momentum, energy, and/or species. Otherwise, the segregated solver is suggested. In this present thesis, a segregated algorithm called SIMPLE is implemented. More detailed information on SIMPLE is provided in [6] and [153].

FLUENT starts the solution calculation by initial guess $p*$ (during update properties). This initial guess is used to solve the descretised momentum equations

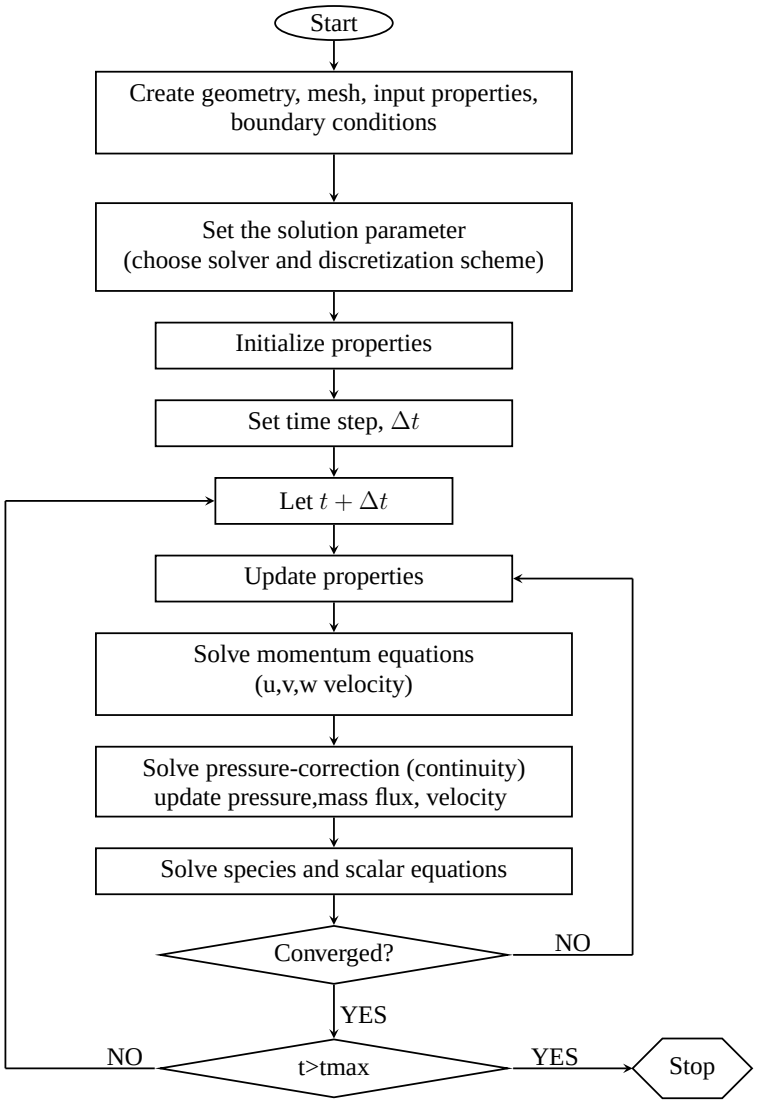

FIGURE 2.6: Flow chart of the simulation procedures.

(2.16) to obtain $\boldsymbol{v}^*$. The correct pressure p is the sum of the guessed pressure $p*$ and the correction p' which is $p = p* + p'$. Similarly,

$$\boldsymbol{v} = \boldsymbol{v}^* + \boldsymbol{v}' \tag{2.19}$$

where $\boldsymbol{v}'$ is the correction to the velocity guess.

Equation (2.19) together with the discretised momentum equation (2.16) yields an equation of the form $\boldsymbol{v}' = f(p')$. Then, substituting into the discretised continuity equation (2.14) yields a discretised continuity equation as an equation for pressure correction p'. More details on this are provided in [6] and [153]. Once p' is solved, the correct pressure and velocity component can be obtained.

The process repeats until convergence achieved. The accuracy of the solution is highly dependent on the numerical approach taken, further details of which will be discussed below.

2.6.3 Spatial discretization schemes

During the discretization process, the field variables that are stored at the cell centers must be interpolated to the faces of the control volume as they are required in (2.14) to (2.18). FLUENT offers a few interpolation schemes such as first and second order upwind, power law and quick scheme [6]. In this present modelling, second order upwinding is implemented.

2.6.4 Temporal discretization schemes

Temporal discretization involves integration of every term in the governing equation over a time step Δt such that for a variable ϕ,

$$\frac{\partial \phi}{\partial t} = F(\phi) \tag{2.20}$$

where $F(\phi)$ incorporates any spatial discretization. In this thesis, a second order implicit time formulation is employed such that $F(\phi)$ is evaluated at the future time level [6]. Therefore

$$\frac{3\phi^{n+1} - 4\phi^n + \phi^{n-1}}{2\Delta t} = F(\phi^{n+1}) \tag{2.21}$$

or

$$\phi^{n+1} = \frac{1}{3}\left(4\phi^n - \phi^{n-1} + \phi^n + 2\Delta t F(\phi^{n+1})\right). \tag{2.22}$$

This implicit equation can be solved iteratively at each time level before moving to the next time step. The advantage of the fully implicit scheme is that it is unconditionally stable with respect to time step size [6]. An under-relaxation factor can be used to control the update of each computed variable at every iteration. The updated value of the variable ϕ within a cell depends upon the old value, the computed change and the under-relaxation factor, α, as follows,

$$\phi^{\text{new}} = \phi^{\text{old}} + \alpha(\phi^{\text{calc}} - \phi^{\text{old}}) = \phi^{\text{old}} + \alpha\Delta\phi. \tag{2.23}$$

In the present study, the under relaxation factors α are set to the FLUENT default values, which are 0.3 for pressure, 0.7 for velocities and 1 for all other quantities. The iteration will only stopped if a convergence criterion is met.

2.6.5 Convergence criterion

The discretized equations yield a linear system of equations that are solved by FLUENT using the iterative Gauss-Seidel method [6]. The residual for a general scalar ϕ, R_ϕ, is used to monitor the convergence of the simulation in FLUENT, namely [5],

$$R_\phi = \frac{\sum_{\text{cells P}} \left|\sum_{nb} a_{nb}\phi_{nb} + b - a_P\phi_P\right|}{\sum_{\text{cells P}} |a_P\phi_P|}. \tag{2.24}$$

For the continuity equation, the residual is defined as [5],

$$R_c = \frac{\sum_{\text{cells P}} |\text{rate of mass creation in cell P}|}{\sum_{\text{5 iterations}} |\text{rate of mass creation in cell P}|} \tag{2.25}$$

Iteration will continue until the sum of residuals for each variable is less than a set convergence criterion. In the this thesis, an absolute convergence criteria of 10^{-6} is adopted for all variables.

2.7 Summary

In this chapter we have presented information that underpins the research conducted in Chapters 3 to 5 ranging from fumigation issues to mathematical mod-

elling and numerical simulation approaches. The main topics discussed were regarding stored grain insects, grain storage types, fumigant application practices and factors that contributed to fumigation failures. In addition, a literature review of previous related mathematical models was presented. The numerical procedures behind the FLUENT and COMSOL software packages were also discussed.

2.7.1 Main findings from the past research and knowledge gaps

The literature review presented here shows that there is a number of published research articles on the fumigant flow and concentration in grain storage. However, for the fumigant flow in a a circular cylindrical store, to date, studies have only been carried out whereby the inlet is treated as a point source. Therefore, there is a need to conduct an investigation for a more realistic finite inlet.

Findings from Section 2.4 show that sorption is a critical component that is lacking in many models and cannot be neglected. Furthermore, previous fumigant transport models considered the fumigant as a single gas rather than as a multicomponent mixture, despite the possibility of two species having different behavior. A multicomponent species formulation has the advantage that sorption can be more precisely modelled. Moreover, the previous models lack an accurate representation of the most suitable boundary conditions, especially at the grain surface. None have considered a storage that has a given HLP, which is a relevant measure to the industry. In addition, none of the previous works try to include insect extinction.

To the best of the author's knowledge, it appears that a 3-dimensional model of phosphine distribution in a vertical silo, both using fan-forced and tablet fumigation and including sorption, insect extinction and gas tightness at the silo has not been attempted.

Such a study is given here in order to facilitate a greater understanding of phosphine behaviour in on-farm storage silos.

Chapter 3

Simulation of phosphine flow in vertical grain storage: a preliminary numerical study

The following paper is presented in this thesis chapter:

- Isa, Z.; Fulford, G. & Kelson, N. Simulation of phosphine flow in vertical grain storage: a preliminary numerical study. ANZIAM J., 2011, 52, C759-C772.

Statement of contribution of Co-Authors

The authors listed below have certified that:

1. they meet the criteria for authorship in that they have participated in the conception, execution, or interpretation, of at least that part of the publication in their field of expertise;
2. they take public responsibility for their part of the publication, except for the responsible author who accepts overall responsibility for the publication;
3. there are no other authors of the publication according to these criteria;
4. potential conflicts of interest have been disclosed to (a) granting bodies, (b) the editor or publisher of journals or other publications, and (c) the head of the responsible academic unit, and
5. they agree to the use of the publication in the student's thesis and its publication on the QUT ePrints database consistent with any limitations set by publisher requirements.

In the case of Chapter 3: Isa, Z.; Fulford, G. & Kelson, N. Simulation of phosphine flow in vertical grain storage: a preliminary numerical study. ANZIAM J., 2011, 52, C759-C772.

Contributor	**Statement of contribution**
Zaiton M.Isa	Conducted CFD simulations, interpreted the numerical results, wrote the manuscript, acted as corresponding author. Signature: [signature] Date: 16/7/2014
Glenn R. Fulford	Directed and guided the work, assisted with the interpretation of results and preparation of paper and proof read the manuscript.
Neil A. Kelson	Directed and guided the work, assisted with the interpretation of results and preparation of paper and proof read the manuscript.

Principal Supervisor Confirmation

I have sighted email or other correspondence from all Co-authors confirming their certifying authorship.

Name: Troy Farrell Signature: Troy Farrell Date: 16/07/14

Abstract

To fumigate grain stored in a silo, phosphine gas is distributed by a combination of diffusion and fan-forced advection. This initial study of the problem mainly focuses on the advection, numerically modelled as fluid flow in a porous medium. We find satisfactory agreement between the flow predictions of two Computational Fluid Dynamics (CFD) packages, COMSOL and FLUENT. The flow predictions demonstrate that the highest velocity ($> 0.1\,\mathrm{m/s}$) occurs less than $0.2\,\mathrm{m}$ from the inlet and reduces drastically over one metre of silo height, with the flow elsewhere less than $0.002\,\mathrm{m/s}$ or 1% of the velocity injection. The flow predictions are examined to identify silo regions where phosphine dosage levels are likely to be too low for effective grain fumigation.

3.1 Introduction

The Australian grain industry seeks strategies that will kill 100% of insects in grain storage. In practice, a common method for killing insects is fumigation by phosphine gas as it is cheap, easy to use, and is a comparatively safe for most common stored grain commodities. There is currently world-wide acceptance of phosphine fumigation as a residue-free treatment [60, 43]. However, failed fumigation has been reported, and the ineffective spatial phosphine distribution in the grain storage is one of the factors contributing to the failure [85]. This, along with a rise in the number of phosphine-resistant stored grain pests, means that a good understanding of how phosphine is distributed in grain storage is needed to ensure its long-term use.

Phosphine gas has a specific gravity that is almost the same as air (air: 1.0, PH_3 : 1.17) [85] and moves very slowly through the grain mass by diffusion if the air in the storage silo is not moving. Therefore, fan-assisted fumigation is used to drive the phosphine gas through the grain from high to low pressure areas. The purpose of this work is to perform an initial study of this advection-driven phosphine transport, and to this end we focus on a prototype geometry for a typical cylindrical farm silo. Knowledge of the flow patterns in the stored grain will, for example, give an indication of the zones in the grain storage that might provide

areas of refuge for breeding insects.

Previous work related to this problem was conducted by Smith et al. [145, 143] who considered the advection-diffusion of CO_2 in a cylindrical storage, assuming a uniform vertical flow. They obtained an analytic solution for the concentration using a perturbation approach based on small curvature of streamlines. A study of moisture transport coupled with heat transport in grain silos assuming Darcy flow in a porous medium was conducted by Singh and Thorpe [141] who numerically solved the governing equations using a finite difference approach. Their objective was to study the cooling of grain masses since stored product insects cannot thrive in low temperatures. Other research has been conducted by Xu et al. [161], who analytically studied the CO_2 distribution in the bulk grain, again assuming Darcy flow.

We describe some initial results for the fan-forced flow of phosphine into the base of a grain silo, numerically modelled as fluid flow in a porous medium. For comparison purposes, the flow is investigated using two CFD packages COMSOL Multiphysics [62] and ANSYS FLUENT [3]. COMSOL is a general purpose PDE solver based on the finite element method whereas FLUENT is a CFD solver based on the finite volume method. The model equations used for each of the software packages are described and compared, and a detailed comparison of numerical results is presented. Implications of the results for phosphine fumigation of grain are discussed along with further work to be undertaken on this problem.

3.2 Model equations and numerical solution

The geometry chosen for this study is a vertical cylinder intended to model a storage facility having a radius 2 m and height 6 m, typical of many domestic silos on farms. A 0.2 m radius inlet pipe is attached to the centre of the silo base. The resulting computational domain is axisymmetric, whereas practical silos may not be due to, e.g., inlets located in the side walls. In view of this, a fully 3D solution methodology has been used in FLUENT and COMSOL as a precursor to future studies involving more complex domains. The current axisymmetric domain does, however, permit a computationally less expensive 3D axisymmetric solution to be

obtained for comparison purposes using FLUENT (COMSOL does not have this simplified modelling capability). Flow predictions are obtained for various phosphine gas and air mixtures pumped continuously at velocity $v_0 = 0.2\,\mathrm{m/s}$ into the storage (filled with wheat). Mixtures of phosphine gas and carbon dioxide are also considered. Because the specific gravity of phosphine is similar to air, it is reasonable to neglect the effect of gravity on the flow. We also assume that the variation in the grain (wheat) temperature is negligible during fumigation [45] and that the pore-size distribution is uniform with height. While some minor compaction is expected, the assumption of uniform pore size distribution is reasonable for an initial study.

3.2.1 Model equations used for COMSOL

The mathematical model of the porous media flow solved using the COMSOL Multiphysics package assumes gas flow through a grain bulk that satisfies Darcy's law [143, 161]

$$\boldsymbol{v} = -\frac{k}{\mu}\boldsymbol{\nabla} p \tag{3.1}$$

with velocity $\boldsymbol{v}$, pressure p, grain permeability k and dynamic viscosity μ. Typically, for a pure phosphine gas in wheat grain, $k = 0.578 \times 10^{-8}\,\mathrm{m}^2$ [161] and $\mu = 1.1 \times 10^{-5}\,\mathrm{kg\,m^{-1}s^{-1}}$. By comparison, for pure CO_2 gas, $k = 2.5159 \times 10^{-8}\,\mathrm{m}^2$ and $\mu = 18.1 \times 10^{-6}\,\mathrm{kg\,m^{-1}s^{-1}}$ [141]. In this initial study we also assume an incompressible flow, $\boldsymbol{\nabla}\cdot\boldsymbol{v} = 0$, following Smith et al. [143, 145], which implies the pressure satisfies Laplace's equation

$$\nabla^2 p = 0. \tag{3.2}$$

Equation (3.2) is solved subject to the following zero normal velocity boundary conditions on the vertical wall boundary

$$\boldsymbol{\nabla} p\cdot\boldsymbol{n} = 0, \qquad \text{for } r = a, \tag{3.3}$$

where $\boldsymbol{n}$ is the unit normal vector to the boundary and a is the radius of the silo. Phosphine gas flows through the grain surface at $z = h$ into the atmosphere. It is reasonable to assume that the gas pressure is constant at $z = h$, and if we assume Bernoulli's equation then $p = p_a - \rho v^2/2$, where p_a is the atmospheric pressure

and ρ is the density. However, v will be small compared to the inlet velocity, so it is reasonable to linearise around the velocity and therefore approximate the boundary condition with

$$p = p_a \qquad \text{on } z = h.$$

On the base of the cylinder,

$$\boldsymbol{\nabla} p \cdot \boldsymbol{n} = \begin{cases} -\dfrac{\mu}{k} v_0 & r < b, \\ 0 & r > b, \end{cases} \qquad \text{at } z = 0, \tag{3.4}$$

where $b = 0.2\,\mathrm{m}$ is the inlet radius and $v_0 = 0.2\,\mathrm{m/s}$ is the velocity injection of the phosphine at the inlet.

3.2.2 Model equations used for FLUENT

In contrast to COMSOL, FLUENT solves the usual Navier–Stokes equations which include conservation equations for mass and momentum, along with an additional resistance term $\boldsymbol{S}$ to account for the porous medium,

$$\rho(\boldsymbol{v} \cdot \boldsymbol{\nabla})\boldsymbol{v} = \mu \nabla^2 \boldsymbol{v} + \boldsymbol{S}, \qquad \boldsymbol{S} = -\frac{\mu}{k} \boldsymbol{\nabla} p. \tag{3.5}$$

In FLUENT, the no-slip wall condition, $\boldsymbol{v} = \boldsymbol{0}$, replaces boundary conditions (3.3) and (3.4) for $r > b$. For this flow, the inertia terms are typically small over most of the domain. Neglecting these in (3.5), taking the divergence of the remaining terms, and using the continuity equation results in an equation which is mathematically equivalent to (3.2).

3.2.3 Numerical solution methods

In this work all simulations were run on a Windows XP PC with 3Ghz Intel(R) Core(TM)2 Duo (E8400). For the 3D computational modelling, an unstructured tetrahedral mesh, with local refinement near the inlet, is used in both COMSOL and FLUENT. Overall, the surface meshing used for both is similar. Inside the flow volume, the FLUENT simulation uses 180,737 cells whereas the COMSOL simulation uses 62,898 cells, the latter being about one third of the former due to software memory limitations. Throughout the computational domain, COMSOL uses an

iterative GMRES linear system solver and geometric multi-grid pre-conditioner to solve for the pressure field, along with post processing to calculate the velocity. FLUENT instead uses an iterative Navier–Stokes solver which separately solves for the pressure and velocity at each step. For the spatial discretisation, first-order upwinding was available for use in both packages, with second-order upwinding available in FLUENT only. The use of higher order upwinding did not affect the results significantly, as expected, since velocities are small.

In the COMSOL simulation, the discontinuous velocity at the bottom surface, $z = 0$, due to gas injection, v_0, is replaced by the hyperbolic tangent function

$$v_0 \times 0.5(1 - \tanh(\alpha(r - b))),$$

with $\alpha = 50$. The use of this expression aims to reduce any local numerical instability caused by the flow discontinuity across the inlet at $r = b$.

3.3 Results

The overall predicted flow features are illustrated in Figure 3.1 which shows the streamlines and a contour plot of the velocity magnitude through a silo 2D vertical slice. The results shown are obtained using the full 3D solver capability of FLUENT, with corresponding results obtained using COMSOL being indistinguishable by eye (not shown for brevity). Overall, the flow moves upward from the inlet at the base ($z = 0$) towards the grain surface, and axial symmetry appears to be preserved throughout the domain. The gas velocity decreases rapidly: over a radial distance of 1 m from the inlet it decreases to less than 1% of the velocity injection v_0. From about a height of 1 m and above, the flow is spread the full extent of the silo radius and the streamlines are almost parallel. Sample computations with viscosity, μ, and permeability, k, changed from pure phosphine to pure carbon dioxide result in very similar velocity and streamline patterns, suggesting that the flow is not overly sensitive to changes in these parameter values. Although not easily seen from the figure, the regions of lowest velocity are near the corners where the base plate and vertical wall meet. Specifically, the velocity magnitude is less than 0.004% of v_0 in the flow region located at the base of the silo and within 0.1 m of the vertical silo

wall. This very slow flow region is likely to be where the distribution of phosphine gas through diffusion plays an important role. It may also be an area of refuge for insects against any grain fumigation treatment of insufficient duration to achieve critical dosage levels throughout the entire storage silo.

Additional flow detail for the 3D simulations is provided in Figure 3.2 and Figure 3.3, where velocity profiles predicted by both COMSOL and FLUENT are plotted at different locations. Along the vertical symmetry line of the silo, the axial velocity v_z decreases rapidly with height from its inlet value at $z = 0$ before tending to approximately constant, as portrayed in Figure 3.2(a). Physically, this demonstrates the inability of the gas to penetrate quickly to the height of the grain mass. Along this same vertical symmetry line, the transverse velocity v_x is expected to be zero for axisymmetric flow. However, in Figure 3.2(b), small nonzero transverse velocities are observed close to the inlet in both the COMSOL and FLUENT predictions, with these being more pronounced for COMSOL.

In Figure 3.3, the axial velocity profiles across the inlet plane and downstream at height $z = 3$ are given. As shown in Figure 3.3(a), essentially top hat inlet profiles are imposed for the axial velocity in both COMSOL and FLUENT, with some smoothing of the COMSOL inlet profile due to the hyperbolic tangent function across the inlet. Despite this smoothing, nonzero variations in the transverse velocity component across the inlet are found in the COMSOL predictions and are attributable to the simplified modelling. In Figure 3.3(b) the downstream behaviour of the flow at $z = 3$ is different for the two models when near the wall, with the FLUENT simulations imposing the no-slip condition on the vertical walls, whereas in COMSOL only the normal component of the velocity is required to be zero. Nevertheless, away from the narrow near-wall region, an essentially uniform unidirectional axial velocity is predicted by both solvers across the entire silo width. Although not shown for brevity, the corresponding predicted transverse velocity components are close to zero. Hence, in the upper regions of the stored grain, it is mainly the magnitude of the axial velocity that determines the rate of phosphine distribution.

As previously mentioned, a simplified 3D axisymmetric formulation of the governing equations is available in FLUENT. This permits flow predictions on a rectan-

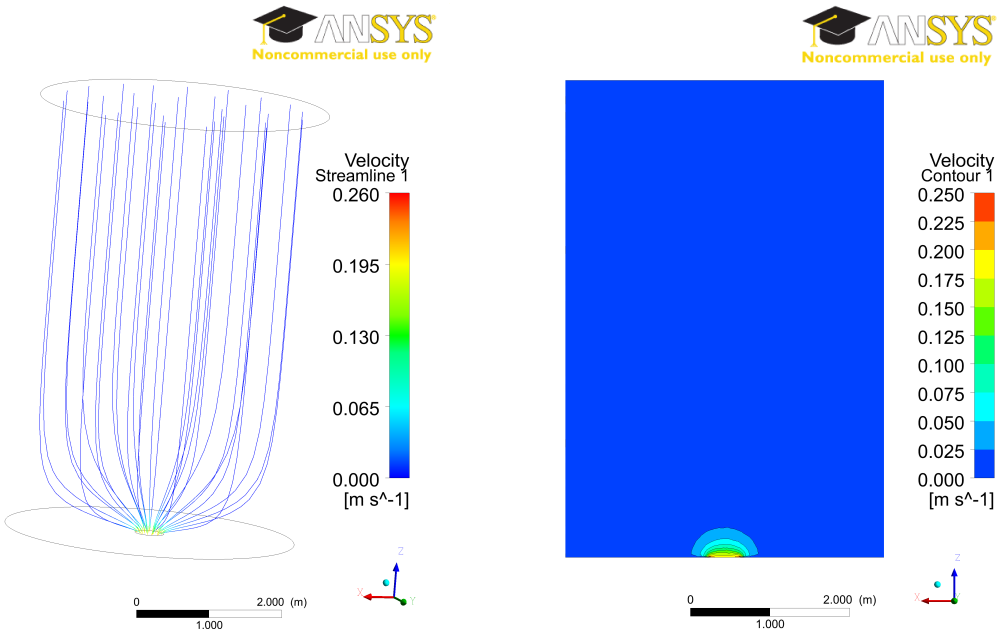

FIGURE 3.1: Streamlines and 2D sliced contour plot from the 3D FLUENT simulations.

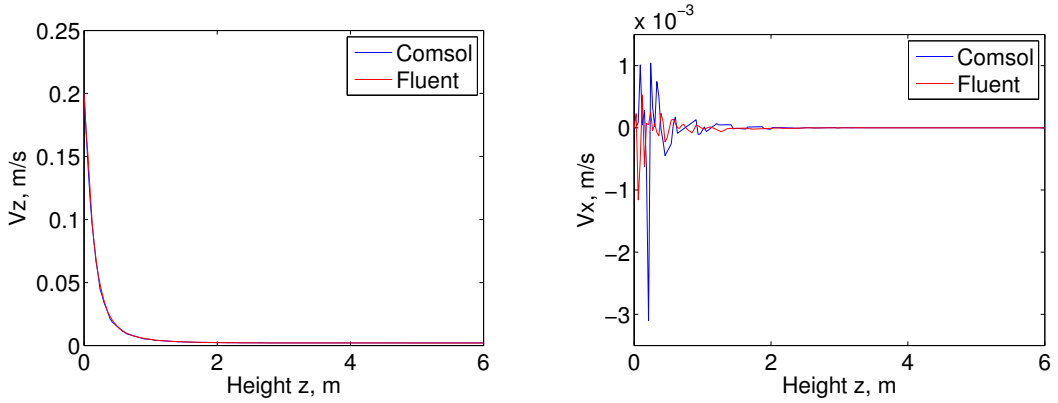

(a) (b)

FIGURE 3.2: Variation with height of (a) axial velocity, v_z, and; (b) transverse velocity, v_x along the symmetry line of the silo.

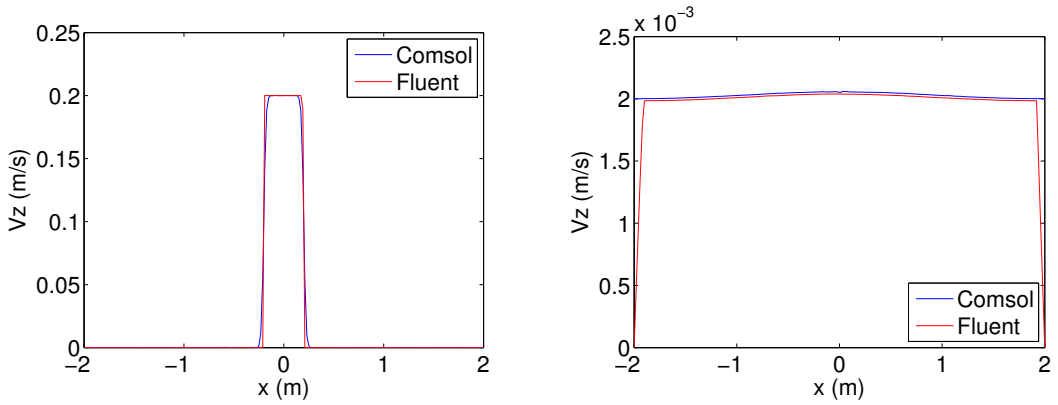

(a) (b)

FIGURE 3.3: Axial velocity profile, v_z (a) at height $z = 0$, and; (b) $z = 3$.

TABLE 3.1: Relative errors of maximum velocities from axisymmetric FLUENT model predictions on three different grids, relative to axisymmetric 300×900 results. Also shown are relative errors for velocities at sample point $(0.2, 0, 1)$ and the number of cells N. Corresponding results for the full 3D FLUENT simulation are also given.

grid size	N	% error			
		max v_z	max v_x	$v_z(0.2, 0, 1)$	$v_x(0.2, 0, 1)$
3D	1.8×10^5	1.9	29.6	2.9	1.5
50×150	7.5×10^3	8.6	44	0.5	1.1
100×300	3×10^4	3.4	26	0.1	0.25
200×600	1.2×10^5	0.8	9.2	0.02	0.04

gular grid corresponding to a vertical slice of the 3D cylindrical storage, at greatly reduced computational cost. Here, we investigate the convergence behaviour of the axisymmetric FLUENT model as the grid is refined using four different grid sizes. Sample results are given in Table 3.1 for the relative error of the three coarsest axisymmetric grids and the FLUENT full 3D simulation results, relative to the finest grid size used (300×900) in the axisymmetric modelling. As expected, the relative error for the peak velocities decreases with increasing number of elements, N, as do the relative errors for the velocities at the point $(0.2, 0, 1)$. Assuming a form $E = kN^\alpha$ then regression on the logarithm of the variables gives an exponent $\alpha \simeq -1.2$ for the peak axial velocity and $\alpha = -1.7$ for both velocity components at the point $(0.2, 0, 1)$. This indicates better than quadratic convergence based on a typical cell length scale $1/\sqrt{N}$. However, for the peak radial velocity, the convergence is slower with $\alpha \simeq -0.7$. While there is reasonable accuracy for the axial peak velocities for the 3D simulation, the tabulated data suggest that further grid refinement is required in the full 3D modelling if more accurate predictions for the transverse velocity components are desirable.

As part of this initial study, we also sought an analytic solution for the axisymmetric version of the model equations used by COMSOL and were able to find a

closed form series solution involving an infinite Fourier-Bessel series,

$$p(r,z) = Dz + E + \sum_{m=1}^{\infty} J_0\left(\frac{\alpha_m}{a}r\right)\left[A_m \cosh\left(\frac{\alpha_m}{a}z\right) + B_m \sinh\left(\frac{\alpha_m}{a}z\right)\right]$$

with

$$D = -\frac{\mu v_0 b^2}{ka^2}, \quad E = p_a - Dh$$

and

$$B_m = -\frac{2\mu b v_0}{k}\frac{J_1(\alpha_m b/a)}{\alpha_m^2[J_0(\alpha_m)]^2} \quad A_m = \frac{-B_m \sinh(\alpha_m h/a)}{\cosh(\alpha_m h/a)}.$$

A detailed analysis of this closed-form solution, including, e.g., convergence behaviour, has not yet been undertaken and remains the subject of future work.

3.4 Conclusions

We used CFD modelling with COMSOL and FLUENT to perform a simulation for phosphine gas flow in a cylindrical grain storage silo. On the whole, COMSOL and FLUENT predict similar flow behaviour with satisfactory agreement. The flow predictions demonstrate that the region with highest velocity ($> 0.1\,\mathrm{m/s}$) occurs within a 0.2 m radius distance from the inlet and reduces drastically over one metre of silo height. A very slow flow region was identified at the base of the silo and within 0.1 m of the silo wall, where diffusion may play an important role in the phosphine gas distribution. Additionally, this region may also be a refuge for insects against any grain fumigation treatments.

In future work, we will consider the advection-diffusion transport of the phosphine, using the flow results in this paper as an input. More complex grain storage geometries will also be explored. Of significant interest to the grain industry is whether "pockets" exist where insects can survive more easily. The critical parameters for such regions include both the local concentration as well as the time of exposure, so some modelling of the mortality of insects should be coupled to this model to provide useful insights for future design of cost effective fumigation strategies.

Chapter 4

Flow field and traverse times for fan forced injection of fumigant via circular or annular inlet into stored grain

The following paper is presented in this thesis chapter:

- Z.M.Isa, G.R.Fulford, N. A.Kelson, T.W.Farrell. Flow field and traverse times for fan forced injection of fumigant via circular or annular inlet into stored grain. Submitted to Applied Mathematical Modelling.

Statement of contribution of Co-Authors

The authors listed below have certified that:

1. they meet the criteria for authorship in that they have participated in the conception, execution, or interpretation, of at least that part of the publication in their field of expertise;
2. they take public responsibility for their part of the publication, except for the responsible author who accepts overall responsibility for the publication;
3. there are no other authors of the publication according to these criteria;
4. potential conflicts of interest have been disclosed to (a) granting bodies, (b) the editor or publisher of journals or other publications, and (c) the head of the responsible academic unit, and
5. they agree to the use of the publication in the student's thesis and its publication on the QUT ePrints database consistent with any limitations set by publisher requirements.

In the case of Chapter 4: Z.M.Isa, G.R.Fulford, N. A.Kelson, T.W.Farrell. Flow field and traverse times for fan forced injection of fumigant via circular or annular inlet into stored grain. Submitted to Applied Mathematical Modelling.

Contributor	**Statement of contribution**
Zaiton M.Isa	Derived the analytic work, interpreted the analytical results, wrote the manuscript, acted as corresponding author. Signature: [signature] Date: 16/7/2014
Glenn R. Fulford	Directed and guided on the analytical work, assisted with the interpretation of results and preparation of paper and proof read the manuscript.
Neil A. Kelson	Directed and guided the overall work, assisted with the interpretation of results and preparation of paper and proof read the manuscript.
Troy W. Farrell	Assisted with justifying the model used and proof read the manuscript.

Principal Supervisor Confirmation

I have sighted email or other correspondence from all Co-authors confirming their certifying authorship.

Name: Troy Farrell Signature: Troy Farrell Date: 16/07/14

Abstract

Fan forced injection of phosphine gas fumigant into stored grain is a common method to treat infestation by insects. For low injection velocities the transport of fumigant can be modelled as Darcy flow in a porous medium where the gas pressure satisfies Laplace's equation. Using this approach, a closed form series solution is derived for the pressure, velocity and streamlines in a cylindrically stored grain bed with either a circular or annular inlet, from which traverse times are numerically computed. A leading order closed form expression for the traverse time is also obtained and found to be reasonable for inlet configurations close to the central axis of the grain storage. Results are interpreted for the case of a representative 6 m high farm wheat store, where the time to advect the phosphine to almost the entire grain bed is found to be approximately one hour.

4.1 Introduction

Infestation of stored grain by insects can cause contamination, odors, molds, and heat damage that reduces the market value of the grain [82] or, if left untreated, makes the grain unsaleable to most buyers [43]. A common method used for eliminating the insect populations in grain storage is fumigation by phosphine, which is cost effective, easy to use, and also a residue-free treatment [60, 43]. However, for successful insect control, the phosphine must be effectively distributed to all areas of the grain bed and kept in contact with the insects for sufficient time at the required concentration. If not, there will be potential zones that can provide areas of refuge where insects can survive and breed.

In view of the above, a good understanding of how the phosphine is distributed in stored grain is important. This can be facilitated by understanding both the flow patterns and the traverse time, defined as the time taken for phosphine entering from the inlet to reach a specified position in the grain bulk. The latter was introduced in early work on grain storage [98] and subsequently employed in a number of studies as a useful interpretive tool (e.g. [100, 144]). In terms of the relevant physics that requires modelling, phosphine gas is driven mainly by advection during fan forced fumigation. While molecular diffusion is involved

the contribution is comparitively small. For example, for stored grain with grain bed height 6 m, typical seepage velocities are of the order 10^{-2} m/s [143] and the diffusion coefficient is of the order 10^{-5} [112], yielding a Peclet number of the order 10^3. Hence, with such an application in mind, fan forced gas flow through the stored grain by advection only is considered here.

The overall objective of this study is to progress further the recently initiated work by the authors [101] to investigate fumigation in stored grain. Here, analytic solutions are the main focus. Apart from providing insights into typically simplified forms of more realistic problems, they can also provide accurate solutions against which numerical simulation models involving more complex physical processes or geometrical grain storage configurations can be validated. The specific aim of the present study is to derive closed form analytic solutions for pressure, velocity and streamlines in a cylindrical grain storage with an annular inlet. The approach also permits the investigation of a circular inlet as a special case. Consistent with earlier studies, incompressible Darcy flow through a porous medium is considered, applicable to relatively low phosphine injection velocity at the inlet.

Regarding earlier work, a number of analytical solutions for two dimensional planar gas flow or traverse times related to grain storage under similar modelling assumptions have been obtained [89, 99, 100, 142, 144, 73], although none investigate the geometrical configurations considered in this study. To the Authors' knowledge, the most relevant prior work to the present one is a closed form solution for the traverse time in a circular cylindrical store open to the atmosphere having a conical base and centrally positioned inlet [100]. However, the expression for the traverse time solution so obtained was an approximation only, and the inlet was treated as a point source. Regarding some other planar two dimensional flows, analytic solutions for calculating the pressure drop within grain storage was obtained in [99] using a conformal mapping approach. Formulae for traverse times were later developed in [100] for a few particular geometries, including some of the plane flows in his earlier work [99]. Incompressible Darcy flow in a rectangular bin open to the atmosphere studied in [100] was further studied in detail in [89]. The gas entering the grain bed was also treated as a point source inlet at the center of the bin floor. They reproduced the analytic solution in [100] for pressure, velocity,

streamlines, and traverse time in the limit of infinite grain height, and also analysed the finite height case. It was found that their limiting solution for semi-infinite height was sufficiently accurate for grain beds higher than 1.25 m. The flow was also extended to investigate Ergun's equation by using perturbation expansions. An analytic solution to this Ergun flow problem was later obtained in [73], but by simplifying from two dimensional to unidirectional flow. A perturbation analysis of Ergun flow was also applied to a triangular domain [142] to infer various bounds for the flow solutions and approximate corrections to model Ergun rather than Darcy flow. Conformal mapping along with matched asymptotic expansions was used in [144] to obtain approximate solutions for incompressible Darcy flow in grain contained by a rectangular symmetrical bin geometry. However, in contrast to [100] and [89], the inlet where the gas entered the bin was treated as a finite curved shape instead of a point source and approximate flow solutions were obtained. The main focus was to understand the conditions under which the traverse time could be used to understand the heat and mass transfer processes that were considered in the study.

4.2 Model equations

The equation of motion used here to model phosphine flow driven by advection in grain storage is Darcy's law [23]

$$\boldsymbol{v} = -\frac{k}{\mu}\boldsymbol{\nabla} p, \tag{4.1}$$

which relates the pressure p and superficial velocity of the gas $\boldsymbol{v}$, defined as the volume of gas crossing a unit area of porous medium per unit time. This equation is accurate for low velocity flows [144] as considered here. A number of other modelling assumptions are also implied in the above formulation. For example, effects of gravity are neglected as the specific gravity of phosphine is similar to air [85]. We also assume negligible temperature variation in the grain bed during fumigation [46] and a uniform pore distribution with height. The permeability k and dynamic viscosity μ are taken as experimentally determined constants, which for the case of pure phosphine in wheat grain are $k = 5.78 \times 10^{-9}\,\mathrm{m}^2$[161], and

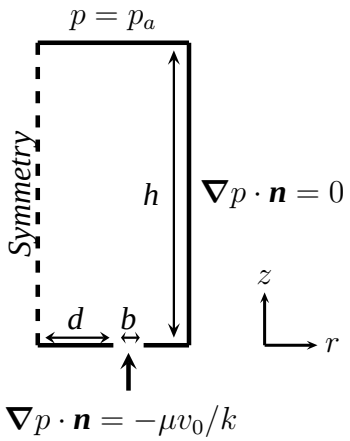

FIGURE 4.1: Axisymmetric vertical cross section of stored grain and the corresponding boundary conditions. Note that $d + b = f$.

$\mu = 1.1 \times 10^{-5}\,\mathrm{kgm^{-1}s^{-1}}$. Further, we assume incompressible flow [143, 145], so (4.1) is solved together with the continuity equation, $\boldsymbol{\nabla} \cdot \boldsymbol{v} = 0$. In this case, the pressure satisfies Laplace's equation $\nabla^2 p = 0$, which expressed in cylindrical coordinates (r, z) is

$$\frac{\partial^2 p}{\partial r^2} + \frac{1}{r}\frac{\partial p}{\partial r} + \frac{\partial^2 p}{\partial z^2} = 0. \tag{4.2}$$

The flow is calculated for a circular cylindrical grain store fumigated with phosphine from a single inlet attached to the base, as illustrated in Figure 4.1. The gas is pumped continuously at velocity $v_0\,\mathrm{m/s}$ into the grain bed through an inlet of size $b = f - d$, where d and f are the radial distances from the central symmetry line to the annular inlet's inner and outer radius, respectively. The case $d = 0$ corresponds to a circular inlet pipe. While in practice, the inlet is sometimes positioned at locations such as the vertical wall, for the purpose of this study the inlet location is restricted to the base to allow an axisymmetric analysis.

The surface $z = h$ is open to the atmosphere and the condition $p = p_a$ is used,

where p_a is the atmospheric pressure. The confining vertical wall and base of the grain bed are assumed impermeable, except at the inlet. Therefore, on the vertical wall (4.2) is solved subject to the zero normal velocity boundary condition

$$\boldsymbol{\nabla} p \cdot \boldsymbol{n} = 0 \qquad \text{for } r = a, \tag{4.3}$$

where $\boldsymbol{n}$ is the unit normal vector to the boundary and a is the radius. On the base $z = 0$ of the cylinder

$$\boldsymbol{\nabla} p \cdot \boldsymbol{n} = \begin{cases} 0 & 0 < r < d, \\ -\frac{\mu}{k} v_0 & d < r < f, \\ 0 & r > f. \end{cases} \tag{4.4}$$

4.3 Flow solution

4.3.1 Series solution for pressure, velocity, and streamlines

The governing equation (4.2) is separable and a solution $p(r, z) = f(r)g(z)$ can be found of the form

$$p(r, z) = Dz + E + \sum_{m=1}^{\infty} J_0\left(\frac{\alpha_m}{a} r\right) \left[A_m \cosh\left(\frac{\alpha_m}{a} z\right) + B_m \sinh\left(\frac{\alpha_m}{a} z\right)\right] \tag{4.5}$$

where α_m is the mth root of the Bessel function, $J_1(\alpha_m) = 0$. Application of the boundary conditions yields

$$D = -(f^2 - d^2)\frac{\mu v_0}{k a^2}, \tag{4.6}$$

$$E = p_a - Dh,$$

$$B_m = \frac{-2\mu}{k} v_0 \frac{\left[f J_1\left(\frac{\alpha_m}{a} f\right) - d J_1\left(\frac{\alpha_m}{a} d\right)\right]}{\alpha_m^2 [J_0(\alpha_m)]^2}, \tag{4.7}$$

and

$$A_m = \frac{-B_m \sinh\left(\frac{\alpha_m}{a} h\right)}{\cosh\left(\frac{\alpha_m}{a} h\right)}.$$

However, the solution as given above is computationally unsuitable in it's current form as the cosh and sinh terms in the series of (4.5) are prone to large numerical errors for evaluation at $z \approx h$. To prevent this, we replace those terms with their exponential forms and substitute A_m as

$$A_m = -B_m \left(\frac{1 - \exp(-\frac{2\alpha_m}{a} h)}{1 + \exp(-\frac{2\alpha_m}{a} h)}\right), \tag{4.8}$$

to obtain

$$p(r,z) = Dz+E+\sum_{m=1}^{\infty} J_0\left(\frac{\alpha_m}{a}r\right)\left(\frac{B_m\left[\exp(-\frac{\alpha_m}{a}(2h-z))-\exp(-\frac{\alpha_m}{a}z)\right]}{1+\exp(-\frac{2\alpha_m}{a}h)}\right) \quad (4.9)$$

which is more stable numerically. Also, the series (4.9) converges. To show the convergence using the limit comparison test, we first note that as m becomes large so does α_m and for large α_m [102],

$$J_n(\alpha_m) \approx \sqrt{\frac{2}{\pi\alpha_m}}\cos(\alpha_m - \frac{n\pi}{2} - \frac{\pi}{4}),$$

which yields $J_n(\alpha_m) \approx O(\alpha_m^{-1/2})$. Now, let

$$T_m = \frac{B_m\left[\exp(-\frac{\alpha_m}{a}(2h-z))-\exp(-\frac{\alpha_m}{a}z)\right]}{1+\exp(-\frac{2\alpha_m}{a}h)}. \quad (4.10)$$

For $z \neq 0$ and $z \neq h$, the mth term in (4.10) decreases exponentially, since it can be written as

$$-B_m\exp(-\frac{\alpha_m}{a}z)\left[1-\exp(-\frac{2\alpha_m}{a}h)-\exp(-\frac{2\alpha_m}{a}(h-z))+\exp(-\frac{2\alpha_m}{a}(2h-z))+...\right].$$

Furthermore, from (4.7), $B_m \approx O(\alpha_m^{-3/2})$ and therefore $T_m = O(\alpha_m^{-3/2}\cdot\exp(-\frac{\alpha_m}{a}z))$. Now, $\lim_{m\to\infty}\alpha_m = \infty$ and $\lim_{m\to\infty}(\alpha_{m+1}-\alpha_m) = \pi$. Thus $\lim_{m\to\infty} T_m = 0$ and

$$\lim_{m\to\infty}\frac{T_{m+1}}{T_m} = \left(\frac{\alpha_m+\pi}{\alpha_m}\right)^{-3/2}\exp(-\frac{\pi z}{a}) = \exp(-\frac{\pi z}{a}) \quad (= r < 1)$$

which converges by comparison with $\sum_{n=1}^{\infty} ar^n$ where $|r| < 1$. Given that (4.10) converges and $J_n(\alpha_m) \approx O(\alpha_m^{-1/2})$, the series (4.9) is also converges.

Having obtained the pressure, the radial (v_r) and axial (v_z) velocity components can be derived via (4.1) and are given by

$$v_r = \frac{k}{\mu}\sum_{m=1}^{\infty}\frac{\alpha_m}{a}J_1\left(\frac{\alpha_m}{a}r\right)\left(\frac{B_m\left[\exp(-\frac{\alpha_m}{a}(2h-z))-\exp(-\frac{\alpha_m}{a}z)\right]}{1+\exp(-\frac{2\alpha_m}{a}h)}\right) \quad (4.11)$$

and

$$v_z = -\frac{k}{\mu}\left\{D+\sum_{m=1}^{\infty}\frac{\alpha_m}{a}J_0\left(\frac{\alpha_m}{a}r\right)\left(\frac{B_m\left[\exp(-\frac{\alpha_m}{a}(2h-z))+\exp(-\frac{\alpha_m}{a}z)\right]}{1+\exp(-\frac{2\alpha_m}{a}h)}\right)\right\}. \quad (4.12)$$

Flow patterns can be described via the stream function (ψ), which is related to the velocity by the equations

$$v_r = \frac{1}{r}\frac{\partial\psi}{\partial z}, \qquad v_z = -\frac{1}{r}\frac{\partial\psi}{\partial r}.$$

Hence, after the necessary working

$$\psi(r,z) = \frac{1}{2}\frac{k}{\mu}Dr^2 + \frac{k}{\mu}\sum_{m=1}^{\infty} rJ_1\left(\frac{\alpha_m}{a}r\right)\left(\frac{B_m\left[\exp(-\frac{\alpha_m}{a}(2h-z)) + \exp(-\frac{\alpha_m}{a}z)\right]}{1+\exp(-\frac{2\alpha_m}{a}h)}\right). \tag{4.13}$$

To determine the likely influence of taking a fixed number of terms only of the infinite series solutions, we plot a representative comparison of the streamlines where between one and five terms of the series given in (4.13) are retained, as depicted in Figure 4.2. Note that only the lower part of the grain bed is shown for clarity because e.g. for heights greater than around 1.5 m the streamlines are virtually coincident. The plot indicates that the streamlines rapidly converge towards a single solution curve as the number of retained terms is increased, with the greatest discrepancies being visible in the region $z < 0.8$ when the number of retained terms is very small.

4.3.2 Leading order flow solution for semi-infinite height

Prior efforts suggest that a simplification in the limit of semi-infinite height may be adequate for modelling purposes [89]. To determine the applicability to our problem, representative streamlines for a range of grain heights are plotted as shown in Figure 4.3. The figure reveals that for heights above 3 m, the streamlines are indistinguishable by eye, suggesting that limiting solutions for semi-infinite height may be adequate for e.g. a 6 m high grain bed in a typical farm storage bin.

Now, by assuming that $h \to \infty$ and taking just one term of the series, the radial component of the velocity, (4.11), is approximated as

$$v_r = -\frac{\alpha_1}{a}\frac{k}{\mu}J_1\left(\frac{\alpha_1}{a}r\right)B_1\exp(-\frac{\alpha_1}{a}z) \tag{4.14}$$

and the stream function, from (4.13), is approximated as

$$\psi = \frac{1}{2}\frac{k}{\mu}Dr^2 + \frac{k}{\mu}rJ_1\left(\frac{\alpha_1}{a}r\right)B_1\exp(-\frac{\alpha_1}{a}z).$$

On a particular streamline we can assign $\psi = \psi_s$, where ψ_s is a constant. With some re-arrangement,

$$\frac{\psi_s}{r} - \frac{1}{2}\frac{k}{\mu}Dr = \frac{k}{\mu}J_1\left(\frac{\alpha_1}{a}r\right)B_1\exp(-\frac{\alpha_1}{a}z). \tag{4.15}$$

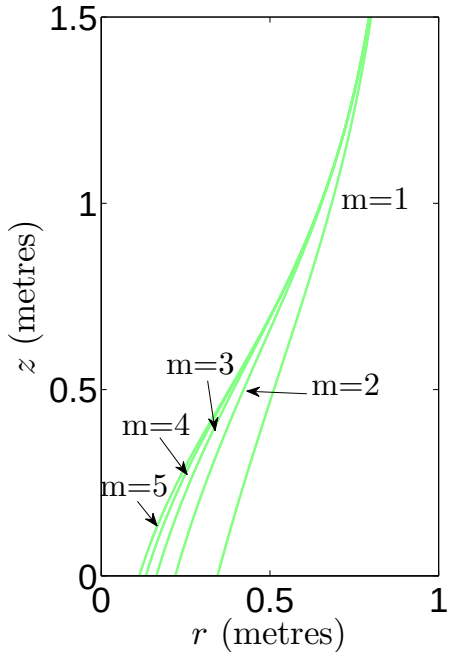

FIGURE 4.2: Streamline $\psi = -0.0008$, $d = 0$, $h = 6$ and $a = 2$ for a range of retained terms (m) in the series solution (4.13). v_0 is chosen corresponding to an inlet volumetric flow rate of $0.02514\,\mathrm{m}^3/\mathrm{s}$. Note that only part of the domain is shown for clarity.

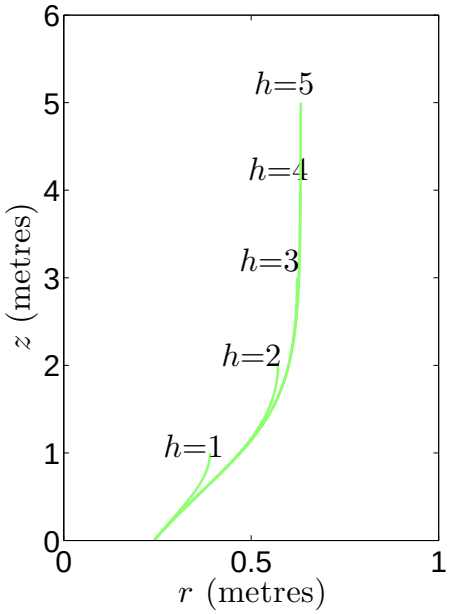

FIGURE 4.3: Streamline $\psi = -0.0004$, $d = 0$ and $a = 2$ for a range of grain surface heights by taking just one term of the series.

Equation (4.15) can be used to eliminate z and reduce (4.14) to

$$v_r = -\frac{\alpha_1}{a}\left(\frac{\psi_s}{r} - \frac{1}{2}\frac{k}{\mu}Dr\right). \tag{4.16}$$

4.4 Traverse time

As previously noted, during fumigation the time taken for the phosphine to reach a specified position is given by the traverse time τ [100], which can be obtained by solving

$$\frac{dr}{dt} = v_r, \qquad \frac{dz}{dt} = v_z \tag{4.17}$$

or alternatively in integral form

$$\tau = \int_0^r \frac{dr}{v_r} = \int_0^z \frac{dz}{v_z} \tag{4.18}$$

using the expressions for the velocity components given in (4.11) and (4.12) above. In general, the traverse time will need to be obtained via numerical means if two or more terms are retained in the series solutions for the velocity components derived earlier. For this purpose, the MATLAB ode45 solver was used to compute the solution of (4.17) with $m = 20$, unless otherwise indicated. We recall from Figure 4.2 that only approximately five terms are required to ensure convergence in (4.13).

4.4.1 Leading order traverse time solution for semi-infinite height

For the leading order $m = 1$ case, numerical integration is not required as a closed form solution for the traverse time can be obtained by applying (4.18) and substituting D from (4.6) into (4.16). The result can be expressed as

$$\tau = -\frac{a^3}{\alpha_1(f^2 - d^2)v_0}\ln\left(1 + \frac{(f^2 - d^2)v_0 r^2}{2a^2\psi_s}\right). \tag{4.19}$$

We note that (4.19) enforces that

$$0 < 1 + \frac{(f^2 - d^2)v_0 r^2}{2a^2\psi_s} < 1 \tag{4.20}$$

for $0 \leq r \leq a$. For the parameters chosen here (4.20) is indeed satisfied. We briefly consider however, the requirement on the parameters such that (4.20) is always satisfied.

Noting (4.6) and (4.15) and substituting into (4.20) we obtain, after some rearrangement, that

$$0 < 1 - \frac{1}{1 + \frac{2}{Dr} J_1\left(\frac{\alpha_1}{a} r\right) B_1 \exp(-\frac{\alpha_1}{a} z)} < 1. \tag{4.21}$$

Assuming that in-flow into the stored grain is positive (i.e $v_0 > 0$) then we note that $D < 0$. Furthermore, $J_1\left(\frac{\alpha_1}{a} r\right) \geq 0$ and $\exp(-\frac{\alpha_1}{a} z) > 0$. Thus, (4.21) can only be satisfied if $B_1 < 0$.

Noting from (4.7) that

$$B_1 = \frac{-2\mu}{k} v_0 \frac{\left[f J_1\left(\frac{\alpha_1}{a} f\right) - d J_1\left(\frac{\alpha_1}{a} d\right)\right]}{\alpha_1^2 [J_0(\alpha_1)]^2}, \tag{4.22}$$

we observe that $\frac{-2\mu}{k} v_0 < 0$ and $\alpha_1^2 [J_0(\alpha_1)]^2 > 0$. Thus $B_1 < 0$ only if

$$f J_1\left(\frac{\alpha_1}{a} f\right) > d J_1\left(\frac{\alpha_1}{a} d\right). \tag{4.23}$$

As long as (4.23) satisfied then (4.20) will be true. Furthermore given that (4.23) is satisfied then equation (4.15) yields that $\psi_s < 0$ (i.e the stream function is always negative).

Now returning to equation (4.19) we recall that it is applicable to an annular inlet setting $d = 0$, however, reduces the problem to the case of a centrally located inlet pipe and (4.19) becomes,

$$\tau = -\frac{a^3}{\alpha_1 (b^2) v_0} \ln\left(1 + \frac{b^2 v_0 r^2}{2a^2 \psi_s}\right). \tag{4.24}$$

Equation (4.24) can be compared to the approximate closed form solution for $d = 0$ with an assumed point source Q obtained in [100], which can be written as

$$\tau = \frac{\pi \epsilon a^2}{Q} \left(\left[2a \tanh^{-1} \frac{r}{a} - 2r\right]^{2/3} + \left[z - \frac{a}{\sqrt{2}} \arctan \frac{z\sqrt{2}}{a}\right]^{2/3} \right)^{3/2}. \tag{4.25}$$

Rewriting Q in terms of v_0 via $Q = \pi b^2 v_0$ and setting $\epsilon = 1$ in (4.25) yields

$$\tau = \frac{a^2}{b^2 v_0} \left(\left[2a \tanh^{-1} \frac{r}{a} - 2r\right]^{2/3} + \left[z - \frac{a}{\sqrt{2}} \arctan \frac{z\sqrt{2}}{a}\right]^{2/3} \right)^{3/2}. \tag{4.26}$$

4.5 Discussion of results

The previously presented closed form series solutions for the hydrodynamics permit a wide range of flow setups to be examined. As a practical application, results are interpreted here for phosphine fumigation of wheat in a representative 6 m high and 2 m radius cylindrical farm store with four different inlet positions corresponding to $d = 0$, 0.5, 1 and 1.5 m. However, the consequences of changing these parameters are also studied for applicability of the model to some larger scale storage facilities. Note that in all cases discussed, indicative values of $b = 0.2$ m and v_0 is chosen corresponding to an inlet volumetric flow rate of 0.02514 m^3/s is maintained for all inlet positions. Note also that our analytical solutions were checked against computed $d = 0$ results obtained in our earlier numerical study [101] using the FLUENT and COMSOL Computational Fluid Dynamic solvers. The predicted traverse times obtained by the computational modelling were in very good agreement with the analytic results presented below, and have been omitted for brevity.

The streamlines obtained from (4.13) and the corresponding traverse times, obtained from the solution of (4.17), are presented in Figure 4.4. Generally, Figure 4.4 (a–d) reveals that the streamlines spread out rapidly within the first 1 m from the base as the gas moves away from the inlet, as expected for this porous flow. Thereafter, the vertical wall confines the flow. The streamlines become almost parallel and the radial velocity component very small for $z > 1$ as the flow moves upward from the inlet towards the grain surface. Further, it can be seen from the figure that a sign change in the radial velocity component v_r with height is evident along some streamlines emanating from certain annular inlet locations. For example, for the case $d = 0.5$ the leftmost streamlines initially trace a path towards, and then away from, the central $r = 0$ symmetry line of the grain bed. The sign change in radial velocity is not evident in the $d = 0$ plot and therefore represents a behaviour distinct to the annular inlet configurations.

Also referring to Figure 4.4, the traverse time contours reveal that advection drives the flow to almost the entire grain bed within a duration of around one hour (3600 s), although not uniformly so. For a central circular inlet case ($d = 0$),

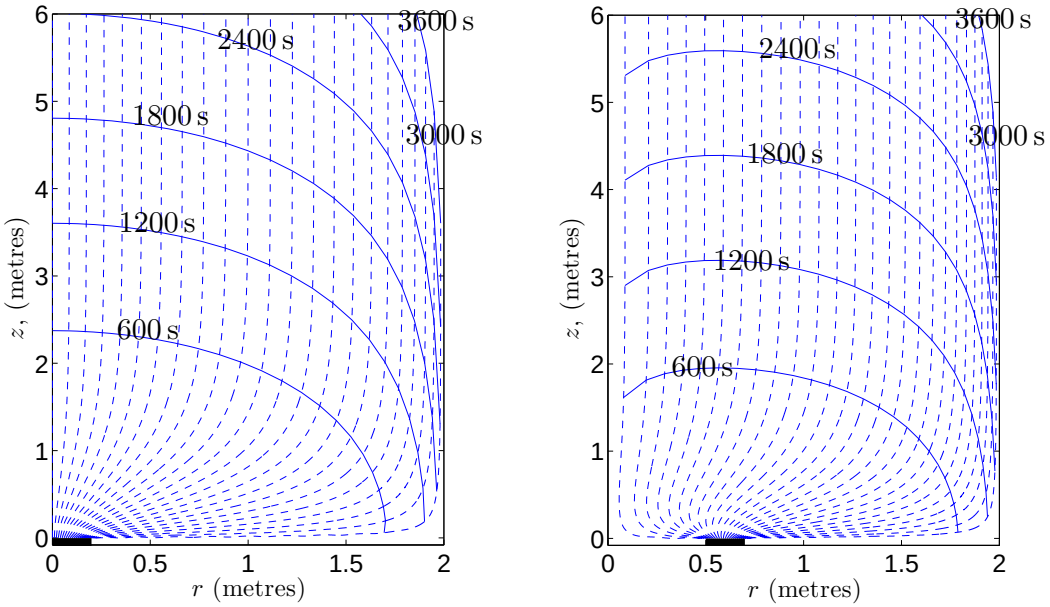

(a) $d = 0$ (b) $d = 0.5$

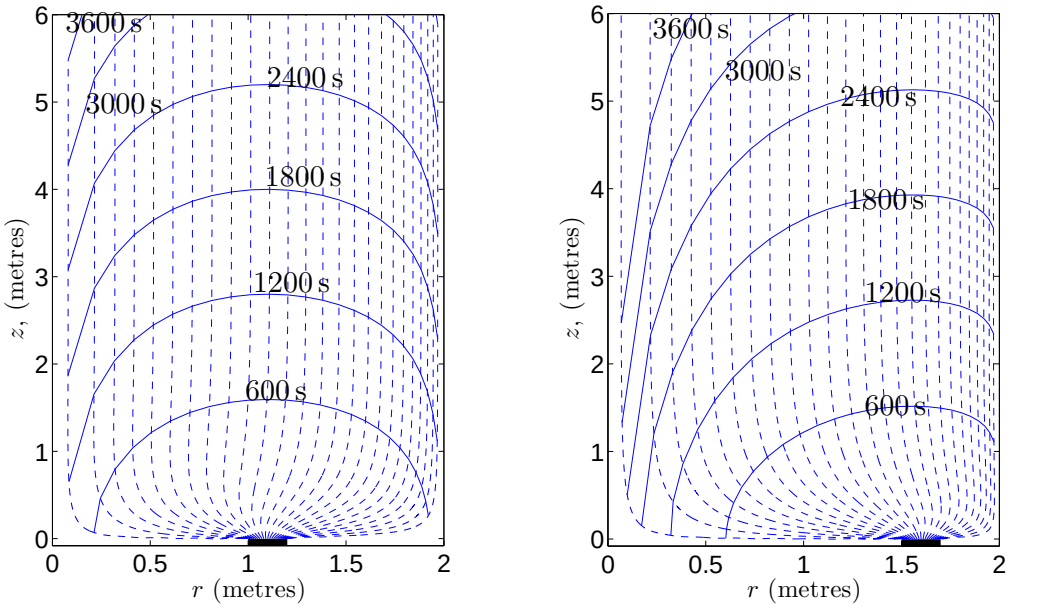

(c) $d = 1$ (d) $d = 1.5$

FIGURE 4.4: The streamlines (- - -), predicted by (4.13), and the traverse time lines(—), predicted by (4.17), for four different inlet positions ($d = 0, 0.5, 1.0, 1.5$ m).

regions where the injected fumigant takes longer to reach are near the vertical wall. In contrast, for the annular $d = 1.5$ inlet case, the corresponding region of slowest phosphine penetration is now near to the central $r = 0$ symmetry line of the grain bed. Although there are identifiable regions to where the gas is more slowly advected, a successful fumigation may still be still possible in a given time if other processes such as molecular diffusion are able to assist in the transport of phosphine to that area. For example, Phosphine has a diffusion coefficient of $1.59 \times 10^{-5}\,\mathrm{m}^2/\mathrm{s}$. This suggests that phosphine will diffuse approximately $0.06\,\mathrm{m}^2$ in 1 hour. In addition, the time taken might be faster due to, e.g. Taylor dispersion effects. Therefore, it is possible that the combination between advection, molecular diffusion, and dispersion will distribute phosphine to every area, but more complex modelling than undertaken in this work would be needed to determine the time to achieve this.

The flow solutions obtaining here also allow a study of the consequences for the flow and traverse time with respect to changes in radius. As an example, Figure 4.5 illustrates the effect of radius on the 900 s traverse time contour for a grain bed with a central $d = 0$ inlet pipe and height maintained at six metres. From the figure it can be seen that less time is needed for the fumigant to reach the same point on the $r = 0$ central symmetry line as the radius is decreased. Specifically, the flow reaches $z = 3\,\mathrm{m}$ on the centre line at 900 s for a radius of 2 m ($a = 2$), whereas the flow only reaches $z < 2.5\,\mathrm{m}$ height in stored grain with larger ($3 \leq a \leq 7$) radii. Additionally, for radii of 4 m or greater, the 900 s traverse time tends to become unaffected with further increases in radius, as expected due to the diminishing influence of the more distant confining vertical wall on the flow transport from the inlet to this contour. Although not shown for brevity, similar behaviour occurs for the three other annular inlet locations.

As a final comparison, Figure 4.6 shows traverse times obtained here via numerical integration of (4.17) using our series solutions (4.11) and (4.12), our leading order closed form solution (4.19), and the approximate analytic solution (4.26) of [100] for the case $d = 0$ and 2 m radius. Along the $r = 0$ symmetry axis, our leading order solution (4.19) remains in fair agreement with that obtained via numerical integration of (4.17) for increasing traverse time, as expected. In contrast,

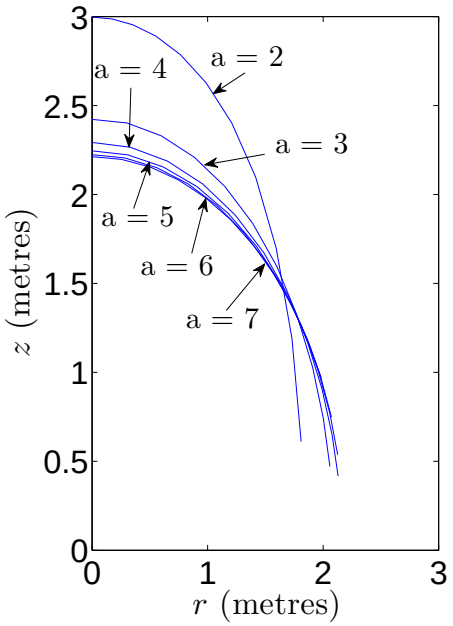

FIGURE 4.5: The traverse time at 900 s for a range of radii a, with an inlet at the floor center ($d = 0$) and height $h = 6$ m maintained.

Hunter's approximate analytic solution (4.26) increasingly over-predicts the axial flow distance travelled for increasing traverse time.

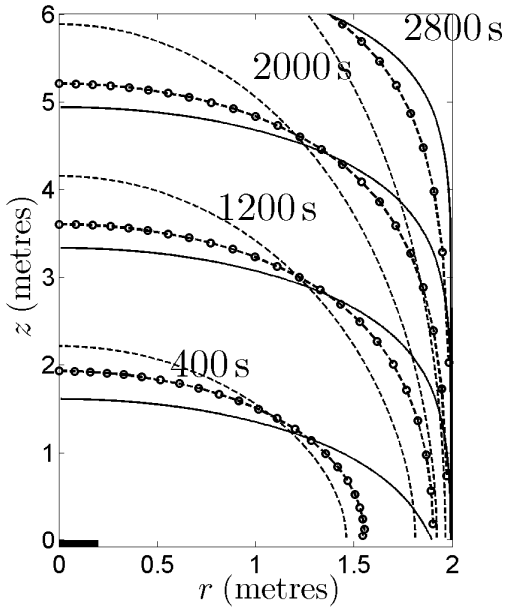

FIGURE 4.6: The traverse time comparison between numerical integration of (4.17) using series solutions (4.11) and (4.12) (-o- - o -), leading order closed form solution (4.19)(—), and Hunter's approximate analytic solution (4.26)(- - -), for the case $d = 0$ and $a = 2\,\mathrm{m}$.

4.6 Conclusion

In this study we have derived analytical series solution expressions for the pressure, flow field and streamlines for phosphine flowing through a cylindrical grain store during fan-forced fumigation. From these, traverse times were computed. Leading order closed form solutions for the flow field and traverse times were also derived. The work differs from prior analytic studies in that a more realistic finite width inlet source is considered, and cylindrical storage of arbitrary height or radius with an annular inlet is mathematically described. A centrally located inlet pipe attached to the silo base is covered as a special case.

Results are interpreted for the case of a wheat bed of height 6 m and radius 2 m, and indicate a number of points of interest. Firstly, the flow moves upward towards the grain surface, and the streamlines are almost parallel at $z > 1$, as expected. However, for the annular inlet case, a sign change in the radial velocity component of the flow along some of the streamlines is evident, in contrast to the central inlet pipe configuration where no such sign change is observed. Also, the advection drives phosphine to reach almost the entire grain bed with a traverse time of approximately one hour, although not uniformly so. Regions where fumigant will reach more slowly are evident and depend on the position of the annular inlet. Further, the traverse time is also found to be affected by the radius, with the influence of the wall proximity diminishing as the radius is increased.

In the fumigation context, if the processes of advection and diffusion can completely distribute the phosphine and no other factors are involved, a complete mortality should be achievable. However, in reality, successful fumigation is not always achieved due to possible issues such as gas leakage, gas sorption into grain, or highly resistant or mobile insects [103, 104], and these issues could provide a focus for future studies. For such studies, the results obtained in this paper should provide a useful starting point for conducting further research by, for example, providing accurate 3D axisymmetric flow and traverse time solutions against which to validate fully 3D computer simulations of more complex fumigant flow in grain storage.

Chapter 5

Mathematical modelling and numerical simulation of phosphine flow during grain fumigation in leaky cylindrical silos

The following paper is presented in this thesis chapter:

- Z.M.Isa, T.W.Farrell, G.R.Fulford and N. A.Kelson. Mathematical modelling and numerical simulation of phosphine flow during grain fumigation in leaky cylindrical silos. Submitted to Journal of Stored Product Research.

Statement of contribution of Co-Authors

The authors listed below have certified that:

1. they meet the criteria for authorship in that they have participated in the conception, execution, or interpretation, of at least that part of the publication in their field of expertise;
2. they take public responsibility for their part of the publication, except for the responsible author who accepts overall responsibility for the publication;
3. there are no other authors of the publication according to these criteria;
4. potential conflicts of interest have been disclosed to (a) granting bodies, (b) the editor or publisher of journals or other publications, and (c) the head of the responsible academic unit, and
5. they agree to the use of the publication in the student's thesis and its publication on the QUT ePrints database consistent with any limitations set by publisher requirements.

In the case of Chapter 5: Z.M.Isa, T.W.Farrell, G.R.Fulford and N. A.Kelson. Mathematical modelling and numerical simulation of phosphine flow during grain fumigation in leaky cylindrical silos. Submitted to Journal of Stored Product Research.

Contributor	Statement of contribution
Zaiton M.Isa	Developed the multicomponent species transport model, conducted CFD simulations, interpreted the numerical results, wrote the manuscript, acted as corresponding author. Signature: [signature] Date: 16/7/2014
Troy W. Farrell	Guided the development of the multicomponent model, assisted with the interpretation of results and preparation of paper and proof read the manuscript.
Glenn R. Fulford	Guided the development of the model, assisted with the interpretation of results and preparation of paper and proof read the manuscript.
Neil A. Kelson	Guided the development of the model, assisted with the interpretation of results and preparation of paper and proof read the manuscript.

Principal Supervisor Confirmation

I have sighted email or other correspondence from all Co-authors confirming their certifying authorship.

Name: Troy Farrell Signature: [signature] Date: 16/07/14

Abstract

The phosphine distribution in a cylindrical silo containing grain is predicted. The transport model is a three-dimensional mathematical model, which accounts for a multicomponent gas phase along with a grain phase. The model also accounts for sorption of phosphine into the grain kernel. In addition, a simple model is presented to describe the death of insects within the grain as a function of their exposure to phosphine gas. The proposed model is solved using the commercially available computational fluid dynamics (CFD) software, FLUENT, together with our own C code to customize the solver in order to incorporate the models for sorption and insect extinction. Two types of fumigation delivery are studied, namely, fan-forced from the base of the silo and tablet from the top of the silo. An analysis of the predicted phosphine distribution shows that during fan forced fumigation, the position of the leaky area is very important to the development of the gas flow field and the phosphine distribution in the silo. If the leak at the lower section of the silo, insects that exist near the top of the silo may not be eradicated. However, the position of a leak does not affect phosphine distribution during tablet fumigation. For such fumigation in a typical silo configuration, phosphine concentrations remain low near the base of the silo. Furthermore, we find that half-life pressure test readings are not an indicator of phosphine distribution during tablet fumigation.

5.1 Introduction

Phosphine gas has been the most preferred fumigant to kill stored grain insects since the mid-1990s [59]. It remains the most relied upon fumigant [47, 96, 154] and comprises approximately 80% of the fumigant usage in Australia [71]. The advantages of phosphine over other fumigants are the low price, ease of application, and minimal residue [35, 43, 50, 60, 132].

However, phosphine sorption into grain kernels has been proven to occur, as described by several authors [17, 49, 70, 72, 82, 135]. Furthermore, the importance of silo sealing has been mentioned to affect phosphine distribution [11, 112, 131, 154, 156]. Both sorption and leakage contribute to an insufficient application rate,

which encourages the development of resistance in grain pests. Such resistance can lead to significance grain loss and has threatened the use of phosphine as a sustainable argichemical [61, 67, 109, 117, 133]. To date, however, alternatives to phosphine are unavailable, since methyl bromide was phased out under the Montreal Protocol on substances that deplete the ozone layer [112, 113, 136].

In view of the above, it is very important to carefully conduct fumigation to make sure that there are no chances of insufficient dosage. Hence, preventing the need for multiple fumigation, which encourages the development of resistance. To achieve this, a good understanding of fumigant behaviour is crucial. Performing field experiments is expensive to organize, and hence, mathematical modelling and computer simulation are alternative, possibly beneficial tools.

Unfortunately, little is known about the behaviour of fumigants in grain storage at this point [59]. In addition, comprehensive studies on the modelling of phosphine distribution in grain silos are lacking, regardless of the application method of fumigation.

Commonly, phosphine is applied through a fan-forced system or tablet formulation. Fan-forced fumigation involves injecting gas through an inlet near the base of the silo. In contrast, tablet fumigation involves placing solid tablets on a basket near the grain surface at the top of the silo, which then dissolve via their interaction with air and moisture.

The aim of this work is to develop a relatively complete model of a leaky grain storage silo, typical of those found in on-farm situations. Given the nonlinear nature of this model and the complicated domain on which it is defined, it is unlikely that closed form analytical solutions exist. Hence a computational fluid dynamics (CFD) approach is used to solve the model equations and investigate the effect of silo gas tightness on the ensuing concentration and flow fields.

A previous study in [16] proposed a mathematical model to predict the average phosphine concentration over time during tablet fumigation. Spatial variation of the gas concentration within the grain is ignored. Given the considerable size of most silos, this is unrealistic. Although leakage and sorption were considered, for simplification, they were both modelled as a constant.

A relatively small number of studies using computational fluid dynamics (CFD)

exist in the literature. For example, [32] predicted the gas flow and heat transfer of a mixture of carbon dioxide and oxygen in a silo with leaky holes at the top boundary. Although a multicomponent gas is considered, sorption of gas into the grain kernel is not accounted for nor is degradation of the phosphine over time, which has proven to be important [70, 72].

The work in [112] investigated the movement of phosphine in a horizontal storage. The fan-forced fumigation involve a gas that is delivered through eight injection inlets and exits through eight recirculation suction outlets. Unfortunately, the model equations are not given. The focus of this work is on the use of CFD to simulate the proposed system. Other examples are the works concerning the distribution of the fumigant, sulphuryl fluoride, in a flour mill [54, 56, 57]. In these works, the whole building was the attention rather than a single storage bin. In addition, the development of the transport modelling equations is not clear.

For tablet fumigation most of the modelling studies of the fumigant distribution have focused on CO_2 gas rather than phosphine. Those in [8, 9, 143, 145] look at CO_2 released from dry ice into a cylindrical storage bin. In these models the dry ice is placed at the bottom of the storage rather than on the surface of the grain or inside the silo. Although the transport model is similar to this present study, sorption and leakage are not considered.

Importantly, none of the theoretical modelling studies mentioned here have tried to account for insect extinction.

Experimentally, phosphine gas distribution has been studied in [35, 42, 49, 105, 157]. With the exception of [105], the experiment incorporate well sealed, large scale silos that range between 2000 to 7000 tonnes (approximately 2600 m^3 to 9210 m^3), whereas here, we consider a small scale "on farm silo" (approximately 100 m^3 or $\approx$ 76 tonne). The experiments in [105] do involve tablet fumigation within a small size silo (240 tonne). However, the silo is equipped with a gas recirculation system, which is beyond the scope of our current investigation as it is not common on farm.

The lack of a comprehensive model for typical small scale (on-farm) grain fumigation practices serves as a primary motivation for this work. In contrast to the reported studies, the present model is developed by considering a binary gas

flow (phosphine and air) in a three-dimensional cylindrical silo filled with grain. Absorption of phosphine into the grain, degradation of the phosphine over time in the silo and extinction of grain pests are included in the current model. In addition, both fan forced and tablet fumigation regimes are considered for silos that range in their "integrity" from being air tight to moderately leaky.

This present study focuses on fumigation with phosphine in accordance with on-farm practices. Although grain storage comes in a range of shapes and sizes, a vertical silo is considered here since this is the most popular method of storing grain, constituting 79% of all on farm storage types [156]. Generally, fan-forced fumigation on farms is unusual since for small silos tablet fumigation is considered to be adequate, however, the results obtained here provides a comparison between the two types of delivery method.

5.2 Model development

Figure 5.1 shows the view of the typical cylindrical silo considered here. The coordinate r (m) denotes the radial distance from the origin ($r = 0$), θ (radians) is the angle from a fixed axis, and z (m) is the vertical height of the silo. Inside the silo, grain occupies the silo up to the height $z = h$ (m) and is porous, while the region from $z = h$ to $z = L$ (m) is called the headspace and is non-porous.

The model assumes that no water or excess water vapour is present, and that the gas present in the pores is a binary mixture of air and phosphine. Therefore, in the porous zone, the total volume will consist of grain and gas such that,

$$\varepsilon_{\text{gr}}(\mathbf{x}) + \varepsilon_g(\mathbf{x}, t) = 1 \tag{5.1}$$

where ε_{gr} and ε_g are the volume fractions of grain and gas, respectively. Furthermore,

$$\varepsilon_g(\mathbf{x}, t) = \varepsilon_{\text{air}}(\mathbf{x}, t) + \varepsilon_{\text{ph}}(\mathbf{x}, t) \tag{5.2}$$

where ε_{air} and ε_{ph} are the volume fractions of air and phosphine gas, respectively. The volume fraction of grain, $\varepsilon_{\text{gr}}(\mathbf{x})$, is considered to be static over time, which means that any deformation of the grain, for example via the consumption of grain by pests, or compaction due to gravity is ignored.

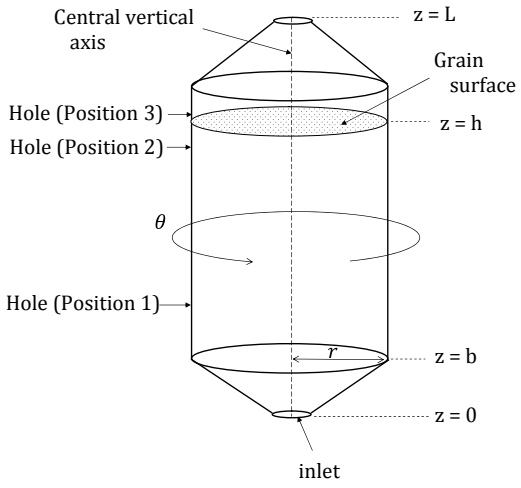

FIGURE 5.1: Schematic of the cylindrical silo (not to scale) considered in this work.

The gas is considered to be an ideal mixture of ideal gases, such that the total gas pressure, $P_g(\boldsymbol{x}, t)$ (Pa), is the sum of the air pressure, P_{air} (Pa), and phosphine pressure, P_{ph} (Pa), namely,

$$P_g = P_{\text{air}} + P_{\text{ph}}. \tag{5.3}$$

Furthermore,

$$P_i = \frac{\rho_i RT}{M_i}, \quad (i = \text{air}, \text{ph}) \tag{5.4}$$

where $\rho_i(\mathbf{x}, t)$ (kg m^{-3}) is the density of component i, R ($\text{J K}^{-1}\text{mol}^{-1}$) is the ideal gas constant, T (K) is the temperature (assumed constant) and M_i is the molar mass of component i.

In using FLUENT [3] to simulate gas flow in our grain silo, the gas velocity, $\boldsymbol{v}_g$ is governed by the equation of motion

$$\frac{\partial}{\partial t}(\varepsilon_g \rho_g \boldsymbol{v}_g) + \boldsymbol{\nabla} \cdot (\varepsilon_g \rho_g \boldsymbol{v}_g \boldsymbol{v}_g) = -\boldsymbol{\nabla} P_g + \boldsymbol{\nabla} \cdot (\varepsilon_g \boldsymbol{\tau}) + \varepsilon_g \rho_g \mathbf{g} + \varepsilon_g \boldsymbol{F}, \tag{5.5}$$

where t (s) is time, ρ_g (kg m^{-3}) is the density of gas, $\boldsymbol{\tau}$ ($\text{kg m}^{-2}\text{s}^{-2}$) is the viscous stress tensor, $\mathbf{g}$ (m s^{-2}) is acceleration due to gravity and $\boldsymbol{F}$ (N m^{-3}) are the external forces on the gas per unit volume.

Noting (5.4), we may rewrite (5.3) to define the density of gas in (5.5) as

$$\rho_g = \frac{P_g}{RT\sum_i \frac{\omega_i}{M_i}}, \quad (i = \text{air}, \text{ph}), \tag{5.6}$$

where $\omega_i = \rho_i/\rho_g$, is the mass fraction of component i in the gas phase.

In FLUENT, for compressible flow

$$P_g = P_{\text{op}} + P_{\text{gauge}} \tag{5.7}$$

where P_{op} (Pa) is the operating pressure and P_{gauge} (Pa) is the local relative pressure predicted by FLUENT. During all simulations, P_{op} =101325 Pa (i.e. 1 atm).

In addition in (5.5), $\boldsymbol{\tau}$ is given in [3],

$$\boldsymbol{\tau} = \mu_g \left[\left(\boldsymbol{\nabla v} + \boldsymbol{\nabla v}^T \right) - \frac{2}{3} \boldsymbol{\nabla} \cdot \boldsymbol{v} \mathbf{I} \right] \tag{5.8}$$

where $\mu_g(\mathbf{x}, t)$ ($\text{kgm}^{-1}\text{s}^{-1}$) is the dynamic viscosity of the gas and $\mathbf{I}$ is the unit tensor. The dynamic viscosity of the air and phosphine mixture is calculated from kinetic theory, such that [33],

$$\mu_g = \sum_i \frac{X_i \mu_i}{\sum_j X_j \phi_{ij}}, \quad (i = \text{air}, \text{ph}; \text{j} = \text{air}, \text{ph}). \tag{5.9}$$

Here, X_i is the mole fraction of species i, and the dimensionless quantities ϕ_{ij} are given by,

$$\phi_{ij} = \frac{1}{\sqrt{8}} \left(1 + \frac{M_i}{M_j} \right)^{-1/2} \left[1 + \left(\frac{\mu_i}{\mu_j} \right)^{1/2} \left(\frac{M_j}{M_i} \right)^{1/4} \right]^2 \quad (i = \text{air}, \text{ph}; \text{j} = \text{air}, \text{ph}), \tag{5.10}$$

where M_i is the molecular weight (kgmol^{-1}) of gas species i.

Finally in (5.5), $\boldsymbol{F}$ is a frictional force due to the resistance to flow in the porous material and is given in [3],

$$\boldsymbol{F} = -\left(\frac{\mu_g}{K_g} + \frac{C_2 \rho_g}{2} |\boldsymbol{v}| \right) \boldsymbol{v} \tag{5.11}$$

where C_2 (m^{-1}) is a constant and $K_g(\mathbf{x}, t)$ (m^2) is the gas permeability (here, in the absence of a liquid phase, equal to the intrinsic permeability of the grain).

Let us now define the conservation of the gas mass in the porous region. In this region, the gas is in contact with the grain, in which sorption of phosphine occurs [17, 49, 82, 135]. Therefore, for phosphine,

$$\frac{\partial(\varepsilon_g \rho_g \omega_{\text{ph}})}{\partial t} + \boldsymbol{\nabla} \cdot (\varepsilon_g \rho_g \omega_{\text{ph}} \boldsymbol{v}_g) = \boldsymbol{\nabla} \cdot (\varepsilon_g \rho_g D_{\text{eff}}^{\text{ph}} \boldsymbol{\nabla} \omega_{\text{ph}}) - B_1 \varepsilon_g \rho_g \omega_{\text{ph}} + B_2 \rho_g \omega_{\text{ph}}^{\text{gr}} \tag{5.12}$$

and

$$\frac{\partial \rho_g \omega_{\text{ph}}^{\text{gr}}}{\partial t} = B_4 \varepsilon_g \rho_g \omega_{\text{ph}} - B_3 \rho_g \omega_{\text{ph}}^{\text{gr}}. \tag{5.13}$$

where ω_{ph} and $\omega_{\text{ph}}^{\text{gr}}$ are the phosphine mass fractions in the gas and grain, respectively and $t\,(\text{s})$ is time. The parameters B_1, B_2, B_3, and B_4 are constant. The sorption term represented in the last two terms of (5.12) and (5.13) is adopted from the model suggested in [70], which asserts that phosphine is absorbed into the grain and at the same time also degrades in air. Both of these processes are taken into consideration through the parameters, B_1 to B_4.

Without sorption, the conservation equation for air is

$$\frac{\partial (\varepsilon_g \rho_g \omega_{\text{air}})}{\partial t} + \boldsymbol{\nabla} \cdot (\varepsilon_g \rho_g \omega_{\text{air}} \boldsymbol{v}_g) = \boldsymbol{\nabla} \cdot (\varepsilon_g \rho_g D_{\text{eff}}^{\text{air}} \boldsymbol{\nabla} \omega_{\text{air}}). \tag{5.14}$$

The parameters D_{eff}^i $(\text{m}^2\text{s}^{-1})$ in (5.12) and (5.14) are the effective diffusivities of phosphine and air, respectively, and are given by

$$D_{\text{eff}}^i = \tau D_\infty^i \varepsilon_g^{3/2}, \quad (i = \text{air}, \text{ph}) \tag{5.15}$$

where τ is the tortuosity of the grain as a porous medium, and D_∞^i $(\text{m}^2\text{s}^{-1})$ is the diffusivity of component i in the absence of any porous structure. Transport is assumed to be isotropic.

In the non-porous region, at the top of the silo, the grain is not present, which means $\varepsilon_g = 1$. Here, the velocity satisfies the equation of motion (5.5) with $\mathbf{F} = 0$, such that

$$\frac{\partial}{\partial t}(\rho_g \boldsymbol{v}) + \boldsymbol{\nabla} \cdot (\rho_g \boldsymbol{v}\boldsymbol{v}) = -\boldsymbol{\nabla} P_g + \boldsymbol{\nabla} \cdot (\boldsymbol{\tau}) + \rho \mathbf{g}. \tag{5.16}$$

Furthermore, there is no grain for phosphine sorption. Hence, air and phosphine share the same conservation equation, namely,

$$\frac{\partial (\rho_g \omega_i)}{\partial t} + \boldsymbol{\nabla} \cdot (\rho_g \omega_i \boldsymbol{v}) = \boldsymbol{\nabla} \cdot (\rho_g D_{\text{eff}}^i \boldsymbol{\nabla} \omega_i) \quad (i = \text{air}, \text{ph}). \tag{5.17}$$

5.2.1 Population extinction

It is known that the effect of phosphine on the mortality of grain insects is due to both the level of the phosphine concentration and the time of exposure. A modified

Haber's rule has been proposed in [61, 67, 68], to capture this joint dependency where

$$C^n t_{0.999} = K. \tag{5.18}$$

Here, C (mg/L) is the concentration of phosphine and $t_{0.999}$ (s) is the time to kill at least 99.9% of the insect population, which is usually taken as an indicator of extinction. The constants n and K are empirical and only depend on the particular species and strain of insect. For one particular grain pest, *Rhyzopertha dominica.*, the strongly resistant genotype has values measured in [61] of $n = 0.6105$ and $K = 349090$. These values are adopted in our model.

Noting (5.18), we define an extinction indicator function, $e(\mathbf{x}, t)$, as

$$e(\mathbf{x}, t) = 1 - \frac{1}{K} \int_0^t C(\mathbf{x}, t)^n dt. \tag{5.19}$$

Here we note that $e(\mathbf{x}, t)$ accounts for the period of exposure to phosphine that an insect has encountered. We assume that it is the cumulative dosage of fumigant (as determined by the integral term in (5.19)) that is important in killing pests and we contest that when the cumulative dosage given to a particular pest reaches K then the pest will die. From (5.19) we see that for a given point in the grain, when $t < t_{0.999}$ (i.e. the cumulative dose of fumigant is less than K) then we have $e(\mathbf{x}, t) > 0$ and, assuming that grain insects are sedintary, we can interpret this as meaning that some measurable number of insects at this point in the grain are still alive. Similarly, when $t \geq t_{0.999}$ then $e(\mathbf{x}, t) \leq 0$, meaning that at least 99.9% of the insect population at this point have been killed.

To incorporate the above extinction model into FLUENT, we solve for the time derivative form of (5.19). In terms of the concentration variables used in the transport model this becomes,

$$\frac{\partial e(\mathbf{x}, t)}{\partial t} = -\frac{1}{K}(10^3 \rho_g \omega_{\text{ph}})^n, \tag{5.20}$$

where 10^3 is the conversion factor from kg/m^3 to mg/L (i.e. $1\,\text{kg/m}^3 = 10^3\,\text{mg/L}$). Furthermore, (5.20) is solved subject to the initial condition $e(\mathbf{x}, 0) = 1$.

As previously mentioned, two types of phosphine application are considered in this paper. Therefore, the following boundary conditions are separated into fan forced and tablet fumigation sections, respectively.

5.2.2 Fan-forced fumigation

During fan-forced fumigation, the fumigant is delivered through an inlet as shown in Figure 5.1. Typically, gas enters the silo through the inlet with a mass flow rate (depending on the capability of the equipment) ranging between 1.2kg/hr - 12 kg/hr [47]. Hence, at the inlet,

$$(\varepsilon_g \rho_g D^i_{\text{eff}} \boldsymbol{\nabla} \omega_i - \varepsilon_g \rho_g \omega_i \boldsymbol{v}_g) \cdot \widehat{\mathbf{z}} = \frac{\dot{m}}{A_{\text{in}}}. \tag{5.21}$$

where $\widehat{\mathbf{z}}$ is a unit normal vector in the z-direction, $\dot{m}$, (kgs^{-1}) is the mass flow rate of gas and A_{in} (m^2) is the inlet area. This mass flow rate is related to the volumetric flow rate Q (m^3s^{-1}) as

$$\dot{m} = \rho_g Q. \tag{5.22}$$

Most grain silos are not gas tight. To investigate the effect of gas leakage on fumigation, we consider here a silo with a single circular hole at various positions in its side wall. A pressure drop boundary condition is assumed to hold at the position of the hole; specifically, the change in pressure is assumed to be proportional to the dynamic head of the fluid, namely [54, 56],

$$\Delta P = P_g - P_{\text{atm}} = \frac{1}{2} k_L \rho_g \left| \boldsymbol{v}_g \right|^2, \tag{5.23}$$

where $P_{\text{atm}} = 101325\,\text{Pa}$, and k_L is a constant of proportionality known as loss coefficient. The value of k_L determines the "leakiness" of the silo.

At all wall boundaries we enforce no flux conditions in the direction normal to the surface, namely,

$$(\varepsilon_g \rho_g D^i_{\text{eff}} \boldsymbol{\nabla} \omega_i - \varepsilon_g \rho_g \omega_i \mathbf{v}_g) \cdot \mathbf{n} = 0, \tag{5.24}$$

where $\mathbf{n}$ is a unit vector normal to the wall. Furthermore, we also apply a no slip condition to the walls of the silo.

At time $t = 0$,

$$\omega_{\text{air}} = 1, \quad \omega_{\text{ph}} = 0 \quad \text{and} \quad \rho_{\text{g}} = \rho^{\text{atm}}_{\text{air}}, \tag{5.25}$$

where $\rho^{\text{atm}}_{\text{air}}$ (kgm^{-3}) is the density of air at 1 atm pressure and 25° C.

Equations (5.12) to (5.17) in addition to the boundary conditions (5.21), (5.23), and (5.24), and the initial conditions (5.25) are our governing equations for the fumigant transport in the grain silo under the condition of fan-forced fumigation.

5.2.3 Tablet fumigation

To model tablet fumigation we modify the domain in Figure 5.1 to include a homogeneous "tablet zone" from $z = h$ to $z = h_t$ $(0 < h_t << L - h)$, with the "headspace zone" then stretching from $z = h_t$ to $z = L$. In the tablet zone, phosphine gas, generated from the sublimation of phosphine tablets, is introduced as a source term, S_t $(\mathrm{kg\,m^{-3}s^{-1}})$, in the phosphine conservation equations, but not in air. Therefore, within the tablet zone, equation (5.17) takes the form,

$$\frac{\partial(\rho_g \omega_{\mathrm{ph}})}{\partial t} + \boldsymbol{\nabla} \cdot (\rho_g \omega_{\mathrm{ph}} \boldsymbol{v}) = \boldsymbol{\nabla} \cdot (\rho_g D^i_{\mathrm{eff}} \boldsymbol{\nabla} \omega_{\mathrm{ph}}) + S_t, \tag{5.26}$$

for phosphine and

$$\frac{\partial(\rho_g \omega_{\mathrm{air}})}{\partial t} + \boldsymbol{\nabla} \cdot (\rho_g \omega_{\mathrm{air}} \boldsymbol{v}) = \boldsymbol{\nabla} \cdot (\rho_g D^i_{\mathrm{eff}} \boldsymbol{\nabla} \omega_{\mathrm{air}}) \tag{5.27}$$

for air and these are solved in place of (5.17) in this zone.

For every $1\,\mathrm{m}^3$ of storage volume, 1.5 tablets are needed [154]. The tablets are assumed to be evenly placed on the grain surface. The tablets are 3 g in weight and each tablet can produce 1 g of phosphine gas [12]. Normally, the tablet disolves completely within 3 days [40]. Based on this information and the experimental study of Xianchang [160], the rate of evolution of phosphine is implemented here as,

$$S_{\mathrm{evol}} = \frac{A X_{\mathrm{tab}}}{\sigma\sqrt{\pi}} \exp\left[-\frac{1}{2}\left(\frac{t - \mu_{\mathrm{tab}}}{\sigma}\right)^2\right]. \tag{5.28}$$

Here $S_{\mathrm{evol}} = S_t \mathrm{V}_{\mathrm{tab}}$ $(\mathrm{kg\,s^{-1}})$ where $\mathrm{V}_{\mathrm{tab}} = \pi r^2 (h_t - h)$ (m^3) is the volume of the tablet zone, A (kg), μ_{tab} (s), and σ (s) are constants and X_{tab} is the number of tablets in the tablet zone. The height of the tablet zone $(h_t - h)$ is taken to be fixed at 0.01 m, which is approximately the height of a tablet. Based on the results of Xianchang and assuming $X_{\mathrm{tab}} = 150$, we find that the best fit of (5.28) with the experimental data is given when $A = 1.559 \times 10^{-3}$, $\mu_{\mathrm{tab}} = 2.88 \times 10^4$ and $\sigma = 7.92 \times 10^4$. Figure 5.2 compares the output of (5.28) under these conditions with the experimental data of Xianchang at $T = 20^\circ$ C and $T = 30^\circ$ C. We note that in our simulation, we take $T = 25^\circ$ C and thus a model curve that sits between the two experimental curves, as ours does, is preferred.

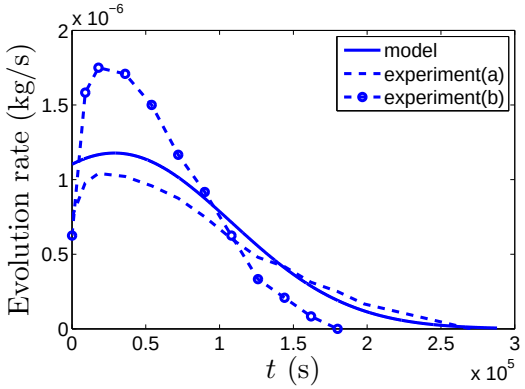

FIGURE 5.2: Rate of evolution of phosphine from tablet during fumigation based on 150 tablets. Comparison is made with the experiment conducted by Xianchang [160] at (a) 20° C and (b) 30° C.

For tablet fumigation the gas is not injected through the inlet, hence the inlet is replaced with a wall condition as in (5.24). At the outlet (hole), the boundary conditions remain as in (5.23).

Equations (5.12) to (5.17) in addition to the equations (5.26) to (5.28), boundary conditions (5.23) and (5.24), and initial conditions (5.25) are our governing equations for the fumigant transport in the grain silo under tablet fumigation.

The parameters used in this paper are given in Table 5.1. The diffusivity D^i_{eff} of air is taken to be that for nitrogen in air, noting that almost 80% volume of air is nitrogen. The values n and K for the extinction model are taken from [61] for strongly resistant *R. dominica*. In the tablet fumigation model, X_{tab} is equivalent to 150 tablets corresponding to the recommended tablet number for a silo size of $100\,\text{m}^3$ as studied here. All of the simulations are undertaken at 298 K (25^oC) as this is the average grain temperature in Australia [61].

As previously mentioned the model equations for fan-forced and tablet fumigation were implemented in FLUENT. The governing equations are spatially discretized using the second order upwind scheme. Simulations were run on a high performance computer. An unstructured tetrahedral mesh is used with a local

Parameter	Value	Comment/Reference
A	1.559×10^{-3} (kg)	Fitted to data of (5.28)
b	1.2 (m)	Dimension of the silo in Figure 5.1
h	8.2 (m)	Dimension of the silo in Figure 5.1
L	9.4 (m)	Dimension of the silo in Figure 5.1
r	2 (m)	Dimension of the silo in Figure 5.1
B_1	8.0833×10^{-6} (s^{-1})	Calculated from [70]
B_2	2.6916×10^{-5} (s^{-1})	Calculated from [70]
B_3	3.6111×10^{-5} (s^{-1})	Calculated from [70]
B_4	6.0833×10^{-6} (s^{-1})	Calculated from [70]
D^i_∞	2.1×10^{-5} (m^2s^{-1}) (air)	For N_2 in air [36]
	1.59×10^{-5} (m^2s^{-1}) (phosphine)	[112]
K_g	5.78×10^{-9} (m^2) (wheat)	[161]
K	349090	Calculated from[61]
M	28.97×10^{-3}($kgmol^{-1}$) (air)	[33]
	34×10^{-3} ($kgmol^{-1}$)(phosphine)	[19]
n	0.6105	[61]
R	8.31 ($JK^{-1}mol^{-1}$)	[19]
ε_g	0.43	[143]
μ_i	1.87×10^{-5} ($kgm^{-1}s^{-1}$)(air)	[74]
	1.1×10^{-5} ($kgm^{-1}s^{-1}$)(phosphine)	[86]
ρ_i^{atm}	1.165 (kgm^{-3})(air)	At 303K [74]
$\boldsymbol{\tau}$	2.4	[119]
P_{atm}	101325 Pa	
T	298 K	
μ_{tab}	2.88×10^4 (s)	Fitted to data of (5.28)
σ	7.92×10^4 (s)	Fitted to data of (5.28)
V_{tab}	0.12566 (m^3)	Calculated from $\text{V}_{\text{tab}} = \pi r^2(h_t - h)$
X_{tab}	150	Based on recommended dosage [154]

TABLE 5.1: Parameters used in the model.

refinement at the inlet. A mesh comprising of 73413 cells and a time step of 900 s were found to produce mesh independent results. During simulations the solution is converged to a tolerance of 1×10^{-5} in all variables.

5.3 Model results and discussion

The simulations conducted here involve fumigation in the three-dimensional silo shown in Figure 5.1. The physical dimensions of the silo are given in Table 5.1 and the total volume is approximately 100 m^3. Two positions of leaky holes (with radius of 0.015 m) are studied for each type of fumigation delivery. For fan-forced fumigation, the first, referred hitherto as Position 1, is located on the sidewall 3.2 m above the base (inlet) of the silo, whilst the second, referred hitherto as Position 2, is located on the sidewall 7.7 m above the base (inlet) of the silo. For tablet fumigation, the first hole is also located at Position 1, but the second, is referred hitherto as Position 3, is located on the sidewall 0.1 m above the tablet zone.

Before the transport model is solved, a pressure test to determine the half-life pressure decay (HLP) is conducted. The HLP is the time required for the pressure within the silo to decay to half of its initial value. A silo filled to capacity is said to have good gas tightness if the HLP achieves 3 min or greater [11]. In order to implement the pressure test in our model, all boundaries of the silo domain are set to be impermeable walls. The initial pressure within the silo is set to be P_g =250 Pa above atmospheric pressure (at $t = 0$). A hole boundary is then (instantaneously) created at either Position 1 or Position 2 and the simulation is started. The time for P_g to reach 125 Pa above atmospheric pressure is recorded. By setting k_L in (5.23) to be 20, 240, and 1000 we obtain HLP times of 1, 3, and 6 minutes, respectively. These correspond to silos that are more leaky (less gas tight) than, equal to, and less leaky (more gas tight) than the benchmark gas tightness, respectively.

5.3.1 Fan-forced fumigation

For each simulation, the fumigant enters the silo through the inlet with a mass flow rate of $\dot{m} = 0.003$ kg/s and a concentration of phosphine of 300 ppm (equivalent to a mass fraction of $\omega_{\text{ph}} = 0.0003$). Figure 5.3 shows the mass fraction of phosphine predicted by the model for a hole at Position 1 for a silo having a HLP of 3 min. From the figure, we observe that the gas flows from the inlet then through the grain before exiting through the hole. However, we note that when the hole is near the base of the silo (Position 1) and the silo is moderately leaky (HLP of 3 min), then the tendency of the gas to flow into the grain above the hole is significantly reduced.

Figure 5.4 shows the gas pressure above atmospheric pressure (i.e $P_g - P_{\text{atm}}$) along the central vertical axis at different times for the silo simulated in Figure 5.3. We observe that the gas pressure profile equilibrates after approximately 8 hours. Figure 5.5 and Figure 5.6 show the three-dimensional gas pressure (above atmospheric) and gas velocity profiles, respectively, in the silo simulated in Figure 5.3 at approximately day 1 (when equilibrium is attained). The fact that the gas pressure (and hence velocity) profiles equilibrate after 8 hours tells us that after this time diffusion is the dominant mechanism for evolving the phosphine concentration profile observed in Figure 5.3. This explains the slow development of phosphine concentration in the silo after day 1 in Figure 5.3(b).

Figure 5.7 compares the predicted phosphine concentration along the vertical central axis at different times for 3 silos having different HLPs and a hole at Position 1. We observe that the concentration of phosphine is similar in all cases at heights less than approximately 5 m. At heights above 5 m, we observe that phosphine concentrations are significantly reduced, which is consistent with our observations following Figure 5.3, and that furthermore, silos that are less leaky (have a higher HLP) develop a significantly lower concentration of phosphine gas above the position of the hole. Our simulations show that, as expected, less leaky silos develop a considerably higher gas pressure when compared with more leaky silos. Furthermore, these pressures develop fairly quickly as a result of the incoming phosphine gas mixture not being able to displace the air in the silo that is initially

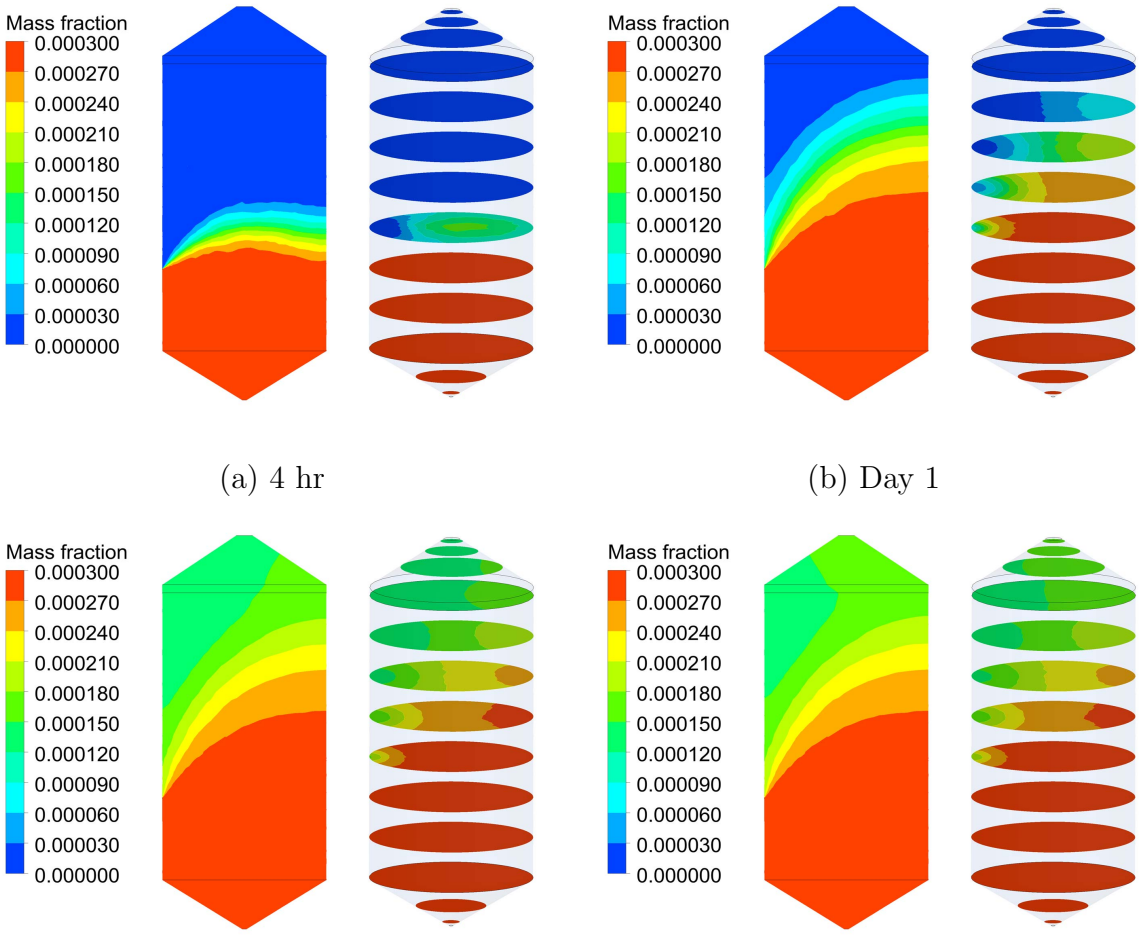

(a) 4 hr (b) Day 1

(c) Day 10 (d) Day 20

FIGURE 5.3: Phosphine mass fraction at 4 hr, 1, 10 and 20 days in a silo having a HLP of 3 min and a hole at Position 1.

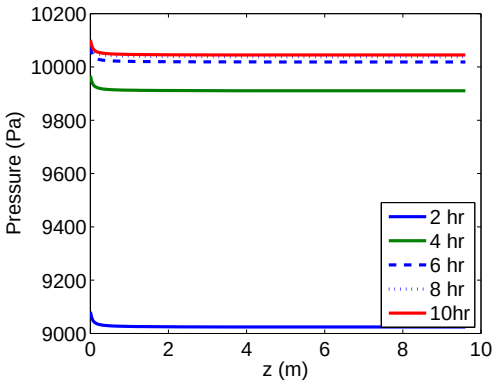

FIGURE 5.4: Gas pressure (above atmospheric pressure) along the central vertical axis at different times in a 3 min HLP silo with a hole at Position 1.

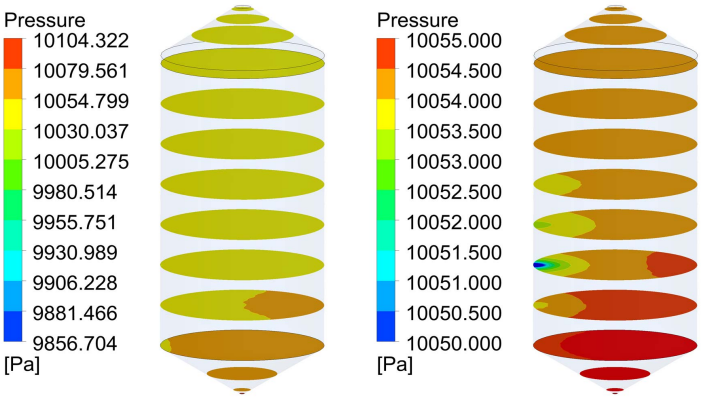

FIGURE 5.5: Gas pressure (above atmospheric pressure) contour plot for a 3 min HLP silo with a hole at Position 1. Note that the scale is changed in the figure on the right.

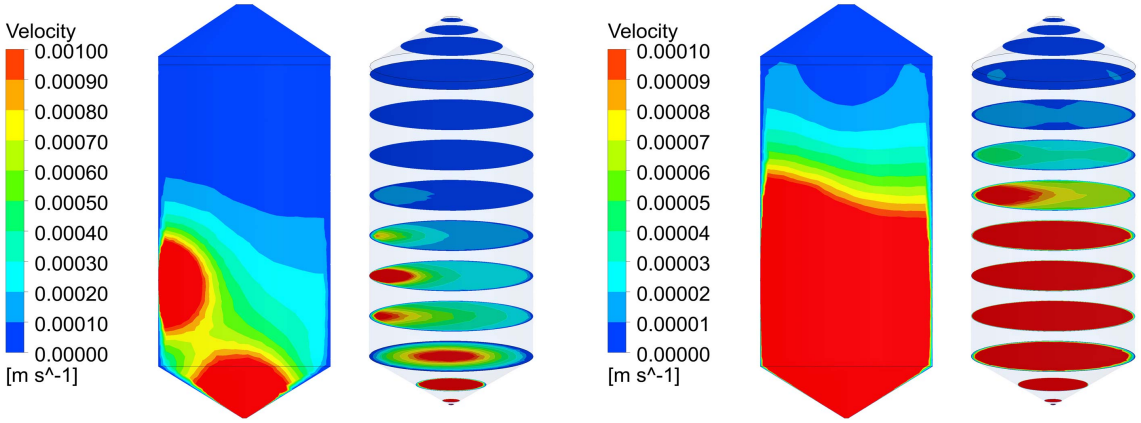

FIGURE 5.6: Velocity contour plot for a silo having a HLP of 3 min and a hole at Position 1. Note that the scale has been refined in the figure on the right.

present. The net result is that, as shown in Figure 5.8, silos having a high HLP (less leaky silos) and a hole at Position 1, develop a gas velocity profile that is lower in magnitude throughout most of the silo. This leads to a lower penetration of phosphine gas vertically within the silo.

As with the silo discussed in Figure 5.3, the gas pressures in silos with higher HLPs also equilibrate. The equilibration pressures are however higher and the equilibration times are longer. A summary of the simulated behaviour is given in Table 5.2. Similar to the discussion above, at times longer than these gas pressure equilibration times, diffusion of phosphine is the dominant transport mechanism in the silo. This could have a significant impact on the extinction of grain pests. Figure 5.9, shows a contour plot of the extinction indicator function, $e(\mathbf{x}, t)$ (see (5.19)) for two silos having different HLPs and a hole at Position 1 at a time of 10 days. We note that values of $e(\mathbf{x}, t) < 0$ correspond to complete extinction of grain pest in our model. We observe that after 10 days of fumigation, total extinction of grain pests does not occur even in a less leaky silo (HLP = 3 min).

Figure 5.10 shows the distribution of phosphine at various times for a silo having a HLP of 3 minutes and a hole at Position 2 (near the top of the silo). We

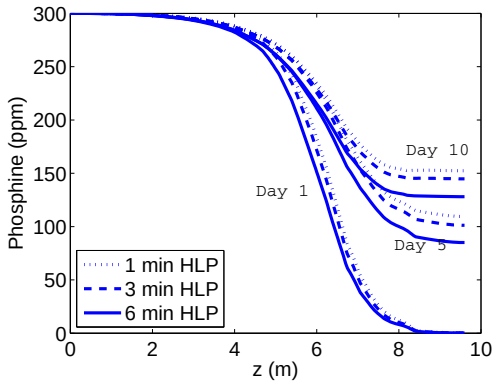

FIGURE 5.7: Comparison of phosphine concentration profiles along the central vertical axis between silos having different HLP values and a hole at Position 1.

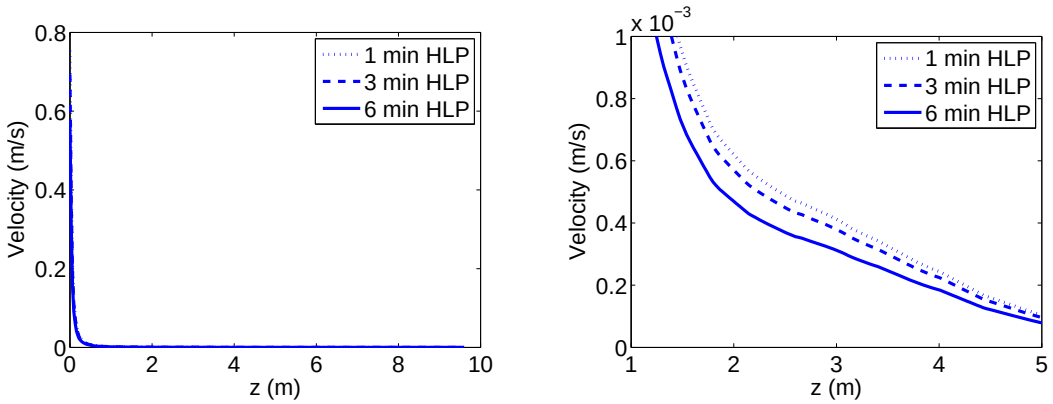

(a) (b)

FIGURE 5.8: Comparison of velocity profiles along the central vertical axis between silos having different HLP values and a hole at Position 1. Note that the scale has been refined in (b).

Properties	**1 min**	**3 min**	**6 min**
Time to achieved steady state	3 hr	8 hr	18 hr
Maximum pressure at steady state	1165 Pa	10104 Pa	33917 Pa
Minimum pressure at steady state	892 Pa	9856 Pa	33708

TABLE 5.2: The pressure properties for silos with different HLPs and having hole at Position 1.

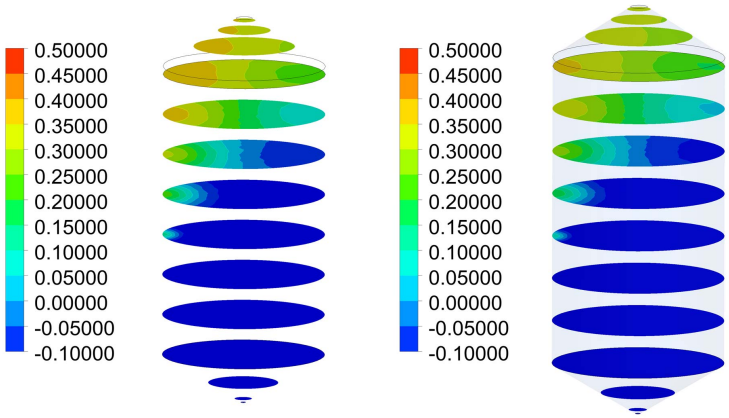

(a) 1 min HLP (b) 3 min HLP

FIGURE 5.9: Contour plot of $e(\mathbf{x}, t)$ at day 10 during fan-forced fumigation for silos with a hole at Position 1.

observe that in contrast to the distributions given for a similar silo in Figure 5.3 with a hole at Position 1, the phosphine reaches a concentration of 300 ppm (the inlet concentration) at essentially all points within the grain zone by approximately 10 hours and at all points in the silo by 16 hours.

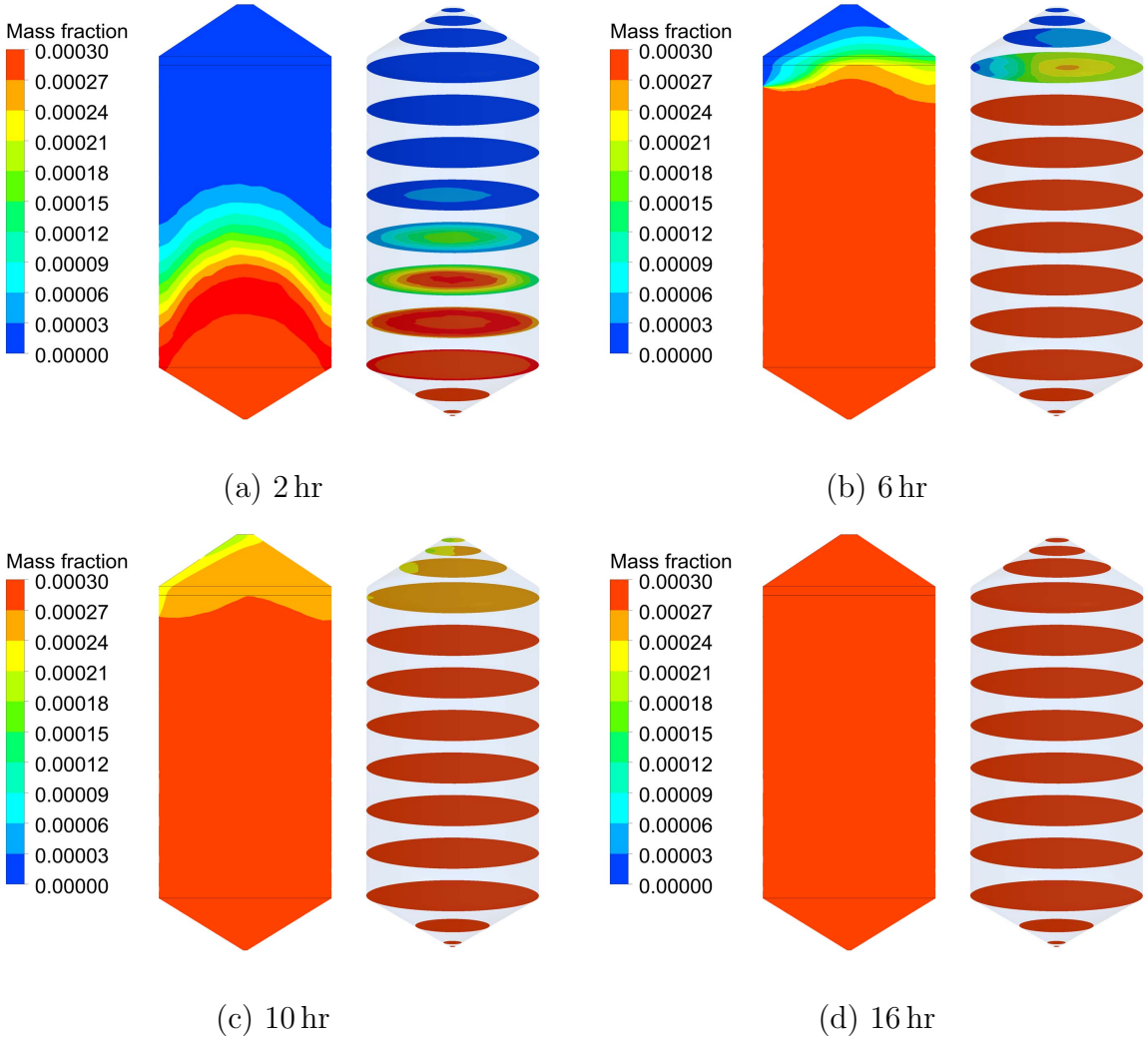

(a) 2 hr (b) 6 hr

(c) 10 hr (d) 16 hr

FIGURE 5.10: Phosphine mass fraction at 2, 6, 10, and 16 hr in a 3 min HLP silo with a hole at Position 2.

Table 5.3 gives the time taken for all points within silos of differing HLPs, to reach a uniform phosphine concentration of 300 ppm. We observe that less leaky silos (having higher HLPs) take longer to equilibrate. This is due to the

aforementioned high gas pressures that build up quickly in these silos and it taking longer for incoming phosphine to displace the air that is in the silo initially.

Half-life pressure test (HLP)	**Time taken**
1 min	14 hr
3 min	16 hr
6 min	24 hr

TABLE 5.3: Time for complete phosphine distribution in a silo with a hole at Position 2.

Figure 5.11 shows a contour plot of $e(\mathbf{x}, t)$ at days 7,8 and 9 for the silo in Figure 5.10. We observe that after 8 days of fumigation, more than 99.9% of insects are dead everywhere in the silo.

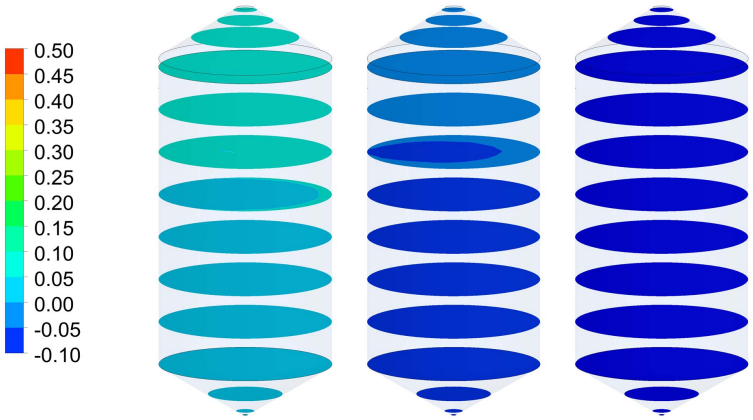

FIGURE 5.11: Contour plot of $e(\mathbf{x}, t)$ at days 7, 8 and 9 (left to right), during fan-forced fumigation within a silo having a HLP of 3 min and a hole at Position 2.

The model developed here can be used to determine the amount of phosphine that has been adsorbed into the grain. For example, Figure 5.12 shows the predicted phosphine absorption into the grain along the central vertical axis of a silo

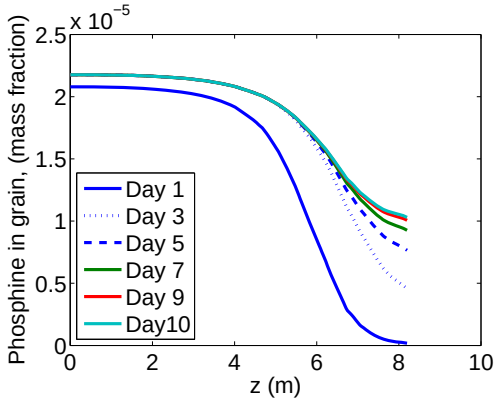

FIGURE 5.12: Mass fraction of phosphine in grain at various time along the central vertical axis of a silo having a HLP of 3 min and a hole at Position 1.

having a 3 min HLP and a hole at Position 1 during fan-forced fumigation. The highest amount of absorption is approximately 22 ppm and occurrs in the lower region of the silo, whereas the minimum is about 10 ppm and occurs at the upper surface of the grain. These values are in the range of 3.3–7.3% of the introduced concentration, which is in excess of the allowed phosphine residue concentration of 0.01 ppm as set by the maximum residue limit standard [7]. In practise, however, the grain would undergo a ventilation process before being distributed to the customer. During this process, further desorption of phosphine will occur, which will reduce the amount of phosphine inside the grain.

5.3.2 Tablet fumigation

Figure 5.13 gives the predicted concentration of phosphine at 1, 3, 10 and 20 days in a 3 min HLP silo undergoing tablet fumigation with a hole at Position 1. We recall that for tablet fumigation, tablets are situated at the top surface of the grain. Furthermore, there is no forced air convection in tablet fumigation. We observe that, close to the tablet zone, in the upper part of the silo, the phosphine level rapidly increases as soon as fumigation begins, reaching a very high concentration at 6,500 ppm on day 3 (refer Figure 5.15). The phosphine diffuses into the

headspace area above the grain and also downwards into the grain. The headspace provides no resistance to the flow of gas and we observe more rapid penetration of phosphine in this area compared with the porous packed grain zone.

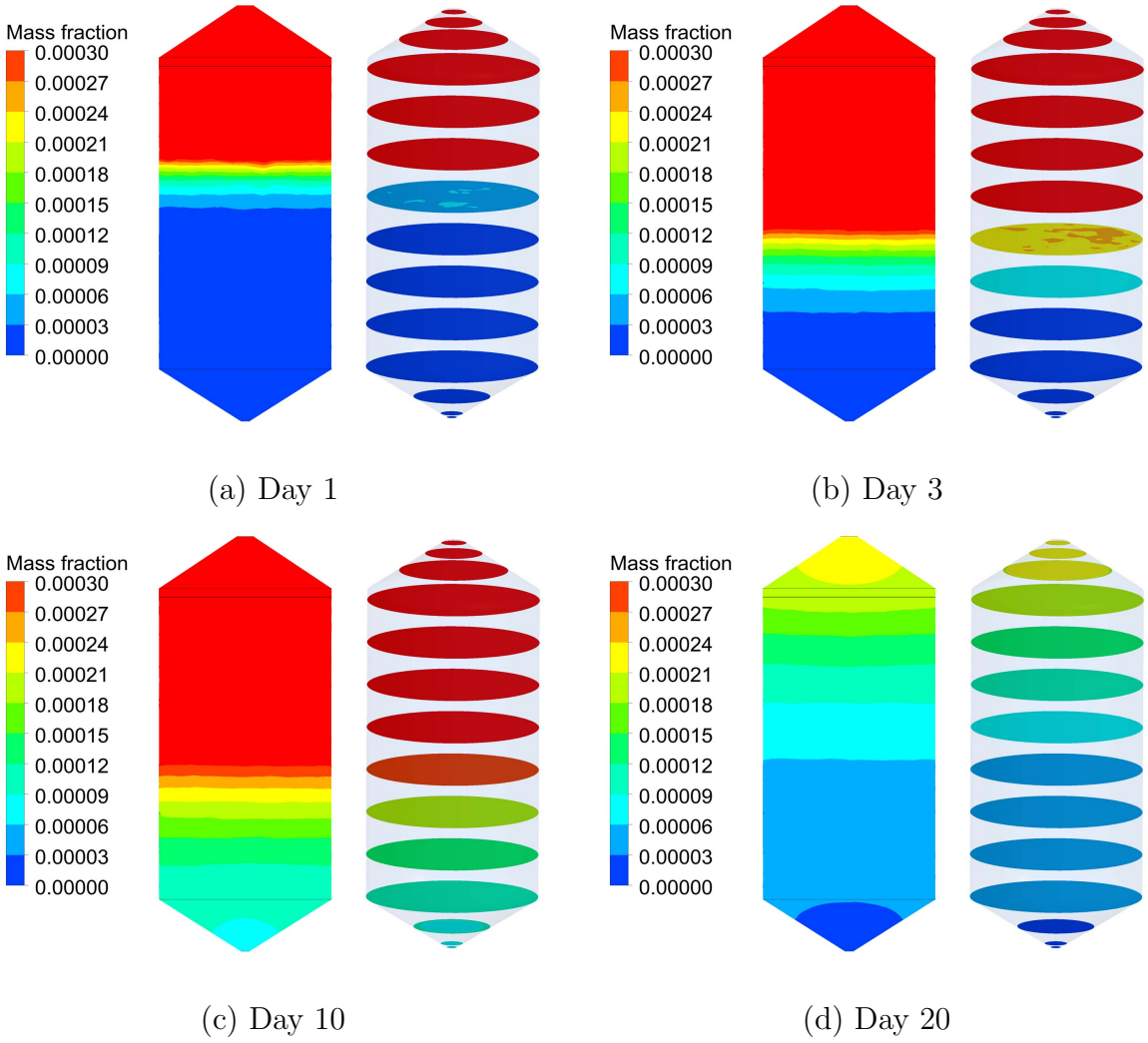

FIGURE 5.13: Phosphine mass fraction at day 1, 3, 10, and 20 during tablet fumigation of a silo having a HLP of 3 min and a hole at Position 1.

By day 3, the tablets in the tablet zone have completely dissolve and we observe that up to approximately day 10, the phosphine gas front continues to diffuse downward into the grain (Figure 5.13). After day 10, the concentration of phosphine gas begins to decline; starting at the bottom of the silo (where the concentration is

lowest). By day 20, the majority of the grain zone has a phosphine concentration below 300 ppm (refer Figure 5.15(b)). This is due to absorption into the grain and degradation in air as described in (5.12) and (5.13).

Figure 5.13 also reveals that the middle and bottom area of the silo do not reach the required concentration level of 300 ppm for seven days. If the phosphine concentration is low then it takes longer for insect extinction to occur. Figure 5.14 shows the contour plot of $e(\mathbf{x}, t)$ for the silo simulated in Figure 5.13. We observe that it takes longer than 25 days for more than 99.9% of insects to be killed in all areas of the silo. This is due to the slow moving nature of the phosphine gas front and the fact that the phosphine concentration is lower at the bottom of the silo. In addition, as mentioned above, after day 10, the concentration of phosphine gas begins to decline.

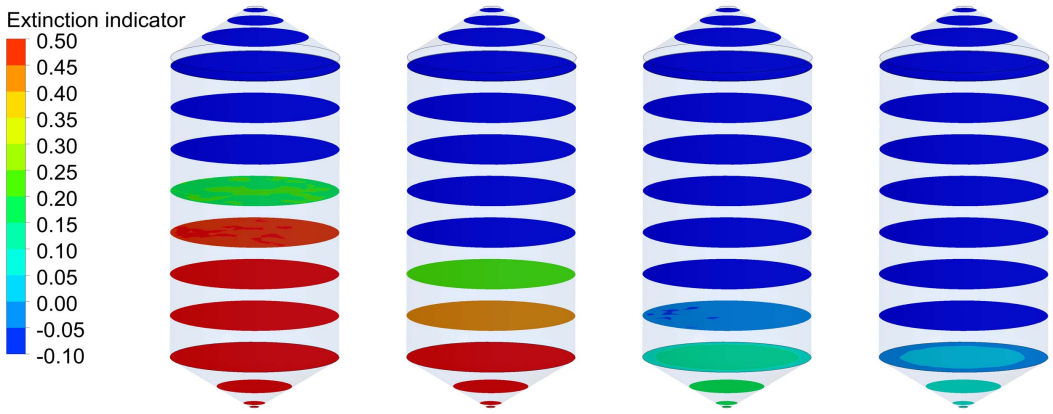

(a) Day 5 (b) Day 10 (c) Day 20 (d) Day 25

FIGURE 5.14: Extinction of insects at day 5, 10, 20, and 25 during tablet fumigation of a silo having a HLP of 3 min and a hole at Position 1.

Importantly, in our findings, we also note that the trends observed in Figure 5.13 are repeated for silos having a different HLP and/or a hole in Position 2. These are shown in Figure 5.15 and Figure 5.16. We note that in Figure 5.15, the concentration profile is identical for each silo having a hole at Position 1, whereas

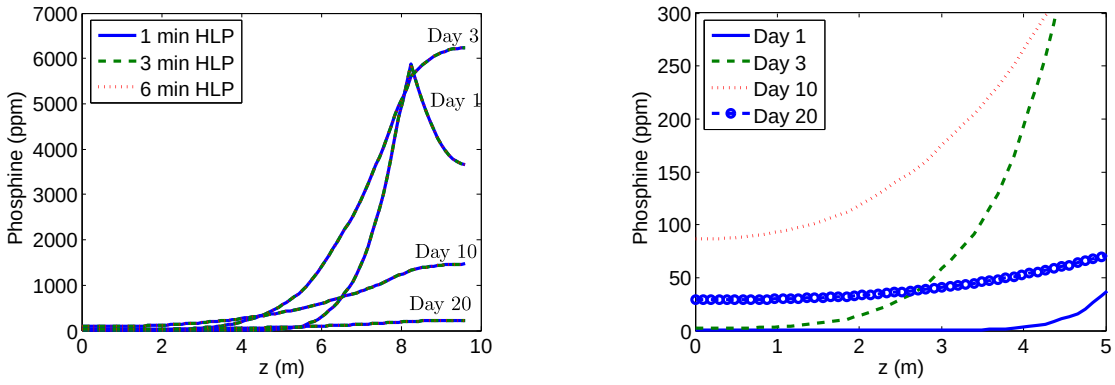

(a) (b)

FIGURE 5.15: (a) Comparison of the phosphine concentration distribution along the central vertical axis between silos having different HLPs and a hole at Position 1. (b) Scale refinement of (a) for a silo having a HLP of 3 min and a hole at Position 1.

in Figure 5.16 we see only a very slight difference between a silo having a HLP of 1 min and a hole at Position 1 and a silo having the same HLP but with a hole at Position 3.

5.4 Conclusion

A mathematical model has been developed that can predict the phosphine concentration within small scale (on farm) leaky grain silos during fan-forced and tablet fumigation. The model equations account for the absorption of phosphine gas into the grain and the degradation of phosphine gas in air. In addition, a simple model, based on empirical evidence, has been included to account for the extinction of grain pests as a result of fumigation. The model equations have been implemented in FLUENT.

For fan-forced fumigation via an inlet at the base of the silo, the model simulations show that the position of a leak can significantly impact on the fumigant

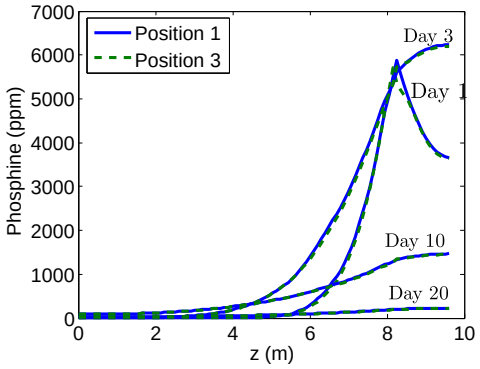

FIGURE 5.16: Comparison of the phosphine concentration distribution along the central vertical axis between silos having different hole positions and a HLP of 1 min.

distribution within the silo. Leaks near the base of the silo serve to inhibit the even distribution of fumigant within the silo. The worst case scenario occurs when an exclusive leak is located near the bottom of the silo (close to the inlet). We have shown for this situation that it is possible that the complete extinction of grain pests within the silo may not occur even after extended periods of fumigation.

The degree of gas tightness (or alternatively "leakiness") of a silo is characterised by the half-life pressure (HLP) time with silos having a high HLP value being more gas tight (less leaky) than those with lower HLP values.

Importantly, our simulation results show that for silos having a leak near the bottom of the silo and undergoing fan-forced fumigation, the concentration of phosphine gas near the top of the silo is slower to evolve. Indeed, after 10 days of fumigation the phosphine concentrations near the top of a silo with a HLP value of 6 min is significantly lower than that for a silo having a HLP value of 1 min. This has important ramifications for the time required to kill grain pests within such silos, with the likelihood being that less leaky silos (having a leak near the base of the silo near the inlet) may not achieve complete extinction of grain pests in the recommended fumigation time.

Leaks near the top of the silo help to distribute fumigant throughout the silo with our simulations showing that even for silos having a HLP of 6 min (i.e. high gas tightness or low "leakiness") the phosphine concentration achieves the inlet concentrations within 24 hours.

Our simulations show that for silos undergoing tablet fumigation, a wave of highly concentrated phosphine gas diffuses downwards into the grain from the tablet zone at the top of the grain surface. Furthermore, the phosphine concentration profile is essentially independent of the HLP time of the silo (for HLPs in the range 1 to 6 mins) and the position of a leak (top or bottom of silo). Our simulations suggest that for a typical small silo ($100\,\mathrm{m}^3$) undergoing fumigation with the recommended dose of phosphine tablets it takes more than 25 days (from initial fumigant application) for complete extinction of grain pests to occur.

In practice of course, it is possible that the position of leaks in silos would not be contained to either the lower or upper sections of the silo exclusively, however, we have simulated these kind of leaks here as they provide us with the extremes of the behaviour that is possible within small scale (on farm) silos under typical fumigation regimes.

Furthermore, we also acknowledge that the results presented here have not been validated against actual experimental data, however, we note that the parameters for the model have been obtained from credible sources and that the gas sorption and insect extinction models included here are empirically based. This gives us some confidence that the model predictions are plausible.

Chapter 6

Conclusions and Further Work

6.1 Summary of thesis objectives

This section summaries the achievement of all objectives given in Chapter 1, which are restated here as follows:

1. To understand the hydrodynamics of fumigant transport in stored grain via:
   - the development of simple analytic models for the flow of gas in open-top silos,
   - the evaluation of relevant computational fluid dynamics packages for the implementation of flow field equations in open and closed grain storage systems.
2. To model the phosphine concentration field in a closed silo whilst accounting for the important factors that characterize realistic grain storage including:
   - gas leaks in the silo,
   - fumigant sorption and degradation,
   - high dimensional geometry of the domain,
   - the multicomponent nature of the fumigant gas,
   - the effect of the fumigant concentration field on the extinction of grain pests.

6.1.1 Achievement of Objective 1

Objective 1 is achieved in Chapters 3 and 4. Computationally, the hydrodynamics of the gas is predicted for a fumigation process in cylindrical storage with a circular inlet attached at the centre of the base as in Chapter 3. We compare the numerical solutions obtained by using the COMSOL and FLUENT CFD packages. Both show satisfactory agreement in predicting the flow.

An analytical solution approach is given in Chapter 4. A new closed form series solution describing the radial and axial velocity, streamlines and traverse time has been presented in Chapter 4. These formulas are general in silo radius and height, which allows for the investigation of any cylindrical storage with an inlet attached at the base. Importantly, the solution obtained extends previous work by accounting for a more realistic finite inlet source. In addition, various cases of annular inlet are also studied.

The fumigant flow behaviour from the numerical and analytical solutions is similar. The streamlines show that the flow moves upward towards the grain surface, and the streamlines are almost parallel at the height $z > 1\,\mathrm{m}$. For a circular inlet on the centreline of the silo, a very slow flow region was identified at the base of the silo and within 0.1 m of the silo wall. For annular inlet, regions where fumigant will reach more slowly depend on the position of the annular inlet. Advection drives phosphine to reach almost the entire grain bed with a traverse time of approximately one hour, although not uniformly so.

The findings provide a hydrodynamic understanding of fumigant flow. In addition, the computational work also serves as a feasibility investigation between COMSOL and FLUENT, showing that both packages are suitable for simulating such flows.

6.1.2 Achievement of Objective 2

Objective 2 is achieved in Chapter 5 where we presented a model of fumigant transport that accounts for multicomponent gas flow, sorption of fumigant in the grain, leaks in the silo and insect extinction. FLUENT is used to solve the model equations. The influence of variations in the HLP values and leaky hole location

are comprehensively investigated to examine the phosphine distribution behaviour. Two types of fumigation application are studied, namely, fan-forced and tablet fumigation. During fan-forced fumigation, phosphine gas is injected through the inlet at the bottom of the silo whereas during tablet fumigation, gas infuses downwards from the grain surface. The number of tablets and the rate of gas evolution has been carefully calculated based on information from the literature. The ability to customize the transport equation in FLUENT has been used to introduce a sorption term and also the evolution of the gas (during tablet fumigation) as a source term. From our model we can predict the pressure, velocity and concentration fields in time and space throughout a three-dimensional silo. This work helps to provide answers to our previous research questions as follows:

How does the half-life pressure test value (HLP) affect the fumigant distribution?

By conducting simulations with different loss coefficients at the leaky boundary, the effect on the fumigant concentration distribution is observed. Our simulation results show that for silos having a leak near the bottom of the silo and undergoing fan-forced fumigation the phosphine concentrations near the top of a silo with a higher HLP value are significantly lower than that for a silo having a lower HLP value. This suggests the likelihood that less leaky silos (having a leak near the base of the silo near the inlet) may not achieve complete extinction of grain pests in the recommended fumigation time. For silos undergoing tablet fumigation, the phosphine concentration profile is essentially independent of the HLP time of the silo (for HLPs in the range 1 to 6 mins).

Does the position of the leaky hole affect the fumigant distribution?

In fan-forced fumigation, our simulation results show that the hole position plays an important role in achieving a good phosphine distribution due to the behaviour of the gas which tend to flow towards the hole. In the case of an inlet at the bottom of the silo investigated here, a hole at the top of the silo will help the phosphine gas to reach all areas of the silo. However, if the hole is located at the bottom of

the silo there will be an area near the top of the silo that does not receive adequate levels of phosphine to kill grain pests.

For tablet fumigation, the simulations suggest that the hole position does not significantly effect the phosphine distribution in the silo.

How much phosphine residue is in the grain kernel?

Using our mathematical modelling we may calculate the amount of phosphine inside a grain kernel at any time. The simulations predict a phosphine residue inside the grain kernel in the range of 10 ppm to 22 ppm (for a silo having a 3 min HLP and a hole at the bottom of the silo during fan-forced fumigation) after 10 days of fumigation. This amount is more than the allowed residue which is 0.01 ppm [7]. However over time, as the grain is aired, this high value is expected to decrease.

We know that the mortality of insects depends on the concentration-time product (Ct). The fumigant concentration fields alone will not provide an exact indication of whether all insects have been killed. Therefore, starting with the relationship $C^n t = k$, an ordinary differential equation is developed and incorporated in the transport modelling. Given the solution for the concentration an extinction indicator, $e(\mathbf{x}, t)$ is calculated whereby the insects are killed if $e(\mathbf{x}, t) < 0$. Incorporating this simple extinction model into our transport model we may determine what regions of the silo could harbor living insects as time progress. The inclusion of an extinction model has allowed us to investigate the research question:

Where are the areas in the grain storage that do not receive sufficient dosage?

An analysis of the predicted phosphine distribution shows that during fan forced fumigation, there is an area at the top part of the silo which received less phosphine. That situation occurs when a leak exists in the lower area of the silo.

However, as noted above, leaks do not significantly affect phosphine distribution during tablet fumigation. For a typical silo configuration, the phosphine concentration at the bottom of the silo is very low for extended periods of time

regardless of the HLP value or the hole location. Due to the small amount of phosphine received at the bottom area, it can take more than 25 days for complete insect eradication.

6.2 Summary of contributions

The work in this thesis involves the hydrodynamical investigation and comprehensive transport modelling of phosphine gas in small, on-farm grain storage. With this, the contributions of the present thesis are as follows:

1. The work provides an analytic solution against which numerical simulation models can be validated.

2. Investigation shows that the position of leaks in the silo significantly effects the fumigant distribution in fan-forced fumigation but not in tablet fumigation.

3. There is an insufficient dosage area at the top part of the silo if leaks are predominant located at the lower part of the silo during fan-forced fumigation.

4. The half-life pressure test value (HLP) is not found to have any significant effect on the fumigant distribution during tablet fumigation.

5. The amount of phosphine in grain kernel is found very high which is in the range of 3.3–7.3% of the introduced concentration. This amount is more than the allowed 0.01 ppm [7]. However, this is the value before ventilation is allowed to take place.

6.3 Recommendations for further work

The grain industry is in need of research into phosphine fumigation. The research conducted here could be improved and extended as follows:

1. The analytic solution in Chapter 4 could be extended to include the fumigant concentration. Integral transform methods could provide a way forward here

as has been shown in [81]. The results would provide an invaluable analytic solution against which numerical simulation models can be validated.

2. Our study could be extended to consider multiple leaky holes as such patterns of leaks may exhibit different fumigant distribution. Such an extension would require significant computational resources since the number of mesh points in the discrete domain would increase dramatically.

3. Our study could be extended to simulate the ventilation process after fumigation by using the results in this present model as an initial condition. In this thesis, the amount of phosphine inside the grain kernel is very high and it is very important to investigate the response of the phosphine in the grain kernel during the ventilation process. From the same mathematical model in Chapter 5, we can determine the amount of phosphine inside the grain kernel after the ventilation by imposing a new boundary condition such that at the inlet only pure air is pumped in.

4. For tablet fumigation, a particularly useful extension to our work would be to consider the phosphine distribution when tablets are probed into the grain mass instead of sitting on the grain surface, as this is a common on-farm practice.

5. The mathematical model developed here for fumigant transport may be made more accurate by including the variation of temperature within the silo. Significant temperature gradients could drive thermal convection of the gas within the silo. In addition the incorporation of an external flow field model on the outside of the silo could also be undertaken. Such a model could be used to investigate the significance of air ingress into the silo via holes in the walls.

Bibliography

[1] *Application Manual for EC02Fume.*

[2] *Application manual for Vaporph3OS phosphine fumigant.*

[3] *FLUENT, Ansys inc. http://www.ansys.com.*

[4] Farmnote (307), April 2008.

[5] *Ansys Fluent - User's guide.* Ansys,Inc., 2009.

[6] *Ansys Fluent- Theory guide.* Ansys,Inc., 2009.

[7] *The MRL Standard : Maximum residue limits in food and animal feedstuff.* Australian Pesticides and Veterinary Medicines Authority, 2012.

[8] K. Alagusundaram, D.S. Jayas, W.E. Muir, and N.D.G. White. Convective-diffusive transport of carbon dioxide through stored grain bulks. *American Society of Agricultural Engineers*, 39(4):1505–1510, 1996.

[9] K. Alagusundaram, D.S. Jayas, W.E. Muir, N.D.G. White, and R.N. Sinha. Finite element model of three-dimensional movement of carbon dioxide in grain bins. *Canadian Agricultural Engineering*, 38(2):75–82, 1996.

[10] V. Ambatipudi, J.Y. Murthy, and D.E. Maier. Detailed and reduced form modeling of structural fumigation in food processing facilities. In *9th International working conference on stored product protection*, 2006.

[11] A.S. Andrews, P.C. Annis, and C.R. Newman. Sealed storage technology on australian farms. In *Proceeding of the 6th international working conference on stored product protection*, 1994.

[12] P. Annis. Phosphine fumigation for farm stored grains. Technical report, CSIRO stored grain reserach laboratory, 2003.

[13] P. C. Annis. Requirements for fumigation and controlled atmodpheres as an option for pest and quality control in stored grain. In B.R. Champ, E. Highley, and H.J. Banks, editors, *Proceedings of an international conference of fumigation and controlled atmosphere storage of grain*, 1989.

[14] P. C. Annis. The relative effects of concentration, time, temperature and other factors in fumigant treatments. In *Proceedings of the 7th International Working Conference on Stored product Protection*, 1998.

[15] P.C. Annis. Sealed silos increase fumigation success. Technical report, CSIRO, 2003.

[16] P.C Annis and H.J. Banks. A predictive model for phosphine concentration in grain storage structures. In S. Navarro and E. Donahaye, editors, *Proceeding International Conference Controlled Atmosphere and Fumigation in Grain Storage*, pages 299–312, 1993.

[17] P.C. Annis and H. A. Dowsett. Time to kill phosphine resistant rhyzopertha dominica using a concentration profile typical of field exposure. In *Proceeding international conference controlled atmosphere and fumigation in stored products*, 2001.

[18] P.C. Annis and H.A. Dowsett. The adequacy of aluminium phosphide dosages used in australia. In *Australian Postharvest technical conference*, 2002.

[19] G. Aylward and T. Findlay. *SI chemical data*. John Wiley & Sons, 6th ed., 2008.

[20] H. J. Banks. Uptake and release of fumigants by grain: sorption/desorption phenomena. In S. Navarro and E. Donahaye, editors, *Proceeding International conference controlled atmosphere and fumigation in grain storages*, 1993.

[21] H.J. Banks and P.C. Annis. On criteria for success of phosphine fumigations based on observation of gas distribution patterns. In *proceeding of an international symposium of controlled atmosphere and fumigation in grain storage*, 1984.

[22] A. Barletta and S. Lazzari. 2d free convection in a porous cavity heated by an internal circular boundary. In *Proceedings of the COMSOL Multiphysics User's Conference*, 2005.

[23] J. Bear. *Dynamics of Fluids in Porous Media*. Dover Publications, Inc., New York, 1988.

[24] S.J. Beckett, , R. Morton, and J.A. Darby. The mortality of rhyzopertha dominica(f.) (coleoptera: Bostrychidae) and sitophilus oryzae(l.)(coleoptera:curculionidae) at moderate temperatures. *Journal of Stored Products Research*, 34:363–376, 1998.

[25] C. H. Bell. Time, concentration and temperature relationships for phosphine activity test on diapausing larvae of ephestia elutella. *Pestic. Sci.*, 35:255–264, 1992.

[26] C.H. Bell. Fumigation in the 21st century. *Crop protection*, 9:563–569, 2000.

[27] C.H. Bell. Phosphine in store: application and alternatives. In *HGCA conference: Crop management into the millenium*, 2000.

[28] C.H. Bell and C.R. Watson. Recent developments in grain storage fumigation technology in the uk. In *Proceeding of the 7th international working conference on stored product protection*, 2000.

[29] H. Benhalima, M.Q. Chaudhry, K.A. Mills, and N.R. Price. Phosphine resistance in stored-product insects collected from various grain storage facilities in morocco. *Journal of Stored Products Research*, 40:241–249, 2004.

[30] B. Berck. Sorption of phosphine by cereal products. *J. AGR. FOOD CHEM*, 16:419–425, 1968.

[31] B. Berck and F. A. Gunther. Rapid determination of sorption affinity of phosphine by fumigation within a gas chromatographic column. *J. Agr. Food Chem*, 18:148–153, 1970.

[32] I.P. Bibby and S.T. Conyers. Numerical simulations of gas exchange in leaky grain silos, using measured boundary conditions. *Journal of stored product research*, 34:217–229, 1998.

[33] R.B. Bird, W.E. Stewart, and E.N. Lightfoot. *Transport phenomena*. John Wiley & Sons, 2007.

[34] S.L. Birla, S. Wang, and J. Tang. Computer simulation of radio frequency heating of model fruit immersed in water. *Journal of Food Engineering*, 84:270–280, 2008.

[35] F.B. Boland. Phosphine fumigations in silo bins. In *Proceeding of an International Symposium "Practical Aspects of controlled atmosphere and fumigation in grain storage"*, 1984.

[36] R.E. Bolz and G.L. Tuve. *Handbook of tables for applied engineering sciences.* CRC Press, Cleveland, Ohio, 1973.

[37] E. J. Bond. Sorption of tritiated phosphine by various stages of tribolium castaneum (herbst). *J. stored product research*, 16:27–31, 1980.

[38] E. J. Bond and H. A. U. Monro. The role of oxygen in the toxicity of fumigants to insects. *Journal of stored product research*, 3:295–310, 1967.

[39] E. J. Bond, J. R. Robinson, and C. T. Buckland. The toxic action of phosphine: Absorption and symptoms of poisoning in insects. *Journal of stored product research*, 5:289–298, 1969.

[40] E.I. Bond. *Manual of fumigation for insect control*. Agriculture and consumer protection,, 1984.

[41] E. L. Bonjour, T. W. Phillips, R. T. Noyes, G. W. Cuperus, D. K. Mueller, and C. Schmidt. Mortality of stored grain insects exposed to cylinderized

phosphine in wheat bins. In *7th International Workmg Conference on Stored-product Protection*, 1998.

[42] B. Bridgeman, R. Ryan, D. Gock, and P. Collins. High dose phosphine fumigation using on site mixing. In *Proceeding international conference controlled atmosphere and fumigation in stored products*, 2000.

[43] K. Bullen. Insect control in stored grain. Technical report, DPI&F, Plant Science, Toowoomba, Queensland., 2007.

[44] J. Canchun, D. Sun, and C. Cao. Finite element prediction of transient temperature distribution in a grain storage bin. *Journal of agriculture and engineering research*, 76:323–330, 2000.

[45] J. Canchun, D. Sun, and C. Cao. Computer simulation of temperature changes in a wheat storage bin. *Journal of Stored Products Research*, 37:165–177, 2001.

[46] J. Canchun, D. Sun, and C. Cao. Mathematical simulation of temperature fields in a stored grain bin due to internal heat generation. *Journal of Food Engineering*, 43:227–233, 2001.

[47] R. Cavasin, M. DePalo, and J. Tumambing. Updates on the global application of eco2fume and vaporph3os phosphine fumigants. In *9th International Working Conference on Stored Product Protection*, 2006.

[48] R. Cavasin, B. McSwigan, R. Ryan, and D. Gock. Eco2fume: Global status update. In *Proceeding international conference controlled atmosphere and fumigation in stored products*, 2000.

[49] B. Chakrabarti, C.R. Watson, C.H. Bell, T.J. Wontner-Smith, and J. Rogerson. Fumigation of a 7000t bulk of wheat with phosphine using the phytoexplo system to assist gas circulation. In *Proceedings of the 6th International Working Conference on Stored-Product Protection*, 1994.

[50] M.Q. Chaudhry. Phosphine resistance. *Pesticide Outlook*, 11:88–91, 2000.

[51] M.Q. Chaudhry, H.A. Bell, N. Savvidou, and A.D. MacNicoll. Effect of low temperatures on the rate of respiration and uptake of phosphine in different life stages of the cigarette beetle lasioderma serricorne (f.). *Journal of Stored Products Research*, 40:125–134, 2004.

[52] M. Qasim Chaudry and Nicholas R. Price. Comparison of the oxidant damage induced by phosphine and the uptake and tracheal exchange of 32p-radiolabelled phosphine in the susceptible and resistant strains of rhyzopertha dominica (f.) (coleoptera: Bostrychidae). *PESTICIDE BIOCHEMISTRY AND PHYSIOLOGY*, 42:167–179, 1992.

[53] M.Q. Chaudry. A review of the mechanisms involved in the action of phosphine as an insecticide and phosphine resistance in stored-product insects. *Pestic. Sci.*, 49:213–228, 1997.

[54] W. Chayaprasert, D.E. Maier, K.E. Ileleji, and J.Y. Murthy. Modeling the structural fumigation of flour mills and food processing facilities. In *International working conference on stored product protection*, 2006.

[55] W. Chayaprasert, D.E. Maier, K.E. Ileleji, and J.Y. Murthy. Real time monitoring of a flour mill fumigation with sulfuryl fluoride. In *International working conference on stored product protection*, 2006.

[56] W. Chayaprasert, D.E. Maier, K.E. Ileleji, and J.Y. Murthy. Development and validation of computational fluid dynamics models for precision structural fumigation. *Journal of stored product research*, 44:11–20, 2008.

[57] W. Chayaprasert, D.E. Maier, and B. Subramaniam. A simplified and improved modeling approach for the structural fumigation process using computational fluid dynamics. In *International working conference on stored product protection*, 2010.

[58] P.J Collins. Resistance to chemical treatments in insect pests of stored grain and its management. In *9th International Working Conference on Stored Product Protection*, 2006.

[59] P.J. Collins. Research on stored product protection in australia: a review of past, present and future directions. In *10th international working conference on stored product protection*, 2010.

[60] P.J. Collins, G.J. Daglish, M.K. Nayak, P.R. Ebert, D. Schlipalius, W. Chen, H. Pavic, T.M. Lambkin, R. Kopittke, and B.W. Bridgeman. Combating resistance to phosphine in australia. In *Proc. Int. Conf. Controlled Atmosphere and Fumigation in Stored Products*, 2001.

[61] P.J. Collins, G.J. Daglish, H. Pavic, and R. Kopittke. Response of mixed-age cultures of phosphine-resistant and susceptible strains of lesser grain borer, *Rhyzopertha dominica*,to phosphine at a range of concentrations and exposure periods. *Journal of Stored Products Research*, 41:373–385, 2005.

[62] COMSOL. *Comsol Multiphysics User's Guide, version 3.5a*.

[63] P.D. Cox and L.E. Collins. Factors affecting the behaviour of beetle pests in stored grain,with particular reference to the development of lures. *Journal of Stored Products Research*, 38:95–115, 2002.

[64] S.A. Cryer. Predicted gas loss of sulfuryl flouride and methyl bromide during structural fumigation. *Journal of Stored Product Research*, 44:1–10, 2008.

[65] Cytec Industries Inc. *Vaporph3OS: Product stewardship training manual*.

[66] G. J. Daglish. Effect of exposure period on degree of dominance of phosphine resistance in adults of rhyzopertha dominica (coleoptera: Bostrychidae) and sitophilus oryzae (coleoptera: Curculionidae). *Pest Management Science*, 60:822–826, 2004.

[67] G.J. Daglish, P.J. Collins, H. Pavic, and R.A. Kopittke. Effects of time and concentration on mortality of phosphine-resistant sitophilus oryzae (l) fumigated with phosphine. *Pest Management Science*, 58:1015–1021, 2002.

[68] G.J. Daglish, R.A. Kopittke, M.C. Cameron, and H. Pavic. Predicting mortality of phosphine-resistant adults of sitophilus oryzae (l) (coleoptera: Cur-

culionidae) in relation to changing phosphine concentration. *Pest Management Science*, 60:655–659, 2004.

[69] Gregory J. Daglish and Hervoika Pavic. Changes in phosphine sorption in wheat after storage at two temperatures. *Pest Management Science*, 2009, 2009.

[70] J.A. Darby. A kinetic model of fumigant sorption by grain using batch experimental data. *Pest Mang Sci*, 64:519–526, 2008.

[71] J.A. Darby and P.C. Annis. Integrating fumigation and aeration. In *Proceedings of the Australian Postharvest Technical Conference*, 2003.

[72] J.A. Darby, T. Willis, and K. Damcevski. Modelling the kinetics of ethyl formate sorption by wheat using batch experiment. *Pest Manag Sci*, 65:982–990, 2009.

[73] A. de Ville and E.A. Smith. Airflow through beds of cereal grains. *Appl. Math. Modelling*, 20:283–289., 1996.

[74] Yeschvant V. Deshmukh. *Industrial heating: Principles, Techniques, Materials, Applications and Design*. CRC Press, 2005.

[75] D.Rees. *Insects of stored products*. CSIRO Publishing, 2004.

[76] R. Driscoll and B.C.Longstaffand S. Beckett. Prediction of insect populations in grain storage.journal of stored products research. *Journal of Stored Products Research*, 36:131–151, 2000.

[77] P.J.F. Ducom. The return of fumigants. In *The 9th International working conference on stored product protection*, 2006.

[78] Peter A. Edde. A review of the biology and control of rhyzopertha dominica (f.) the lesser grain borer. *Journal of Stored Products Research*, 48:1–18, 2012.

[79] S.E.A. El-Aziz. Control strategies of stored product pests. *Journal of entomology*, 8(2):101–122, 2011.

[80] National Farmer's Federation. Nff farm facts:2012. Technical report, National Farmer's Federation, 2012.

[81] J. L. Feike and J. H. Dane. Analytical solutions of the one dimensional advection equation and two or three dimensional dispersion equation. *Water resources research*, 26:1475–1482, 1990.

[82] M.A. Ferrell. Fumigation of farm stored grain and structures. Technical report, Dept. of Plant, Soil and Insect Sciences, The University of Wyoming, 1996.

[83] P.G. Fields and N.D.G. White. Alternatives to methyl bromide treatments for stored-product and quarantine insects. *Annual Review of Entomology*, 47:331359, 2002.

[84] K. Flanders and S. Brown. Fumigating agricultural commodities with phosphine. Technical report, Alabama Cooperative extension system, 2005.

[85] P.W. Flinn and C.Reed. Effects of outside air temperature on movement of phosphine gas in concrete elevator bins. In *Proceedings of the International Conference on Controlled Atmosphere and Fumigation in Stored Products*, 2008.

[86] E. Fluck. The chemistry of phosphine. In *Inorganic Chemistry*, chapter Topics in current chemistry, pages 1–64. Springer Berlin Heidelberg, 1973.

[87] D. Garg and D.E. Maier. Modeling non-uniform airflow distribution in large grain silos using fluent. In *9th international working conference on stored product protection*, 2006.

[88] A. Gaston, R. Abalone, R.E. Bartosik, and J.C. Rodriguez. Mathematical modelling of heat and moisture transfer of wheat stored in plastic bags(silobags). *Biosystems Engineering*, 104:72–85, 2009.

[89] J.M. Goudie, E.A. Smith, and A. De Ville. Modelling the velocity of air thfough beds of cereal grains. *Journal of Mathematics applied in business and industry*, 5:325–335, 1995.

[90] Graintec. Grain testing method. Technical report, Graintec Scientific, 2010.

[91] J.S. Graver and R.G. W inks. A brief history of the entomological problems of wheat storage in australia. In *Proceeding of the 6th international working conference on stored product protection*, 1994.

[92] D.W. Hagstrum, C. Reed, and P. Kenkel. Management of stored wheat insect pests in the usa. *Integrated Pest Management Reviews*, 4:127–142, 1999.

[93] D.W. Hagstrum and B. Subramanyam. *Fundamental of stored product entomology*. AACC International, USA, 2006.

[94] B. El Hajjar and A. Mojtabi. Numerical and analytical studies of thermogravitational diffusion in a horizontal cell. In *Proceedings of the COMSOL Multiphysics User's Conference*, 2005.

[95] B.D. Hole, C.H. Bell, K. A. Mills, and G.Goodship. The toxicity of phosphine to all developmental stages of thirteen species of stored product beetles. *Journal of stored product research*, 12:235–244, 1976.

[96] F. Horn, P. Horn, J. Tumambing, D. Gock, and B. McSwigan. Fumigation field trial tour of the horn diluphos system using cytec vaporph3os. In *Proceedings of the Australian Postharvest Technical Conference*, 2003.

[97] P. Horn and F. Horn. Large scale grain fumigations using pure cylinderized phosphine together with the horn diluphos system. In *Proceeding of the 6th International Working Conference on Stored Product Protection*, 2006.

[98] W.V. Hukill and C.K. Shedd. Non-linear air flow in grain drying. *Agricultural Engineering*, 36:462–466, 1955.

[99] J.A. Hunter. Pressure difference across an aerated seed bulk for some common duct and store cross sections. *Journal of Agricultural Engineering Research*, 28:437–450, 1983.

[100] J.A. Hunter. Traverse time for gas flow through porous media for some particular geometries. *Journal of Agricultural Engineering Research*, 35:11–23, 1986.

[101] Z.M. Isa, G.R. Fulford, and N.A. Kelson. Simulation of phosphine flow in vertical grain storage: a preliminary numerical study. *ANZIAM J. (Proceedings of the 15th Biennial Computational Techniques and Applications Conference, CTAC-2010)*, 52:C759–C772, 2011.

[102] A. Jeffrey and H. Dai. *Handbook of mathematical formulas and integrals*. Elsevier USA, 2008.

[103] F. Jian, D.S. Jayas, and N.D.G. White ans E¿A Smith. Two dimensional diffusion of cryptolestes ferrugineus (stephens)(coleoptera:laemophloeidae) populations in stored wheat under constant environmental conditions. *Journal of Stored Products Research*, 43:342–348, 2007.

[104] F. Jian, D.S. Jayas, and N.D.G. White. Vertical movement of rusty grain beetles,cryptolestes ferrugineus. *Journal of Insect Science*, 2006:1–9, 2006.

[105] L. Jianhua, L. Qin, H. Shutian, and Q. Jinsheng. Experiment in recirculation fumigation with low dosage phosphine in silos. In *Proceeding of the 7th international working conference on stored product protection*, 2000.

[106] Carol Jones, James Hardin, and Edmond Bonjour. Design of closed-loop fumigation systems for grain storage structuresin. Technical report, Division of agricultural sciences and natural resources, Oklahoma State University.

[107] G. Khodabakhshi and M. Parvazinia. Stabilized finite element modeling of the flow through porous medium. In *Proceedings of the COMSOL Multiphysics User's Conference*, 2005.

[108] F. Longobardi, M. Pascale, M. Silvestri, and A. Visconti. Rapid method for determination of phosphine residues in wheat. *Food Anal. Methods*, 1:220225, 2008.

[109] I. Lorini, P.J. Collins, G.J. Daglish, M.K. Nayak, and H. Pavic. Detection and characterisation of strong resistance to phosphine in brazilian rhyzopertha dominica (f.) (coleoptera: Bostrychidae). *Pest Management Science*, 63:358–364, 2007.

[110] A.V. Lyubimov and V.F. Garry. *Hayes handbook of pesticide toxicology*, chapter Phosphine, pages 2259–2266. Elsevier, Burlington, 2010.

[111] G. Masters and J. Marszal. Siroflo usage in south australia. In *Australian Postharvest Technical Conference*, 1998.

[112] K.A. Mills, T.J. Wontner-Smith, D.I. Bartlett, and B.B. Harral. A new positive pressure system for combating dilution during phosphine fumigation of bulk grain. In K.A Mills, T.J. Wontner Smith, D.I Bartlet, and B.B. Harral, editors, *Proc. Int. Conf. Controlled Atmosphere and Fumigation in Stored Products*, 2000.

[113] Wayne A. Morrissey. Methyl bromide and stratospheric ozone depletion. Technical report, Congressional research service, 2006.

[114] N.S. Nath, I. Bhattacharya, A.G. Tuck, D.I. Schlipalius, and P.R. Ebert. Mechanisms of phosphine toxicity. *Journal of toxicology*, 2011:1–9, 2011.

[115] S. Navarro. New global challenges to the use of gaseous treatments in stored products. In *9th International Working Conference on Stored Product Protection*, 2006.

[116] S. Navarro, R. Noyes, and D.S. Jayas. *The mechanics and physics of modern grain aeration management*. CRC Press, 2002.

[117] M. Nayak, J. Holloway, H. Pavic, M. Head, R. Reid, and C. Patrick. Developing strategies to manage highly phosphine resistant populations on flat grain beetles in large bulk storages in australia. *10th International working conference on stored product protection*, pages 396–401, 2010.

[118] M.K. Nayak and P.J. Collins. Influence of concentration, temperature and humidity on the toxicity of phosphine to the strongly phosphine-resistant psocid liposcelis bostrychophila badonnel (psocoptera: Liposcelididae). *Pest Management Science*, 64:971–976, 2008.

[119] S. Neethirajan, D.S. Jayas, N.D.G. White, and H. Zhang. Investigation of 3d geometry of bulk wheat and pea pores using x-ray computed tomography images. *Computers and electronic in agriculture*, 63:104–111, 2008.

[120] C. Newman, G. Russell, W. Shore, D. Gock, and R. Ryan. Australian siro-circ recirculatory phosphine fumigation systems at xizui grain terminal and inland depots in china. In *Proc. Int. Conf. Controlled Atmosphere and Fumigation in Stored Products*, 2000.

[121] C.R. Newman. Application of sealing technology to permanent grain storage in australia. In *9th international working conference on stored product protection*, 2006.

[122] C.R. Newman. A novel approach to limit the development of phosphine resistance in western australia. In *10th International working conference on stored product protection*, 2010.

[123] Ronald T. Noyes, Thomas W. Phillips, Gerrit W. Cuperus, and Edmond L. Bonjour. Advances in recirculation fumigation technology in the u.s.a. In *Proceedings of the 7th international working conference on stored product protection*, 1998.

[124] R.T. Noyes and T.W. Phillips. A model for selecting tablet vs pellet dosages in storags with closed loop fumigation (CLF) system. In *Proce. Int. Conf. Controlled Atmosphere and fumigation in stored products*, 2004.

[125] J.L. Parry. Mathematical modelling and computer simulation of heat and mass transfer in agricultural grain drying: A reviews. *Journal agricultural engineering researh*, 32:1–29, 1985.

[126] W. Peng, E.A. Smith, and de Ville. Airflow and temperature distribution in two-dimensional drying bins. *Journal of Engineering Mathematics*, 36:241–254, 1999.

[127] M.A.G. Pimentel, L.R.DA. Faroni, R.N.C. Guedes, A.H. Sousa, and M.R. To tola. Phosphine resistance in brazilian populations of sitophilus zeamais

motschulsky (coleoptera: Curculionidae). *Journal of Stored Products Research*, 45:71–74, 2009.

[128] CRC plant biosecurity. Effective phosphine application: ensuring effective phosphine application in grain stores. Project proposal.

[129] N. R. Price. The effect of phosphine on respiration and mitochondrial oxidation in susceptible and resistant strains of rhyzopertha dominica. *Insect Biochem.*, 10:65–71, 1980.

[130] N. R. Price and S. J. Dance. Some biochemical aspects of phosphine action and resistance in three species of stored product beetles. *Camp. Biochem. Physiol*, 76C:277–281, 1983.

[131] D.I. Proctor, editor. *Grain storage techniques - Evolution and trends in developing countries*. Agriculture and consumer protection, 1994.

[132] S. Rajendran. Benchmarking – what makes a good fumigation? In *Proc. Int. Conf. Controlled Atmosphere and Fumigation in Stored Products*, 2007.

[133] S. Rajendran and N. Gunasekaran. The response of phosphine-resistant lesser grain borer rhyzopertha dominica and rice weevil sitophilus oryzae in mixed-age cultures to varying concentrations of phosphine. *Pest Management Science*, 58:277–281, 2002.

[134] H. Rauscher, G.E. Mayr, and J. B. Sullivan. Sorption and recovery of phosphine. *J. AGR. FOOD CHEM*, 20:331–333, 1972.

[135] C. Reed and H. Pan. Loss of phosphine from unsealed bins of wheat at six combinations of grain temperature and grain moisture content. *Journal of Stored Products Research*, 36:263–279, 2000.

[136] Manager Pesticides Review. Final review report and regulatory decision: the reconsideration of registrations of products containing methyl bromide and their associated approved labels. Technical report, Australian Pesticides and Veterinary Medicines Authority, 2007.

[137] L. D. Rodriguez. *Fumigation training manual*. UK Cooperative extension service, Universityof Kentucky-College of Agriculture.

[138] Kimihiko Sato and Masano Suwanai. Adsorption of hydrogen phosphide to cereal products. *Appl. Ent. Zool*, 9(3):127–132, 1974.

[139] D. Schonstein, W. Shore, R. Ryan, and S. Waddell. Controlled release of phosphine - an update. In *6th INternatiocal working conference on stored product-protection*, 1994.

[140] M. Shi, M. Renton, and P.J. Collins. Mortality estimation for individual-based simulations of phosphine resistance in lesser grain borer (rhyzopertha dominica). In *19th International Congress on Modelling and Simulation*, 2011.

[141] A.K. Singh and G.R. Thorpe. A solution procedure for three-dimensional free convective flow in peaked bulks of grain. *Journal of Stored Products Research*, 29:221–235, 1993.

[142] E.A. Smith. Pressure and velocity of air during drying and storage of cereal grains. *Transport in Porous Media*, 23:197–218, 1996.

[143] E.A Smith and D.S. Jayas. Modeling the movement of fumigant gas within grain beds. *American Society of Agricultural Engineers*, 44(3):661–667, 2001.

[144] E.A. Smith and D.S. Jayas. Air traverse time in grain bins. *Applied Mathematical Modelling*, 28:1047–1062, 2004.

[145] E.A. Smith, D.S. Jayas, and A. De Ville. Modelling the flow of carbon dioxide through beds of cereal grains. *Transport in Porous Media*, 44:123–144, 2001.

[146] A.H. Sousa, L.R.D.A. Faroni, M.A.G. Pimentel, and R.N.C. Guedes. Developmental and population growth rates of phosphine-resistant and -susceptible populations of stored-product insect pests. *Journal of Stored Products Research*, 45:241–246, 2009.

[147] R. W. D Taylor. Phosphine: A major grain fumigant at risk. *International Pest Control*, 31:10–14, 1989.

[148] J. Thorne, G. Fulford, A. Ridley, D. Schlipalius, and P. Collins. Life stage and resistance effects in modelling phosphine fumigation of rhyzopertha dominica (f.). In *10th International Working Conference on Stored Product Protection*, 2010.

[149] G.R. Thorpe. Engineering design equations for grain fumigation systems. In *Conference of Agricultural Engineering*, 1990.

[150] G.R. Thorpe. The application of computational fluid dynamics codes to simulate heat and moisture transfer in stored grains. *Journal of Stored Products Research*, 44:21–31, 2008.

[151] P. Trematerra and A. Sciarretta. Spatial distribution of some beetles infesting a feed mill with spatio-temporal dynamics of oryzaephilus surinamensis,tribolium castaneum and tribolium confusum. *Journal of Stored Products Research*, 40:363–377., 2004.

[152] A. Varnava, J. Potsos, G. Russell, and R. Ryan. New phosphine grain fumigation technology in cyprus using the siroflo/eco2fume flow through method. In *Proceeding of the 7th international working conference on stored product protection*, 2001.

[153] H.K. Versteeg and W. Malalasekera. *An introduction to computational fluid dynamics. The finite volume method.* Pearson education limited, 2007.

[154] C. Warrick. Fumigating with phosphine, other fumigants and controlled atmosphere. Technical report, Grains Research & Development Corporation, 2011.

[155] C.R. Watson, N. Pruthi, D. Bureau, C. Macdonald, and J. Roca. Intransit disinfestation of bulk and bagged commodities: a new approach to safety and efficacy. In *Proceeding of the 7th international working conference on stored product protection*, 2000.

[156] B. White. Grain storage facilities: Planning for efficiency and quality. Technical report, Grain research & development corporation, 2012.

[157] P. Williams, P.J. Nickson, M.F. Braby, and A.P. Henderson. Phosphine fumigations of wheat in 2500^3 steel bins without recirculation facilities. *Journal of Stored Products Research 32, 153–162.*, 32:153–162, 1996.

[158] R.G. Winks and C.J. Waterford. The relationship between concentration and time in the toxicity of phosphine to adults of a resistant strain of tribolium castaneum (herbst). *J. Stored Product Research*, 22:85–92, 1986.

[159] E. J. Wright, P. Annis, and R. Qaisrani. Stored grain australia. Technical report, Stored Grain Research Laboratory, CSIRO Entomology, 2000.

[160] T. Xianchang. Evolution of phosphine from aluminium phosphide formulations at various temperatures and humidities. In *Proceeding of the 6th international working conference on stored product protection*, 1994.

[161] S. Xu, D.S. Jayas, N.D.G. White, and W.E. Muir. Momentum-diffusive model for gas transfer in granular media. *Journal of Stored Products Research*, 38:455–462., 2002.

[162] A. Yazdani and L. Shojai. Solution of a scalar convection-diffusion equation using femlab. In *Proceedings of the COMSOL Multiphysics User's Conference*, 2005.

[163] B. X. Zhao. Generation of phosphine gas for the control of grain storage pests. In *10th International Working Conference on Stored Product Protection*, 2010.